Supporting Information

Psiguadiols A–J, rearranged meroterpenoids as potent PTP1B inhibitors from *Psidium guajava*

Ji-Qin Hou,[†] Chun-Lin Fan,[‡] Xin Pei,[†] Pei-Lin Zhang,[†] Fan Deng,[†] Wan-Qiang Jiang,[†] Guo-Cai Wang,[‡] Xiao-Qi Zhang,[‡] Wen-Cai Ye,[‡] and Hao Wang*[,†]

[†]State Key Laboratory of Natural Medicines, Department of TCMs Pharmaceuticals, School of Traditional Chinese Pharmacy, China Pharmaceutical University, Nanjing 210009, People' s Republic of China

[‡]Institute of Traditional Chinese Medicine and Natural Products, Jinan University, Guangzhou 510632, People' s Republic of China

Supporting information list:

For compound 1

For compound 2

For compound 3

For compound 4

For compound 5

For compound 6

For compound 7

For compound 8

For compound 9

For compound 10

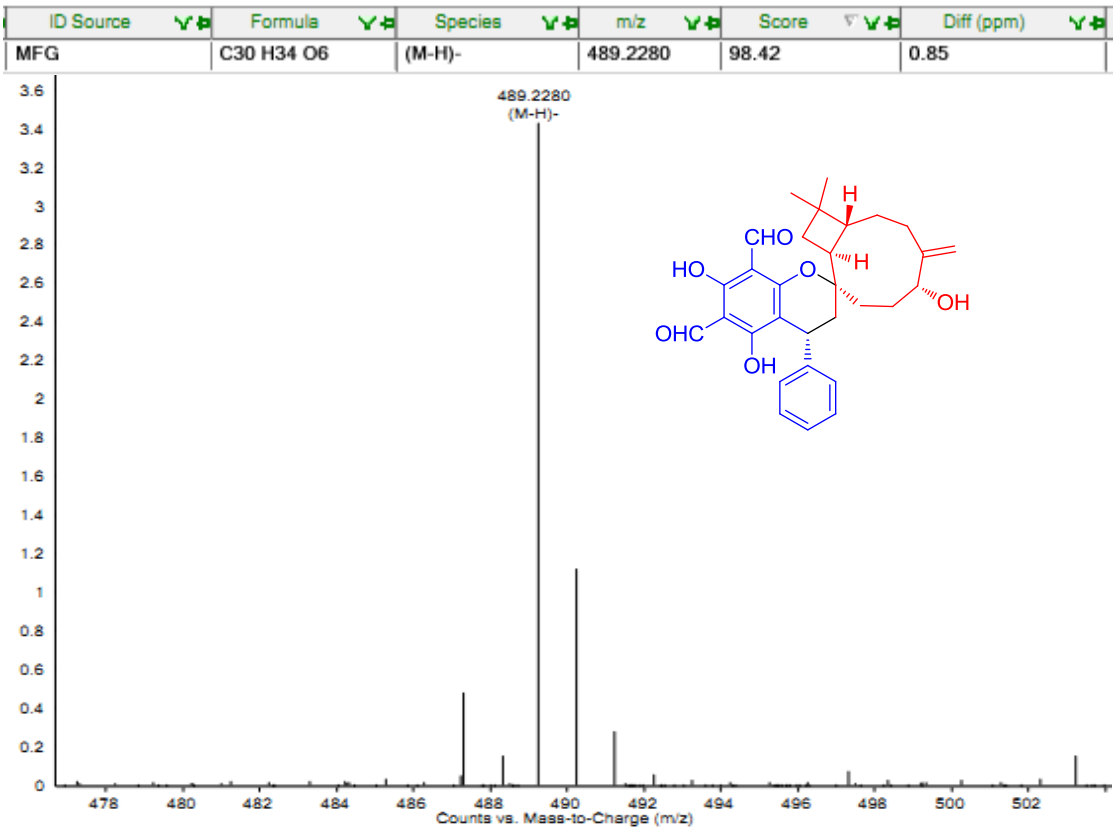

Figure S1-1. HR-ESI-MS spectrum of **1**

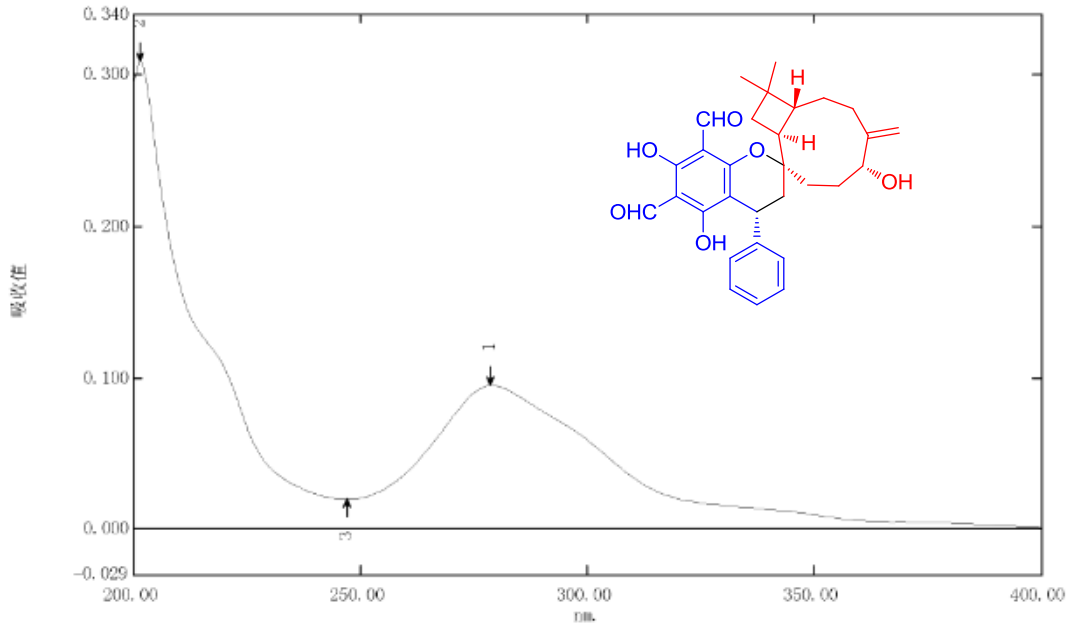

测定属性
波长范围（nm.）：200.00 到 400.00
扫描速度：中速
采样间隔：0.2
自动采样间隔：启用

No.	P/V	波长(nm)	吸收值
1	↑	278.60	0.095
2	↑	201.40	0.309
3	↓	247.20	0.020

Figure S1-2. UV spectrum of **1** in MeOH

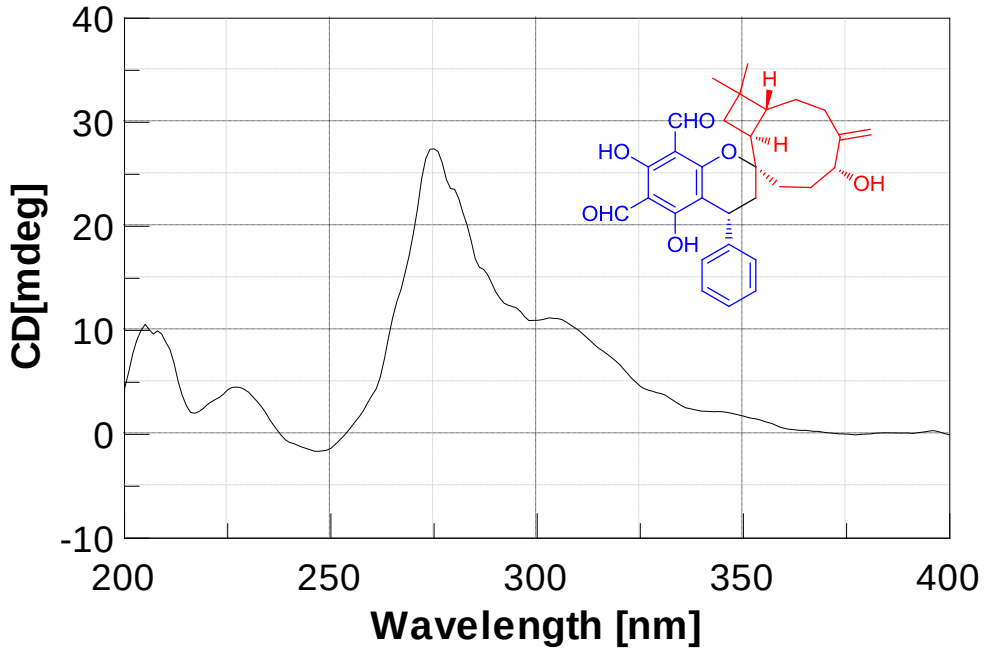

Figure S1-3. CD spectrum of **1** in MeOH

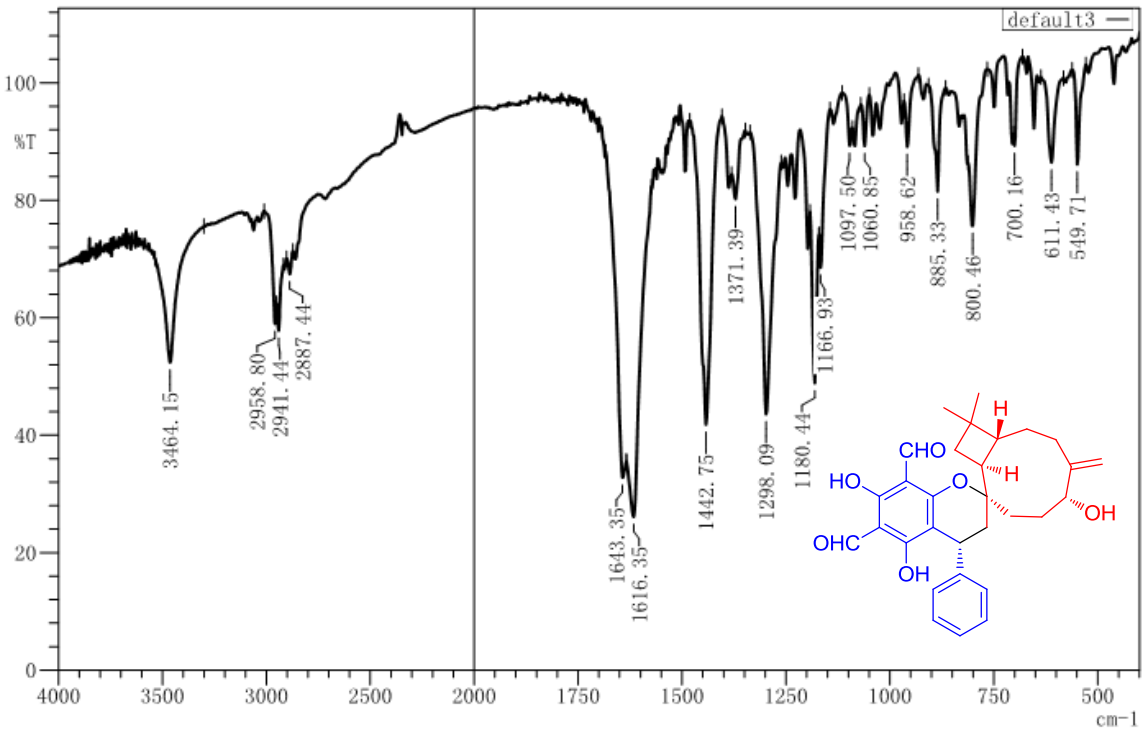

Figure S1-4. IR spectrum of **1**

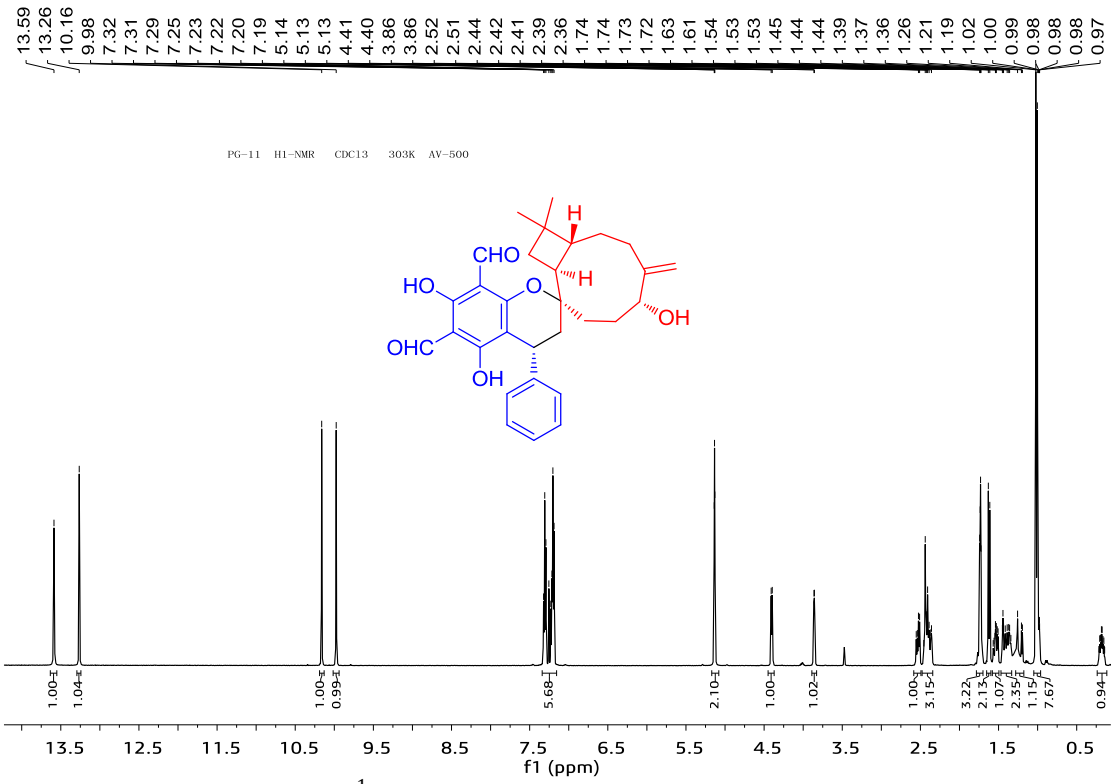

Figure S1-5. ^{1}H NMR spectrum of **1** in $CDCl_3$ (500 MHz)

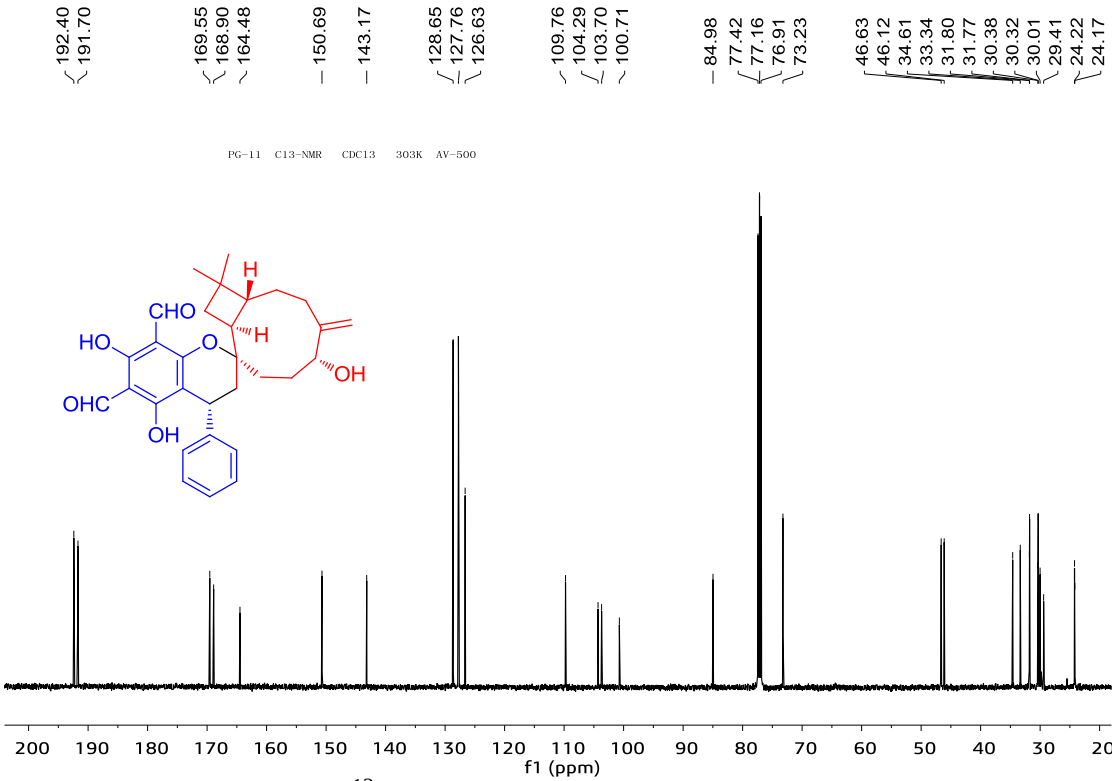

Figure S1-6. ^{13}C NMR spectrum of **1** in $CDCl_3$ (125 MHz)

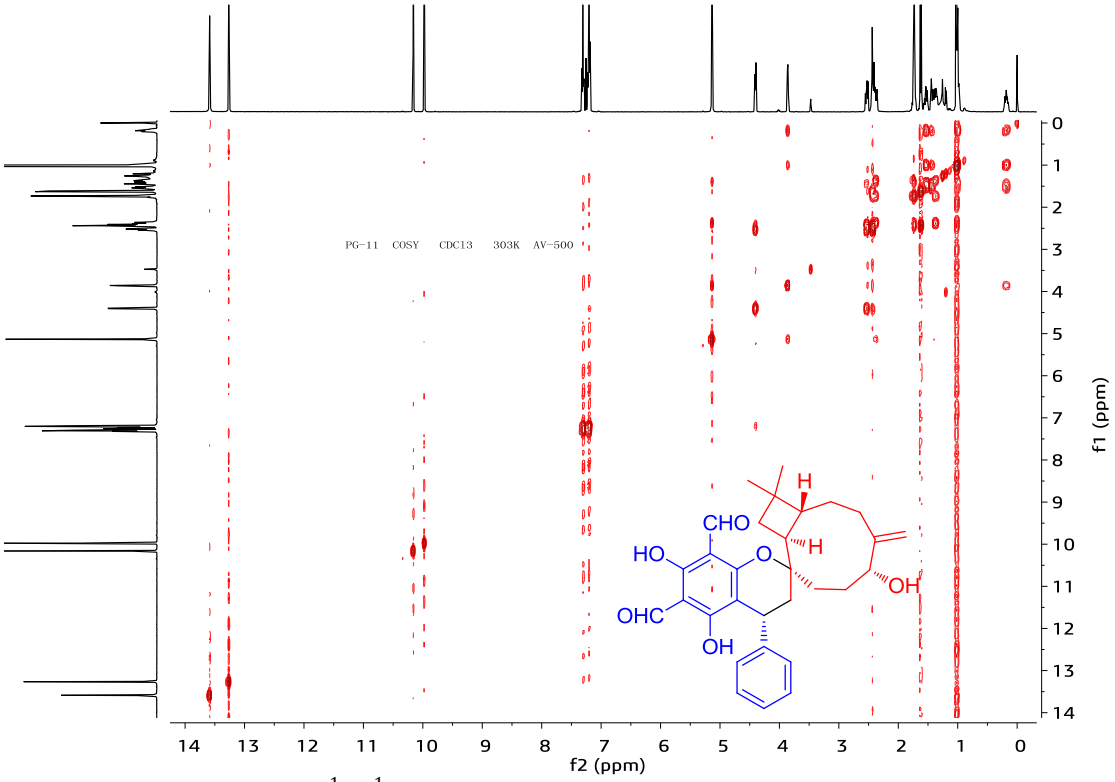

Figure S1-7. ^{1}H-^{1}H COSY spectrum of **1** in $CDCl_3$ (500 MHz)

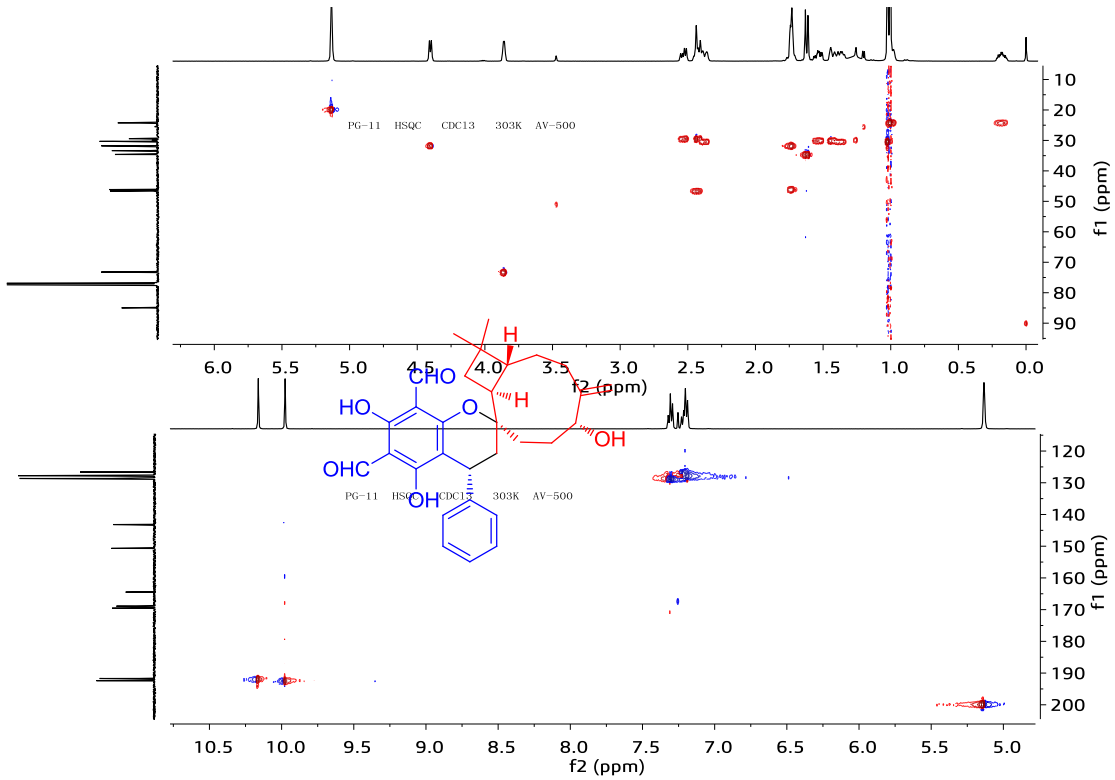

Figure S1-8. HSQC spectrum of **1** in $CDCl_3$ (500 MHz)

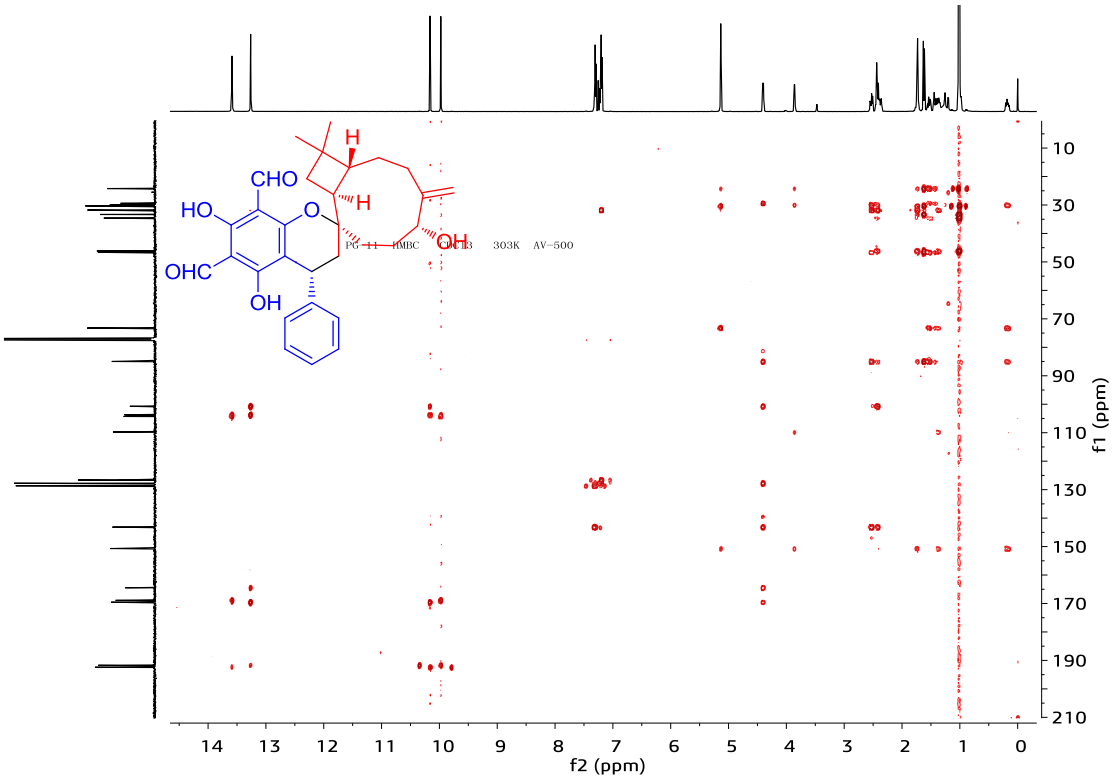

Figure S1-9. HMBC spectrum of **1** in $CDCl_3$ (500 MHz)

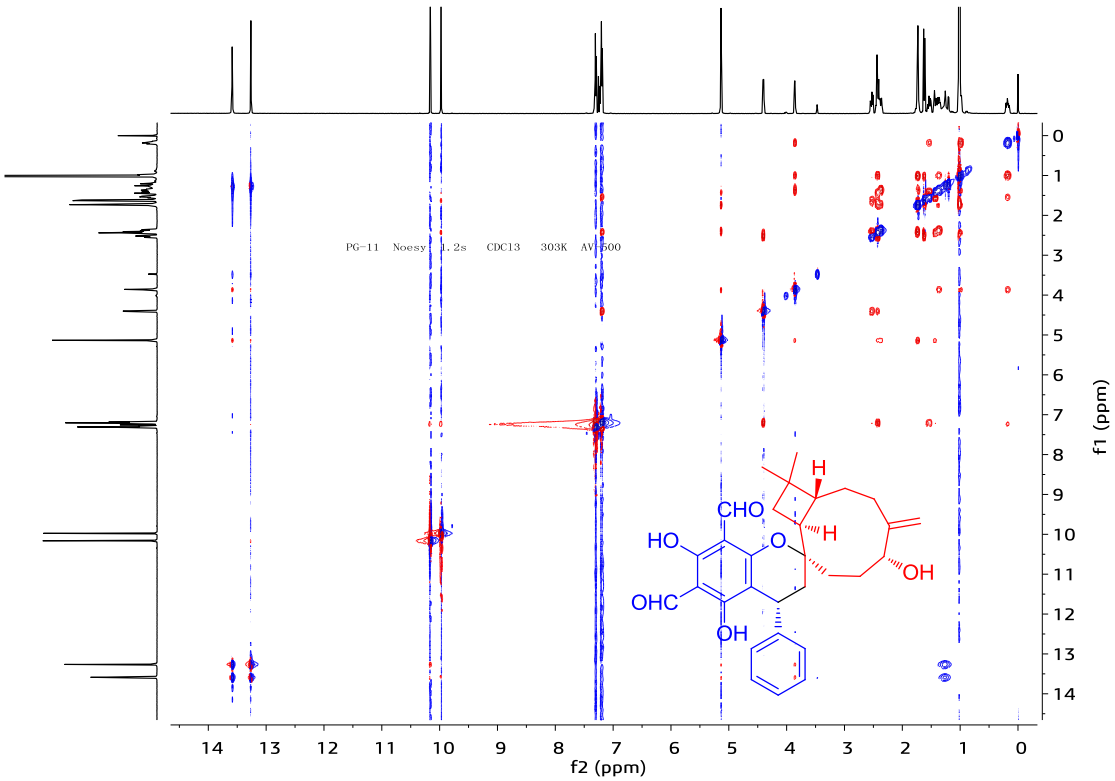

Figure S1-10. NOESY spectrum of **1** in $CDCl_3$ (500 MHz)

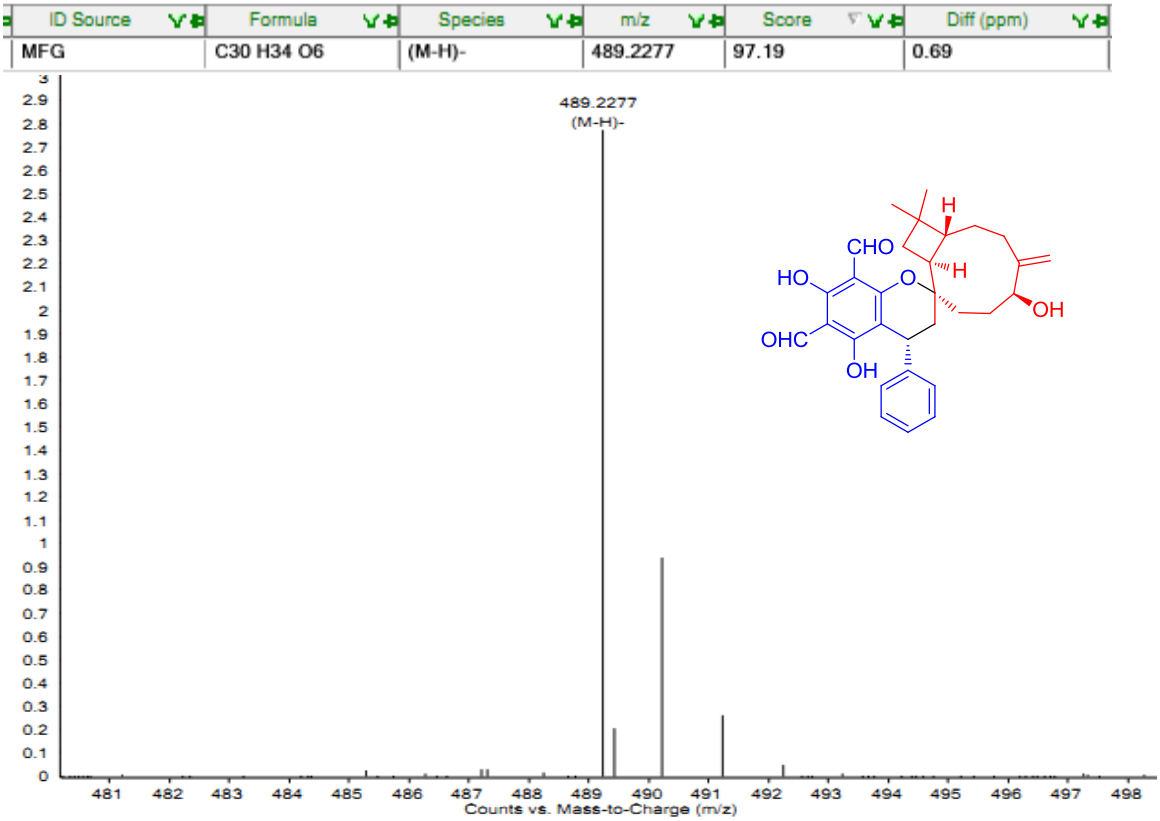

Figure S2-1. HR-ESI-MS spectrum of **2**

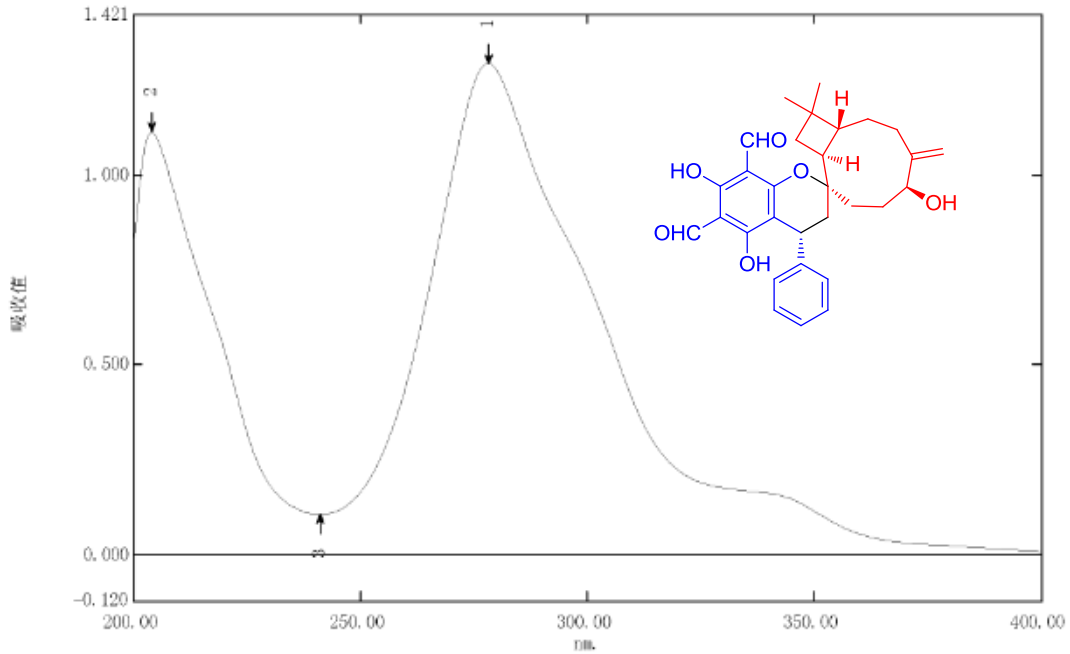

测定属性
波长范围（nm.）：200.00 到 400.00
扫描速度：中速
采样间隔：0.2
自动采样间隔：启用

No.	P/V	波长(nm)	吸收值
1	↑	278.20	1.293
2	↑	204.00	1.112
3	↓	241.20	0.106

Figure S2-2. UV spectrum of **2** in MeOH

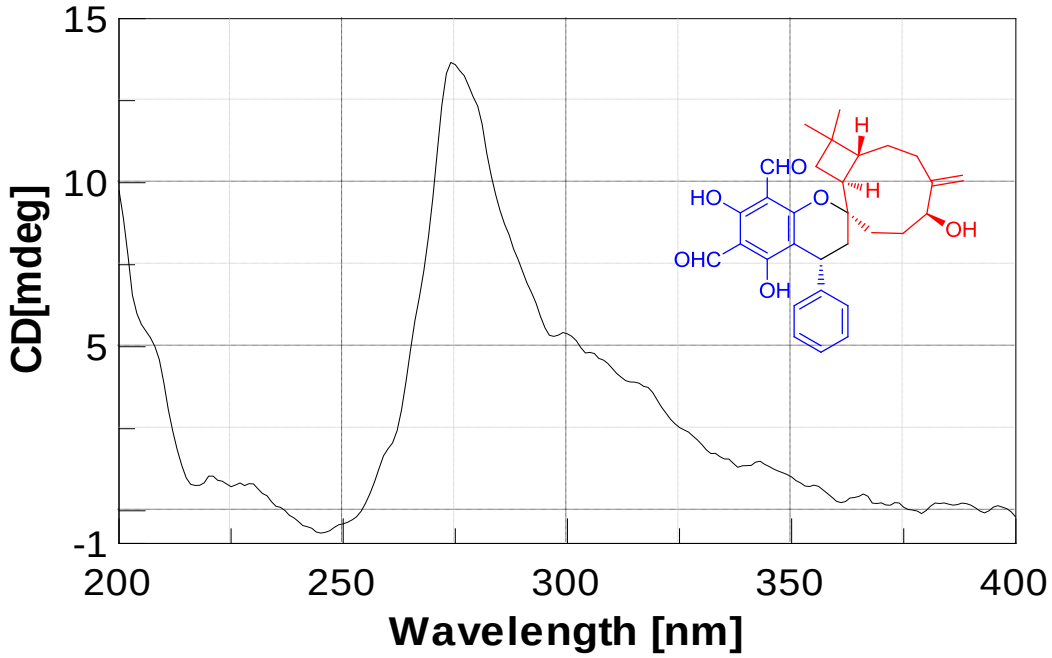

Figure S2-3. CD spectrum of **2** in MeOH

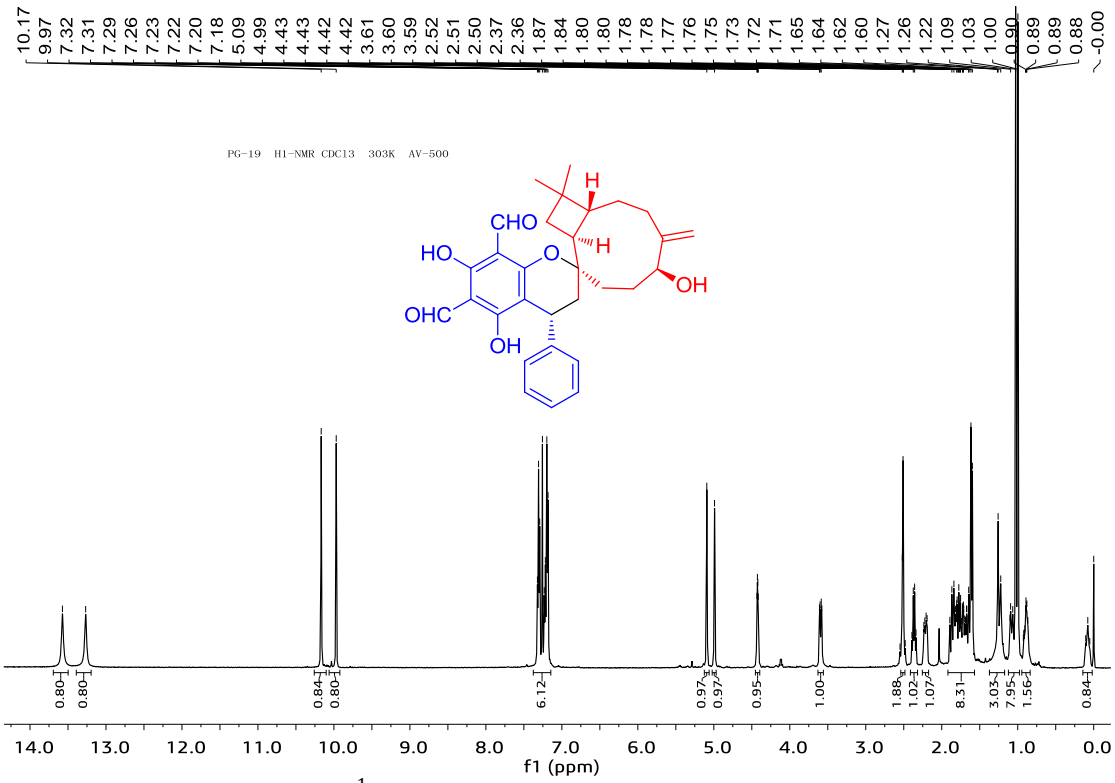

Figure S2-4. ^{1}H NMR spectrum of **2** in $CDCl_3$ (500 MHz)

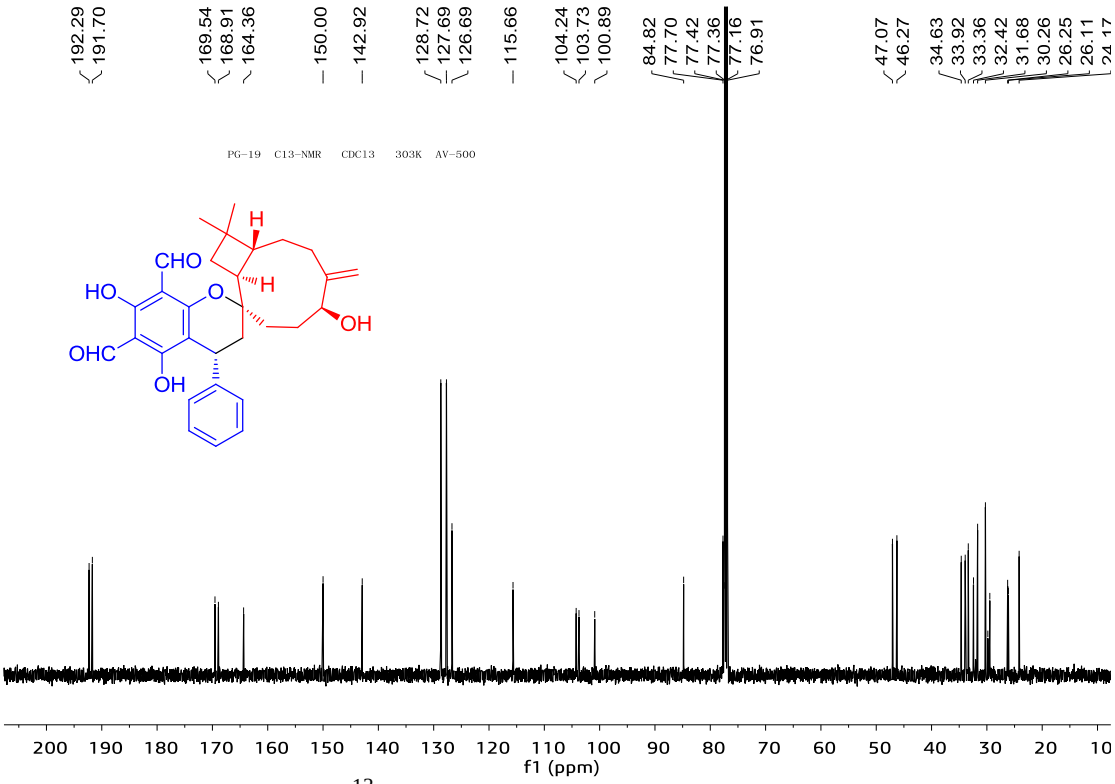

Figure S2-5. ^{13}C NMR spectrum of **2** in $CDCl_3$ (125 MHz)

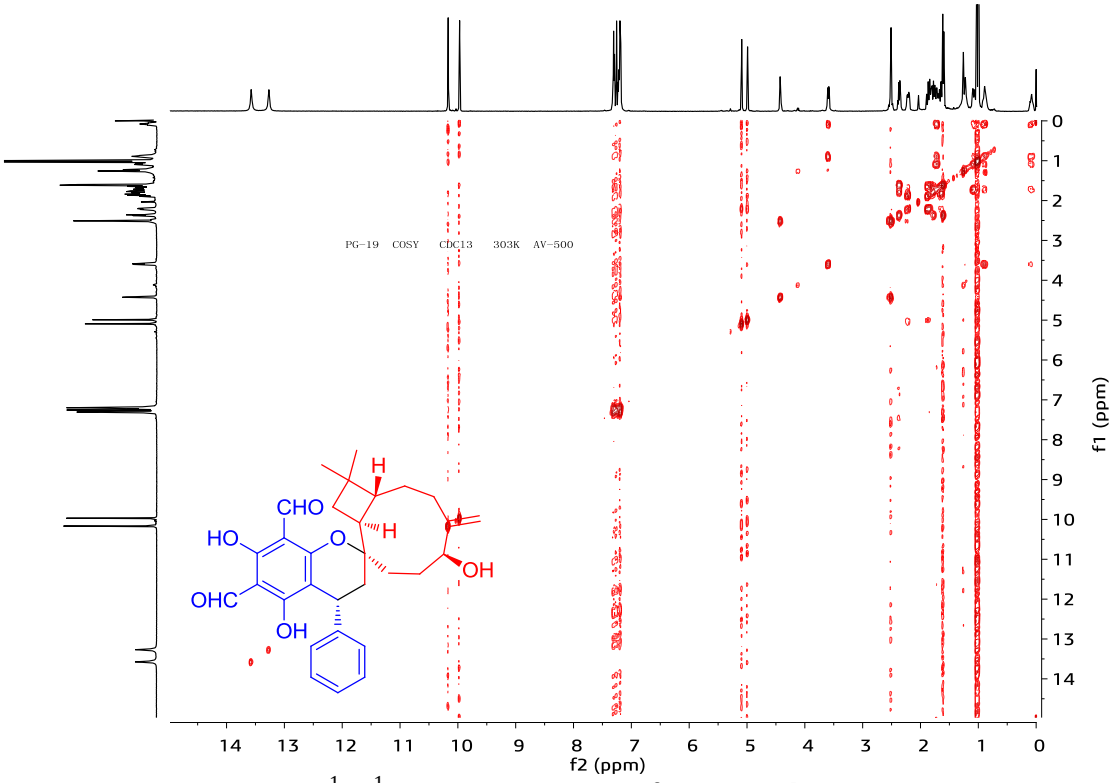

Figure S2-6. ^{1}H-^{1}H COSY spectrum of **2** in $CDCl_3$ (500 MHz)

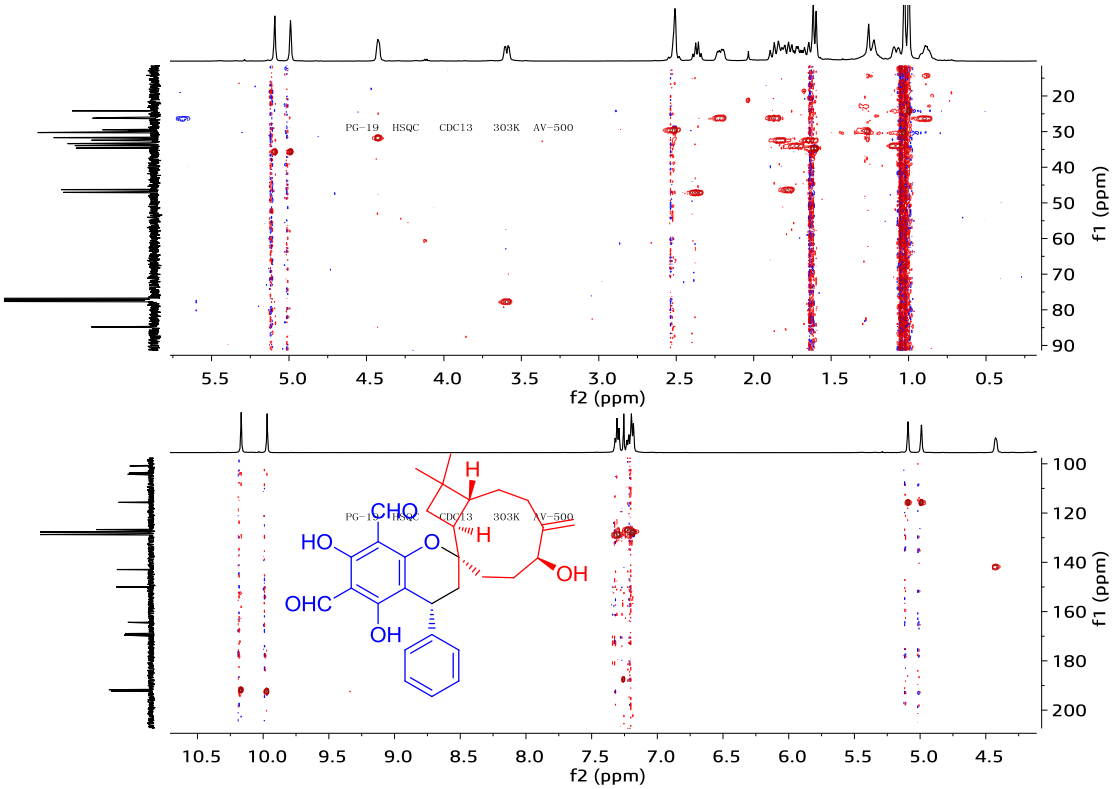

Figure S2-7. HSQC spectrum of **2** in $CDCl_3$ (500 MHz)

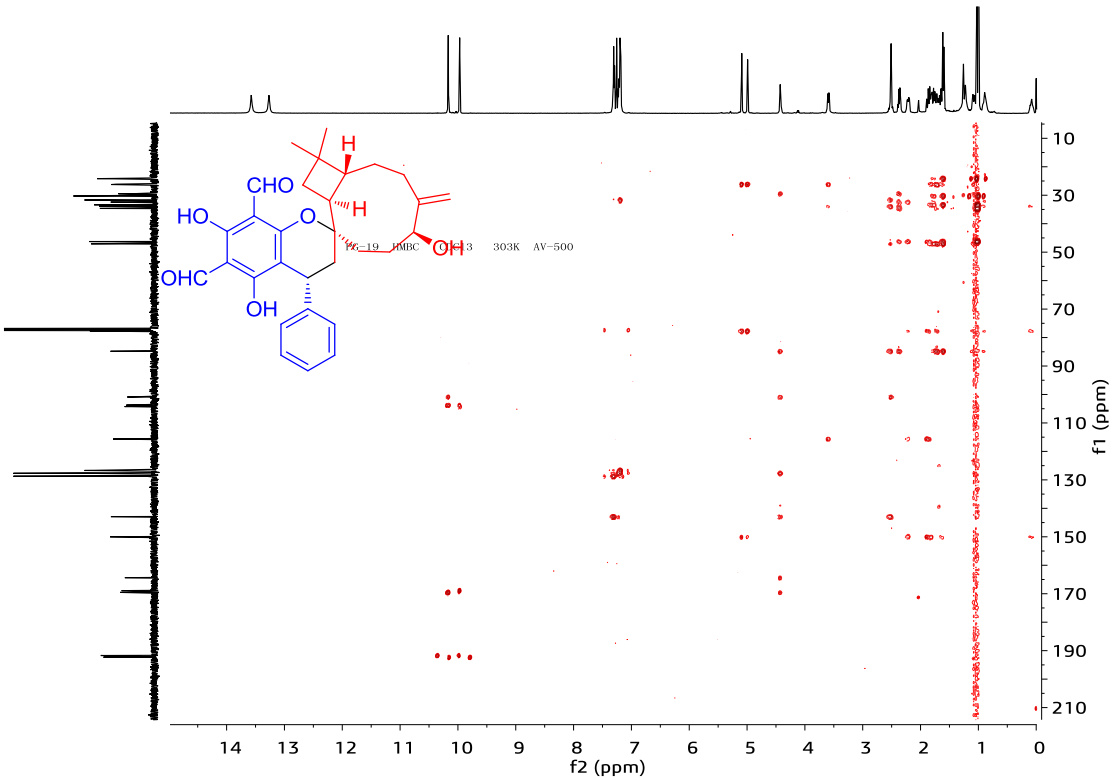

Figure S2-8. HMBC spectrum of **2** in $CDCl_3$ (500 MHz)

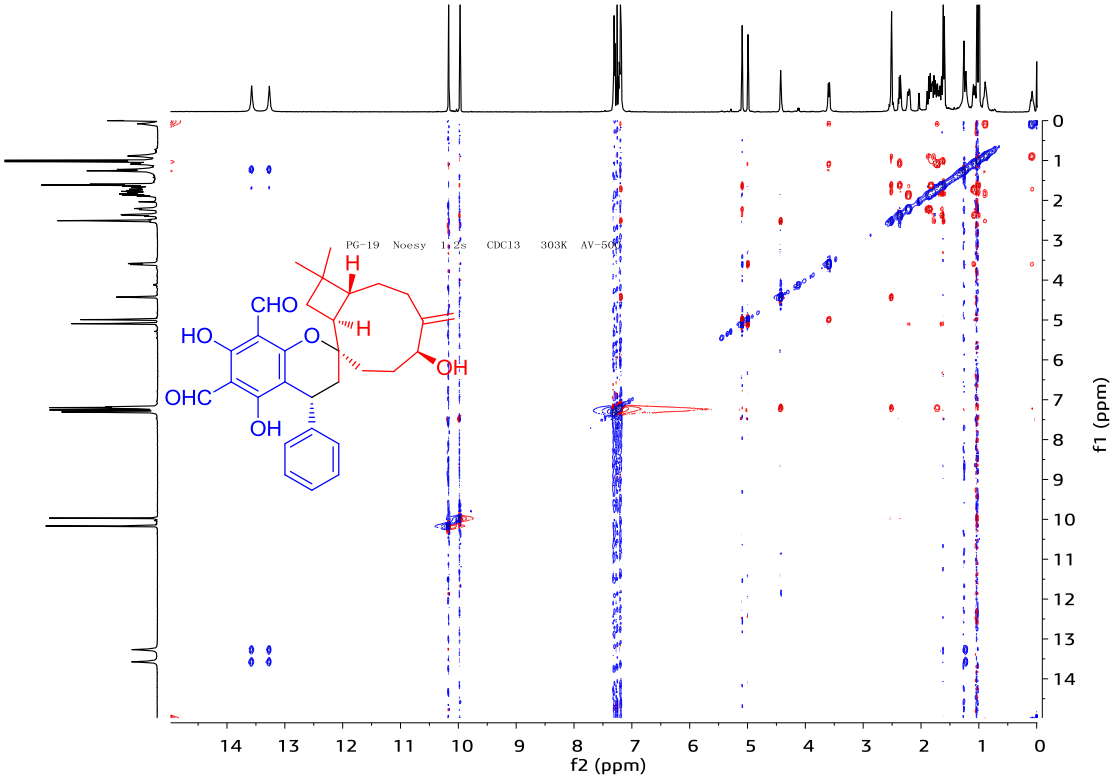

Figure S2-9. NOESY spectrum of **2** in $CDCl_3$ (500 MHz)

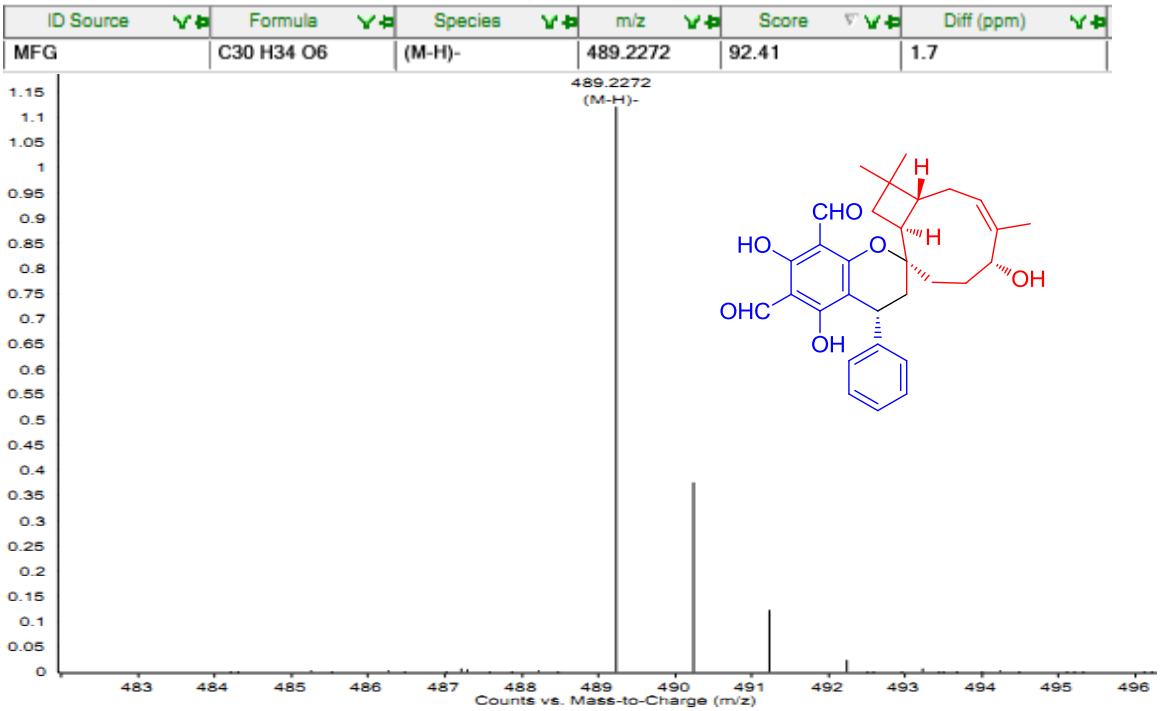

Figure S3-1. HR-ESI-MS spectrum of **3**

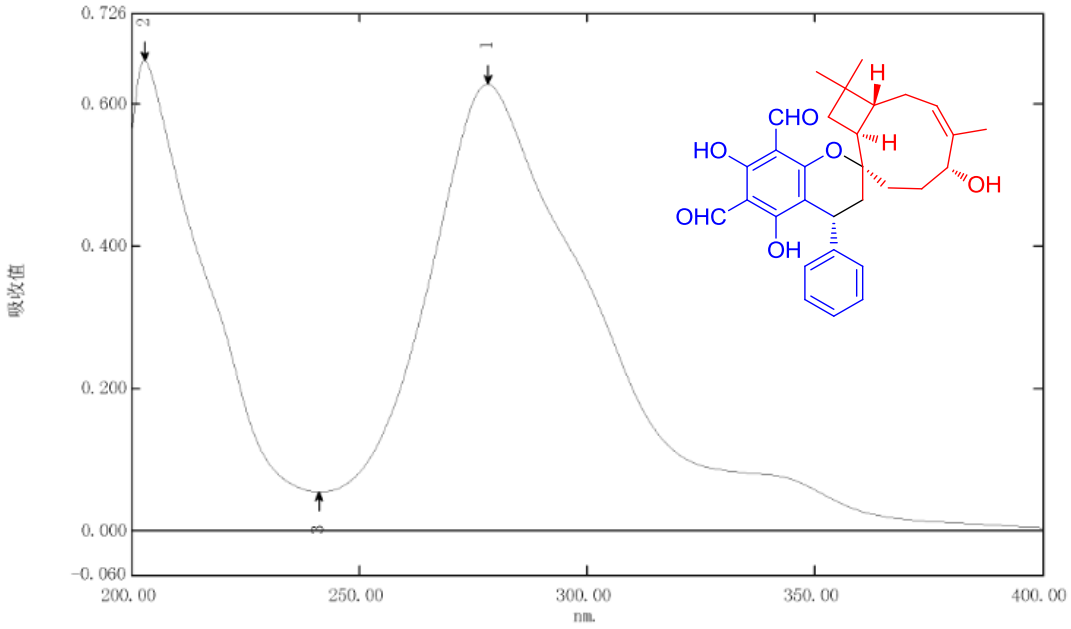

测定属性
波长范围（nm.）: 200.00 到 400.00
扫描速度: 中速
采样间隔: 0.2
自动采样间隔: 启用

No.	P/V	波长(nm)	吸收值
1	↑	278.20	0.627
2	↑	202.80	0.660
3	↓	241.20	0.055

Figure S3-2. UV spectrum of **3** in MeOH

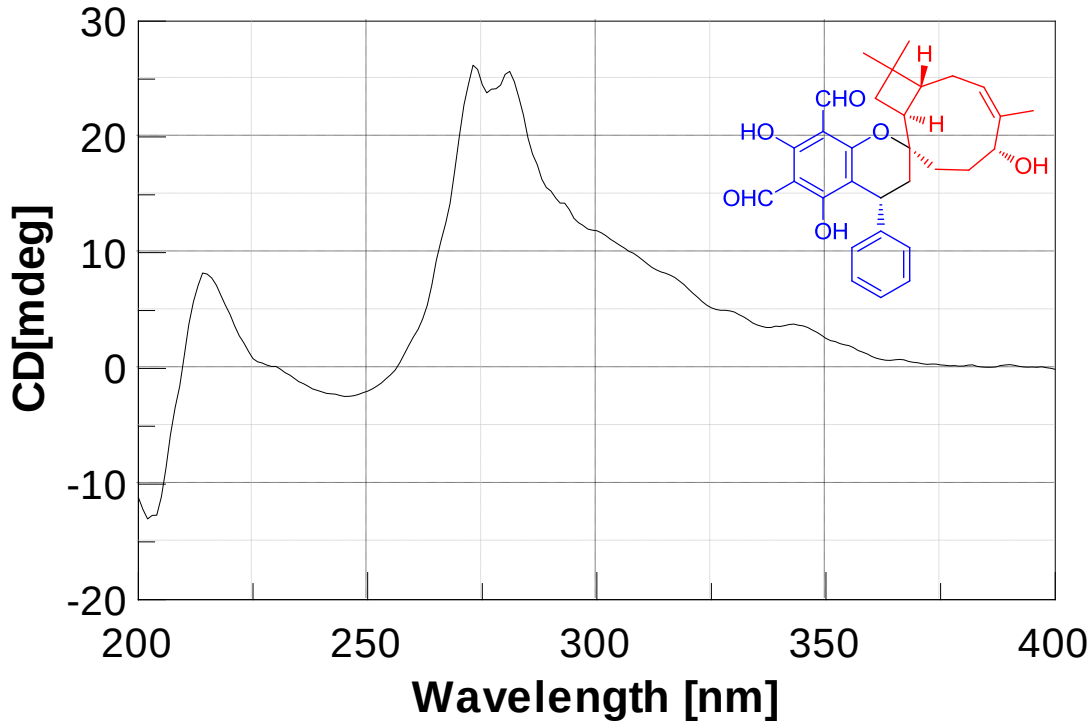

Figure S3-3. CD spectrum of **3** in MeOH

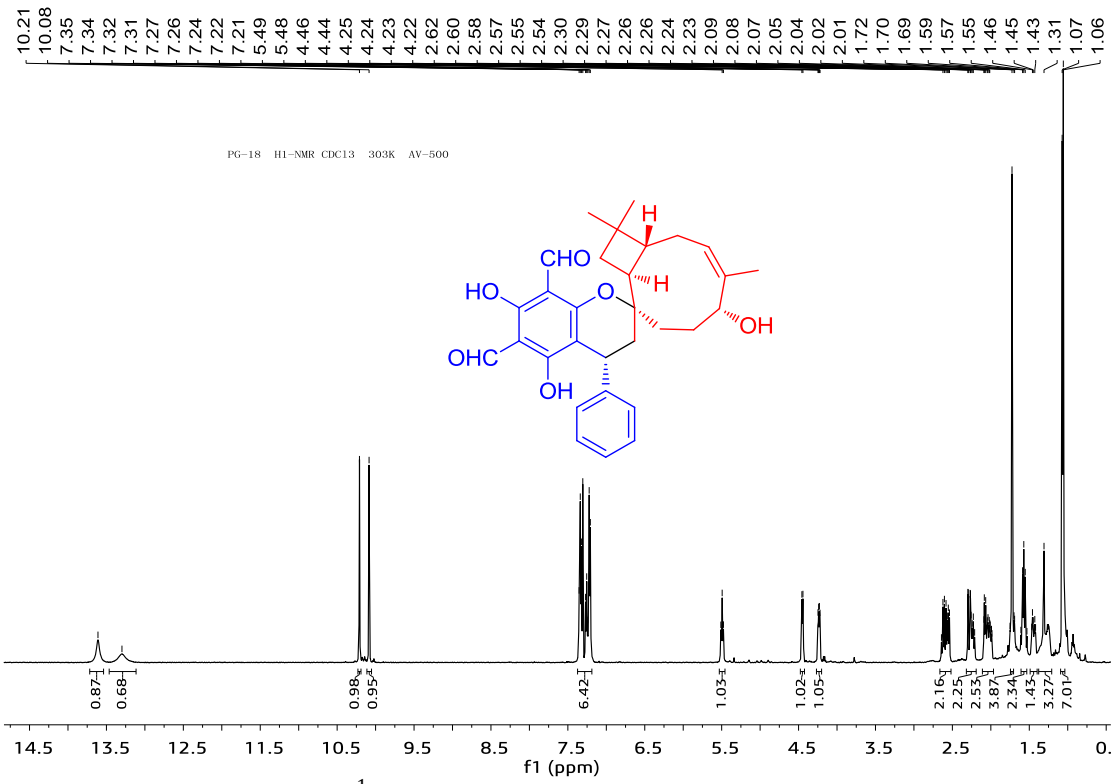

Figure S3-4. ^{1}H NMR spectrum of **3** in $CDCl_3$ (500 MHz)

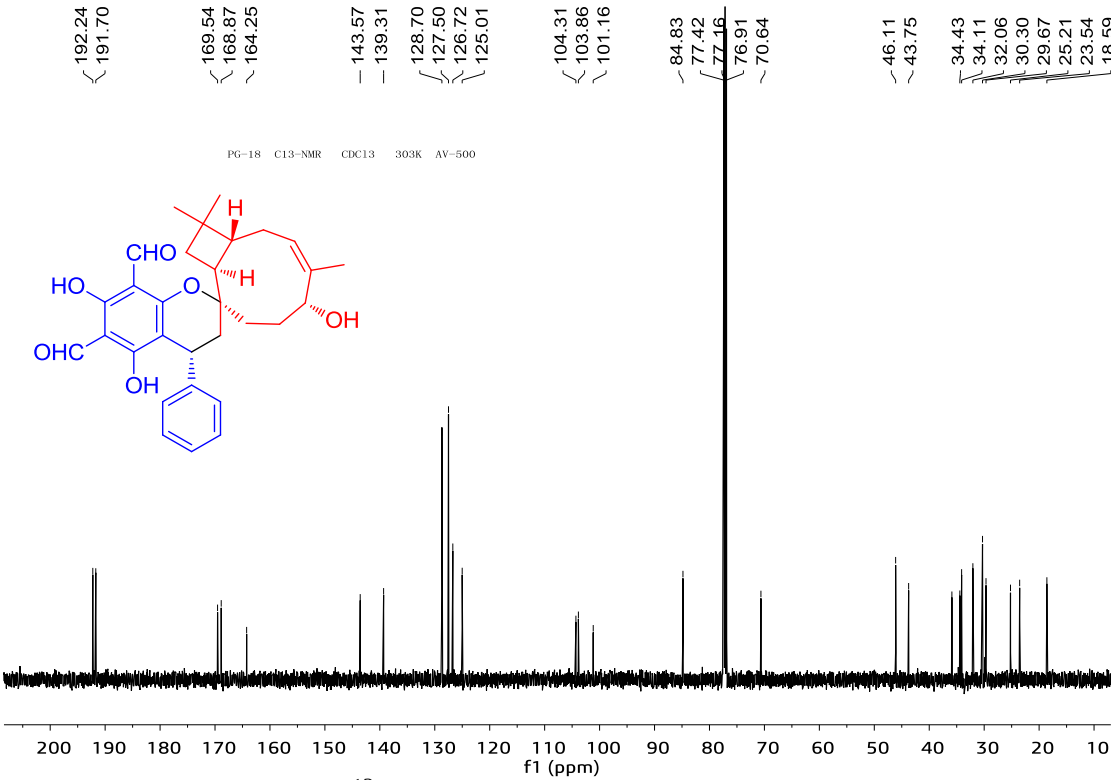

Figure S3-5. ^{13}C NMR spectrum of **3** in $CDCl_3$ (125 MHz)

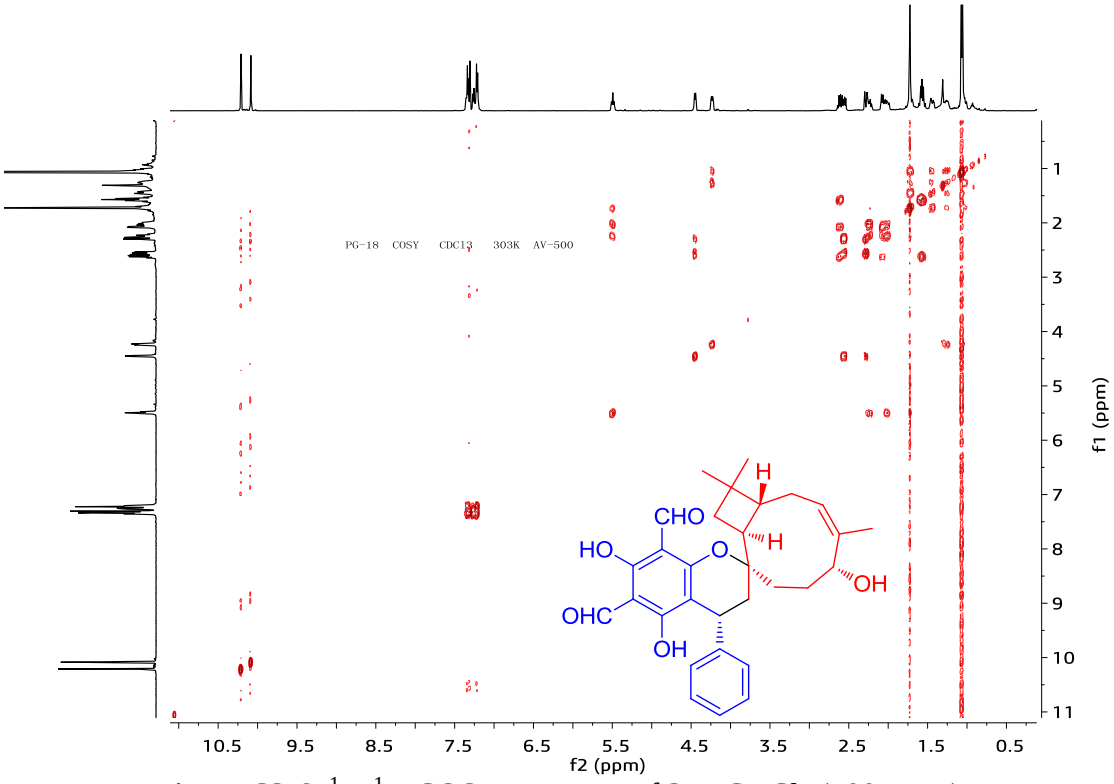

Figure S3-6. ^{1}H-^{1}H COSY spectrum of **3** in $CDCl_3$ (500 MHz)

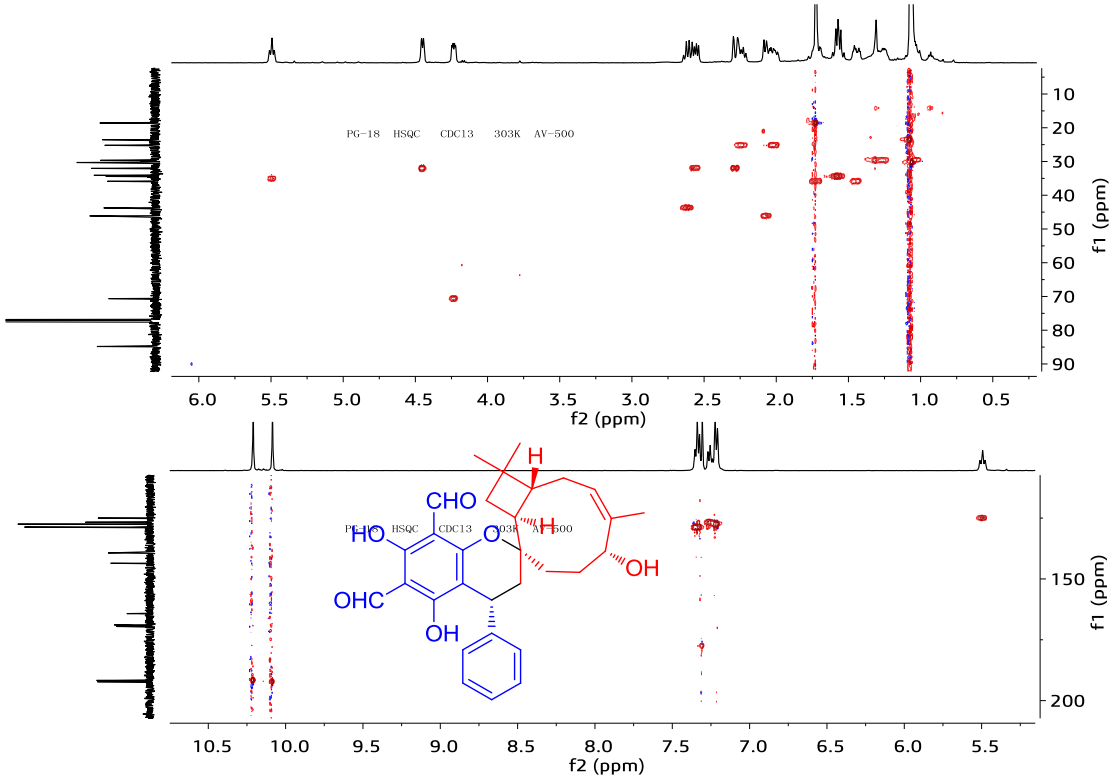

Figure S3-7. HSQC spectrum of **3** in $CDCl_3$ (500 MHz)

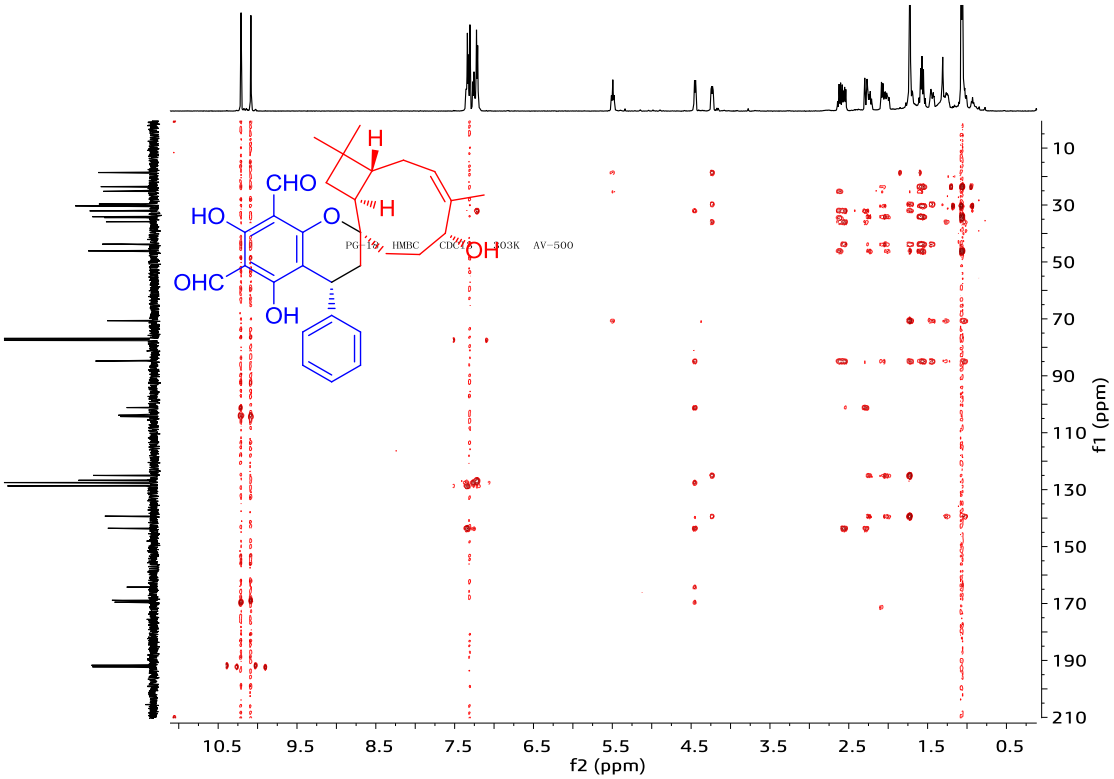

Figure S3-8. HMBC spectrum of **3** in $CDCl_3$ (500 MHz)

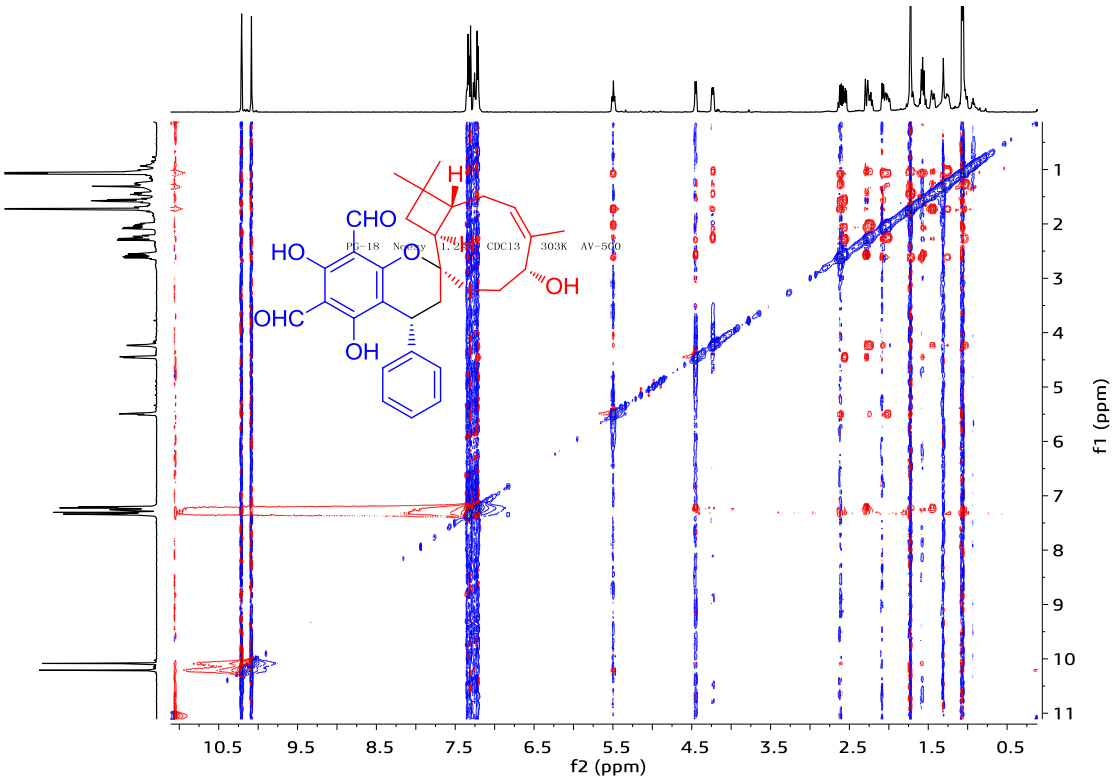

Figure S3-9. NOESY spectrum of **3** in $CDCl_3$ (500 MHz)

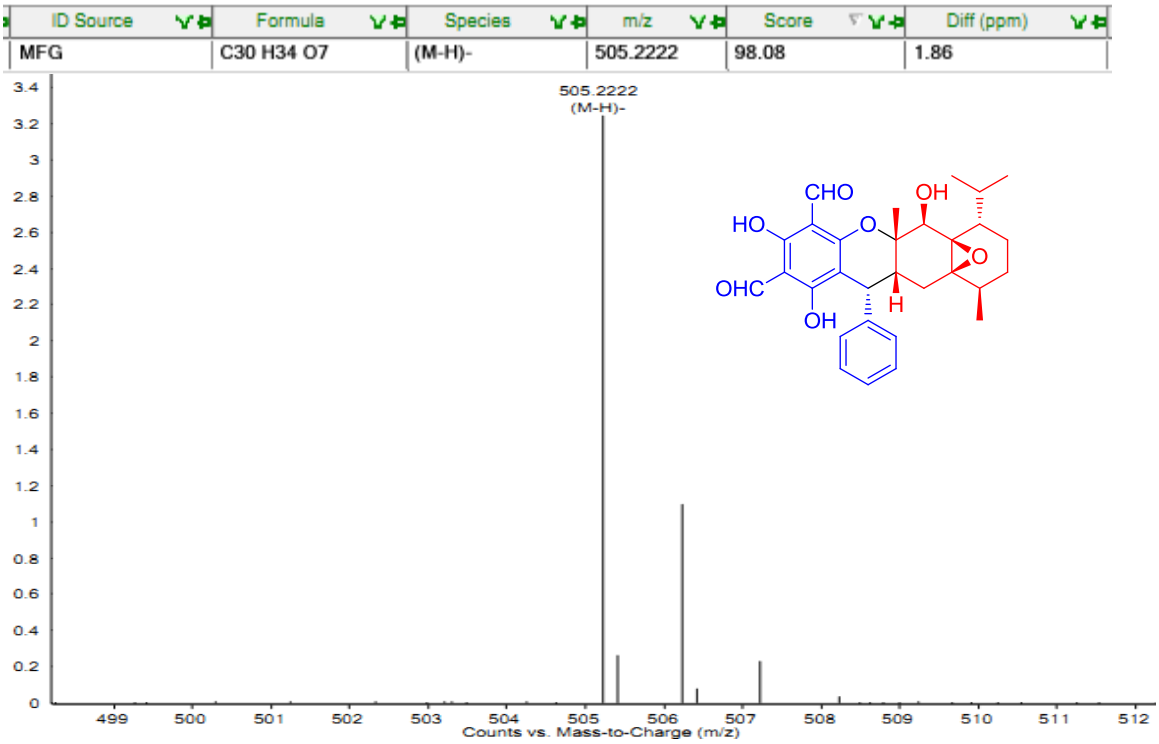

Figure S4-1. HR-ESI-MS spectrum of **4**

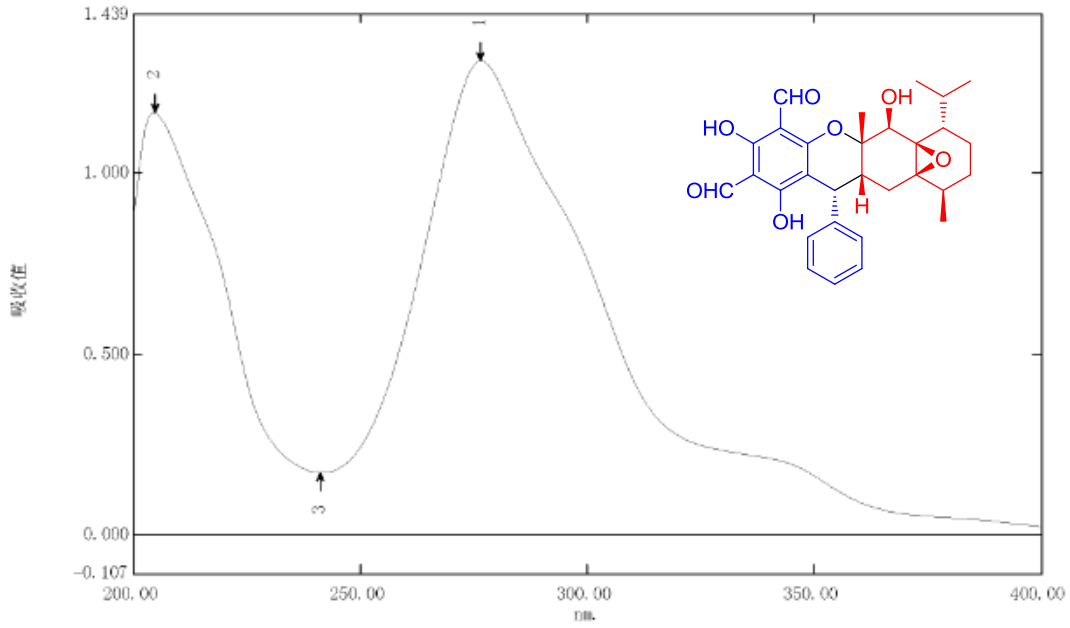

测定属性
波长范围（nm.）：200.00 到 400.00
扫描速度：中速
采样间隔：0.2
自动采样间隔：启用

No.	P/V	波长(nm)	吸收值
1	↑	276.60	1.310
2	↑	204.60	1.166
3	↓	241.20	0.170

Figure S4-2. UV spectrum of **4** in MeOH

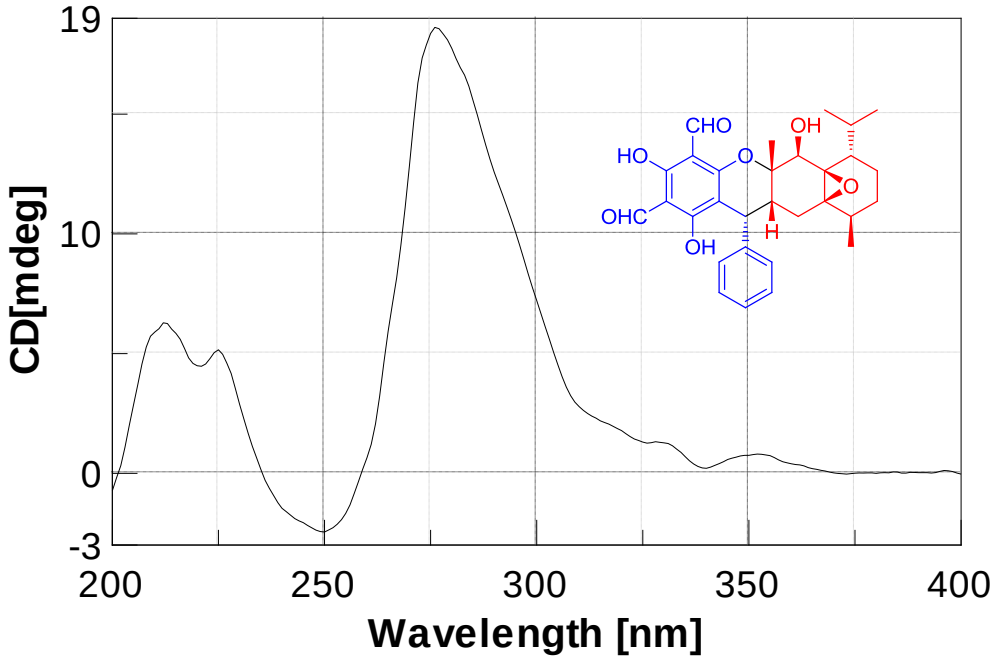

Figure S4-3. CD spectrum of **4** in MeOH

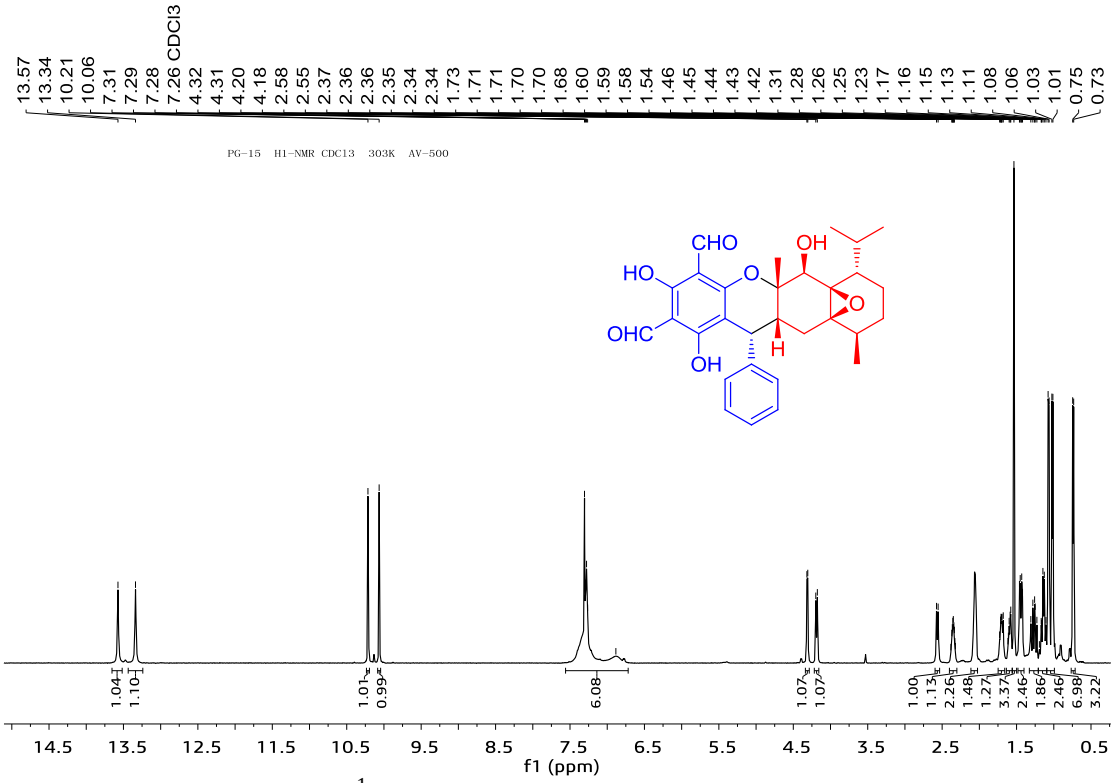

Figure S4-4. ^{1}H NMR spectrum of **4** in $CDCl_3$ (500 MHz)

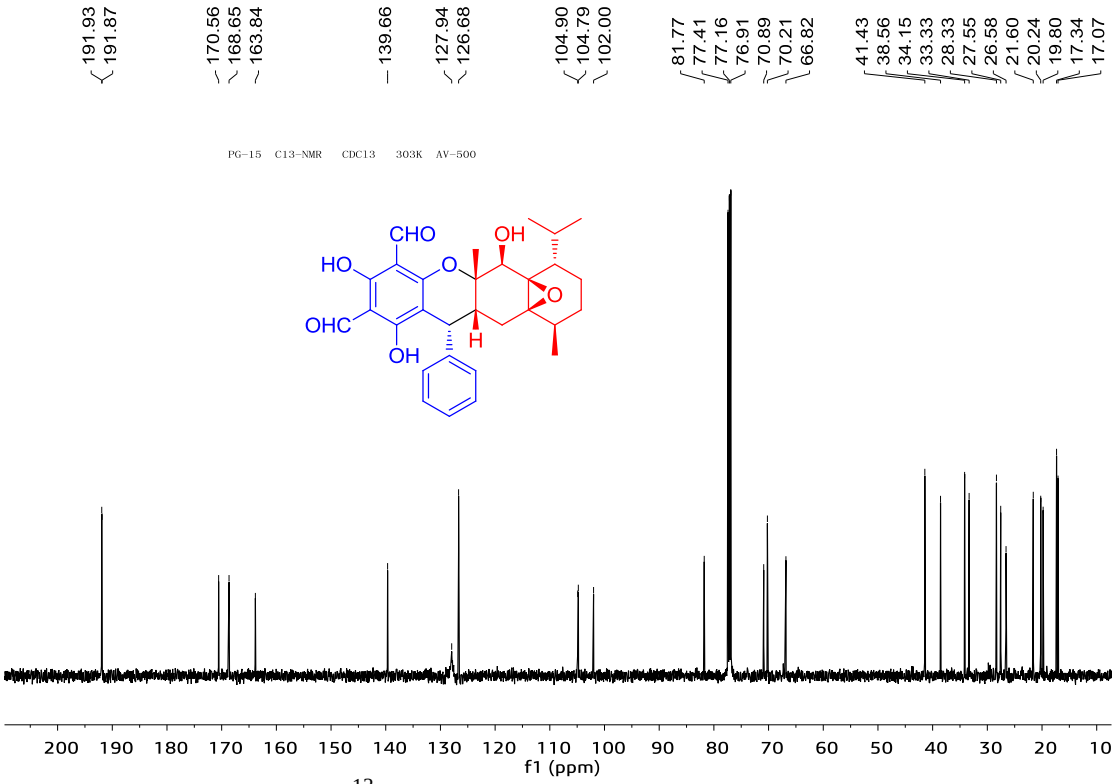

Figure S4-5. ^{13}C NMR spectrum of **4** in $CDCl_3$ (125 MHz)

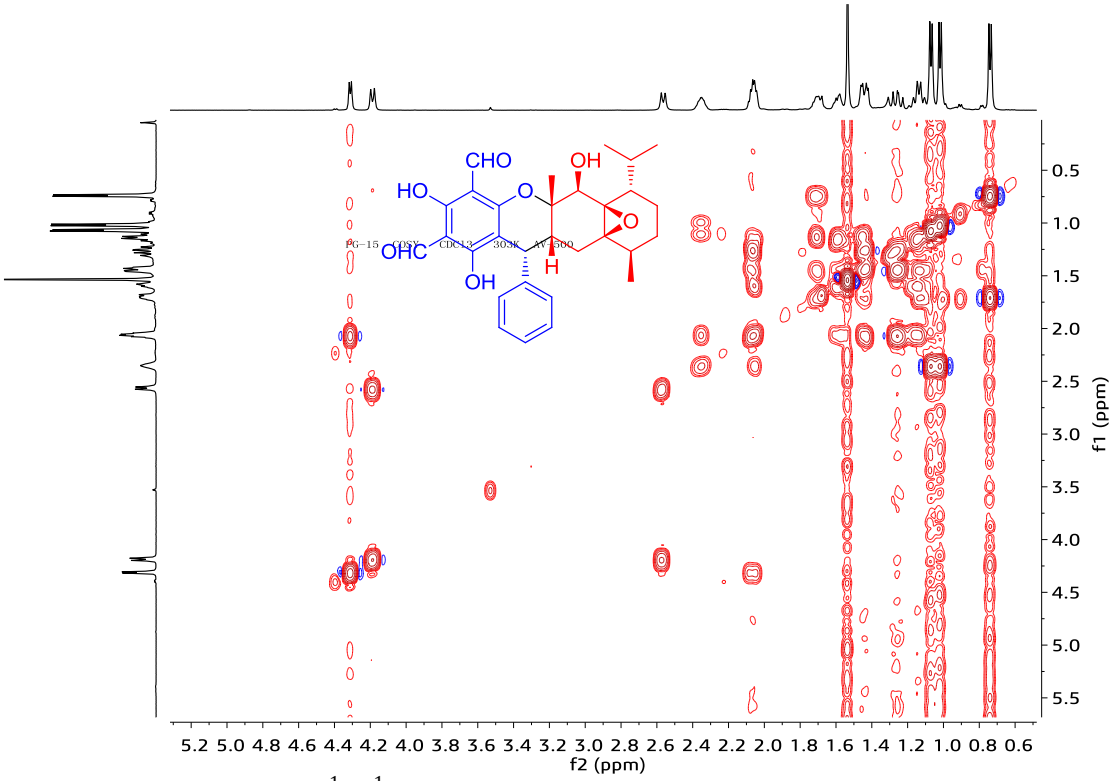

Figure S4-6. ^{1}H-^{1}H COSY spectrum of **4** in $CDCl_3$ (500 MHz)

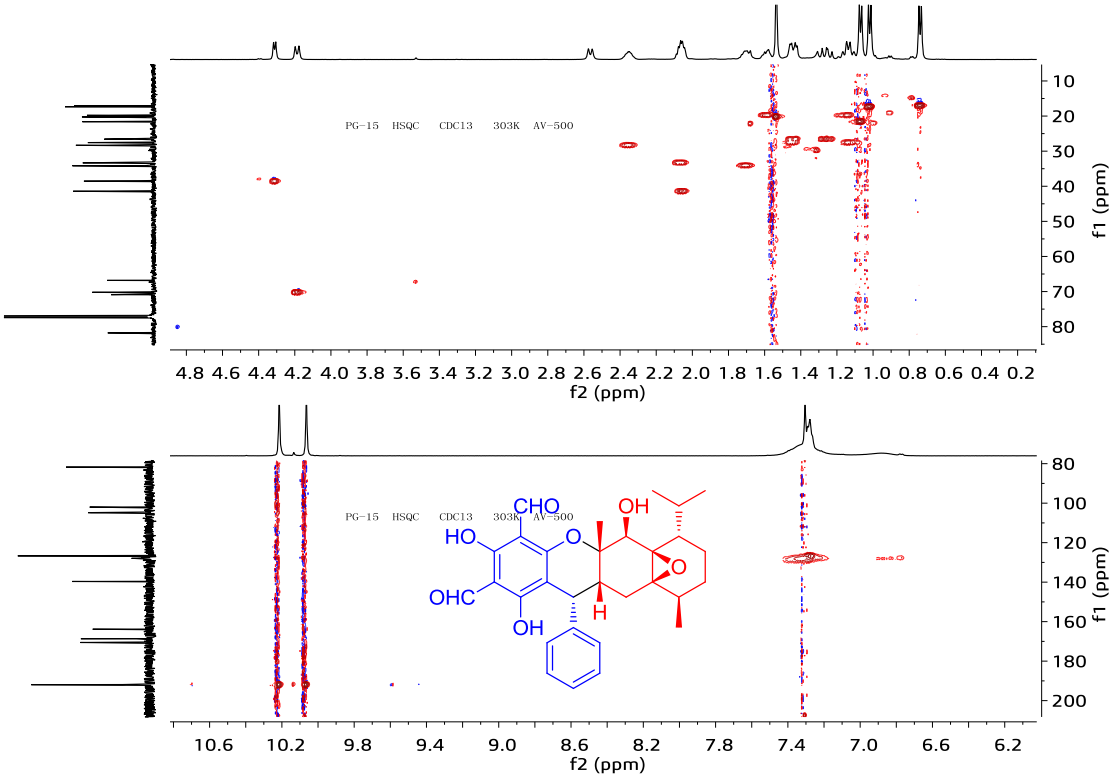

Figure S4-7. HSQC spectrum of **4** in $CDCl_3$ (500 MHz)

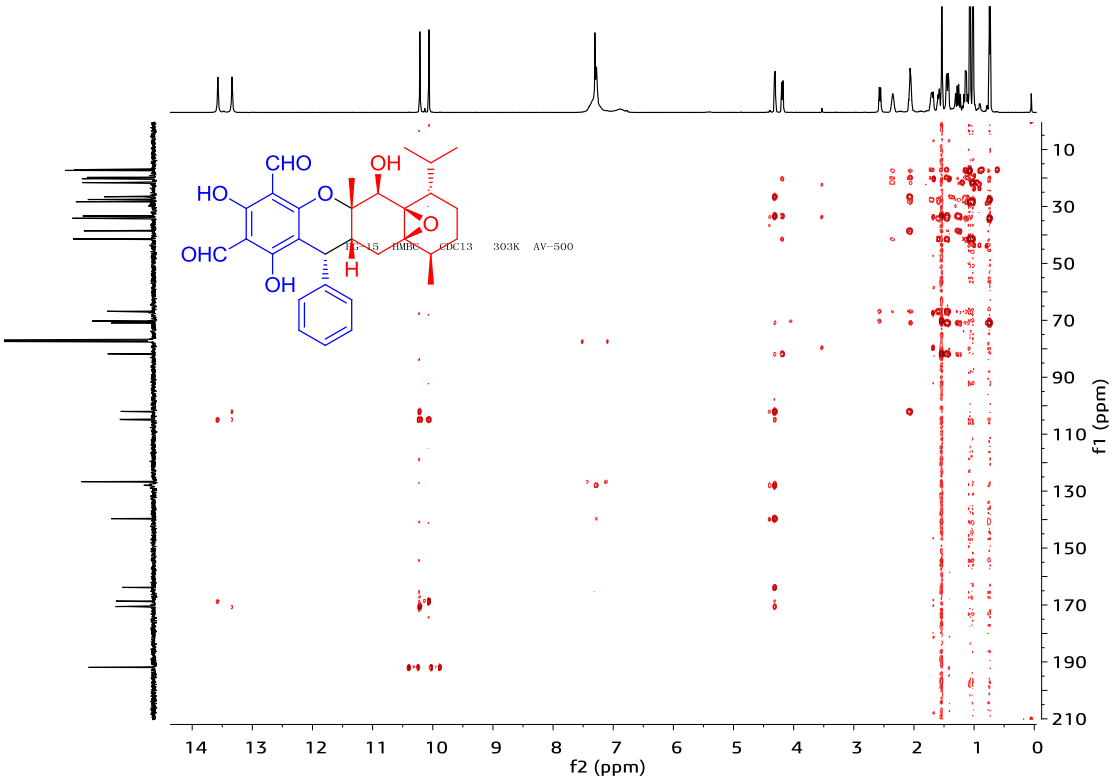

Figure S4-8. HMBC spectrum of **4** in $CDCl_3$ (500 MHz)

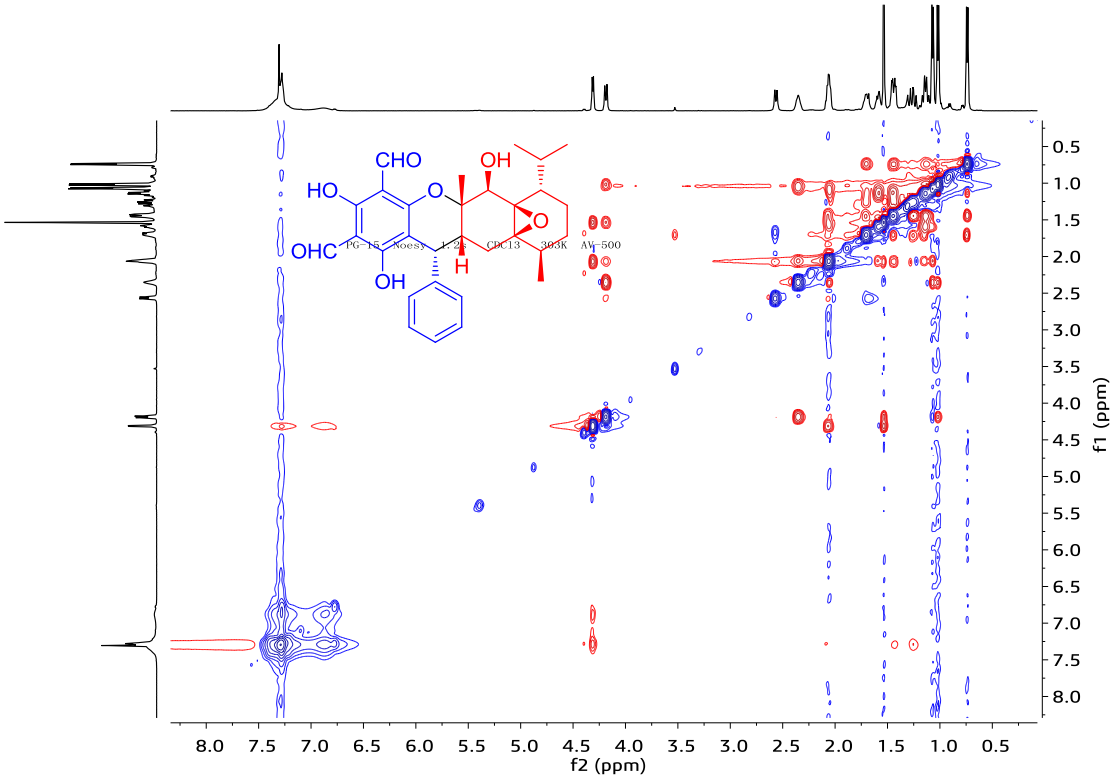

Figure S4-9. NOESY spectrum of **4** in $CDCl_3$ (500 MHz)

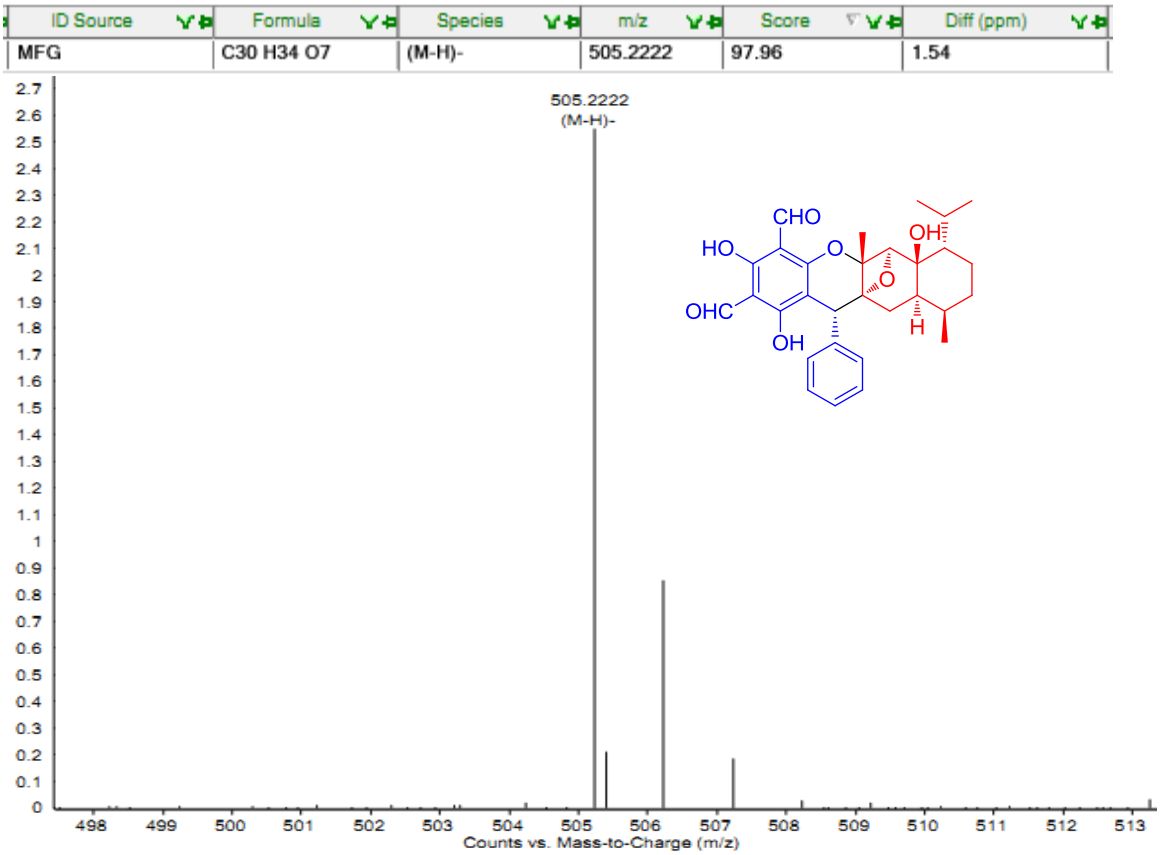

Figure S5-1. HR-ESI-MS spectrum of **5**

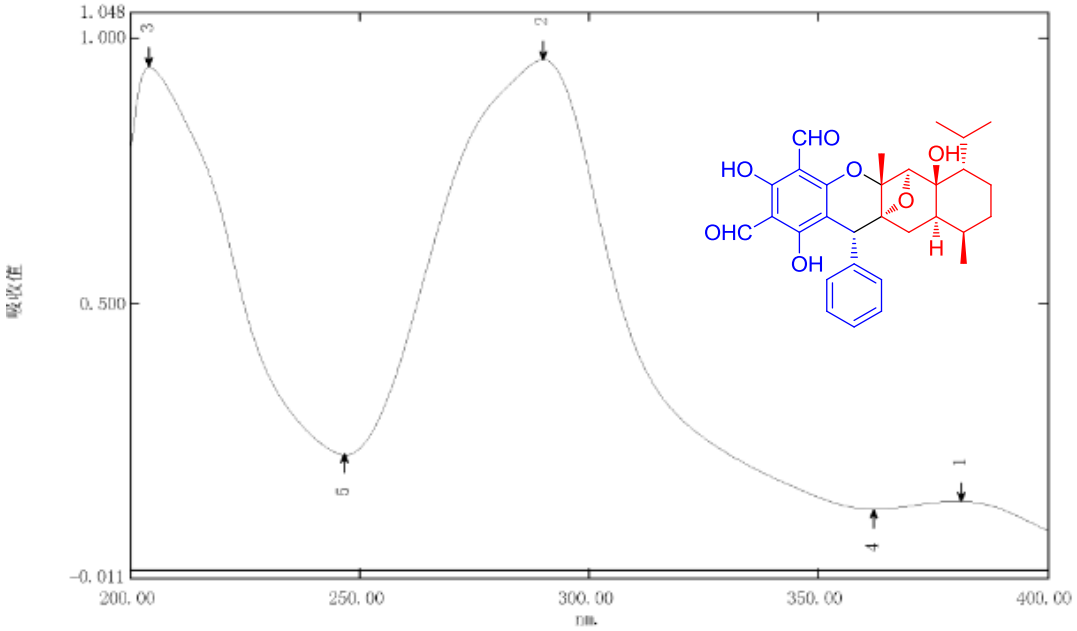

测定属性
波长范围（nm.）：200.00 到 400.00
扫描速度：中速
采样间隔：0.2
自动采样间隔：启用
扫描模式：单个

No.	P/V	波长(nm)	吸收值
1	↑	381.20	0.132
2	↑	290.00	0.959
3	↑	204.20	0.945
4	↓	362.00	0.117
5	↓	246.80	0.218

Figure S5-2. UV spectrum of **5** in MeOH

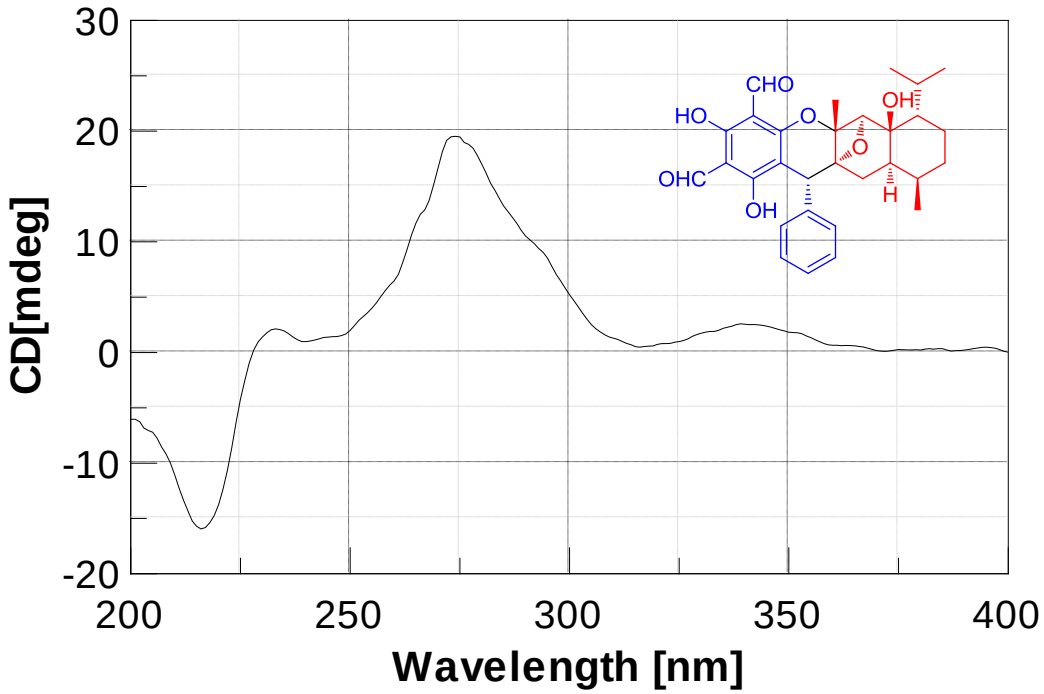

Figure S5-3. CD spectrum of **5** in MeOH

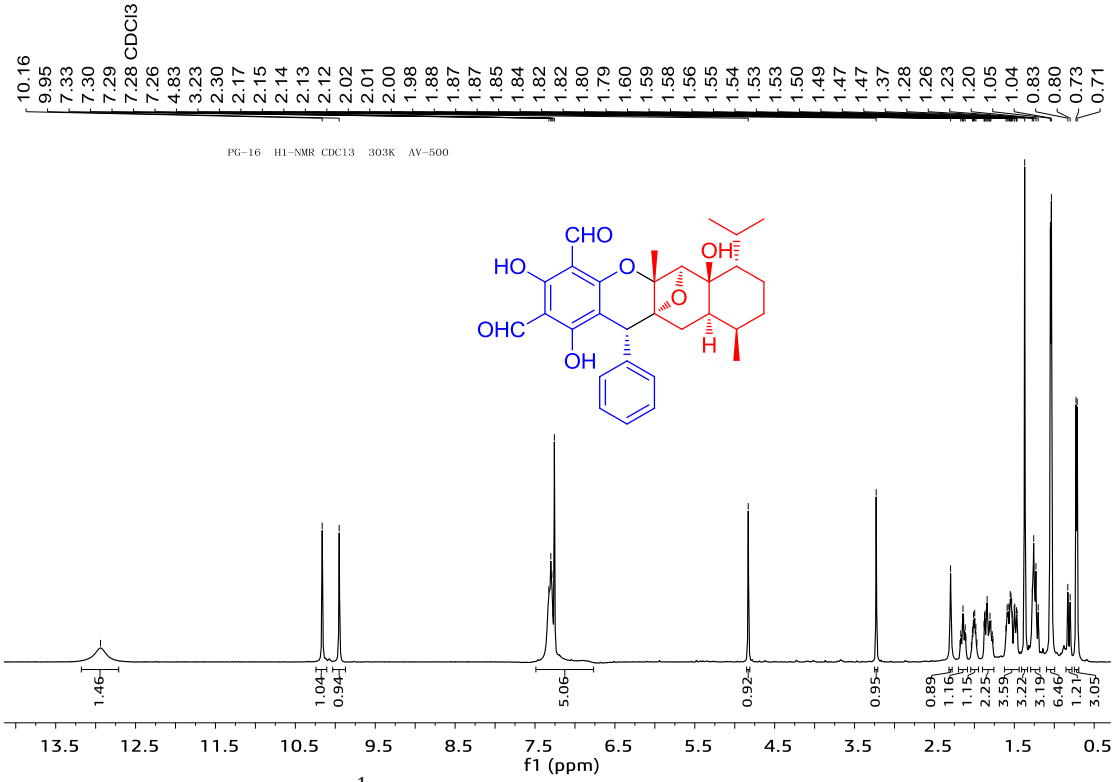

Figure S5-4. ^{1}H NMR spectrum of **5** in $CDCl_3$ (500 MHz)

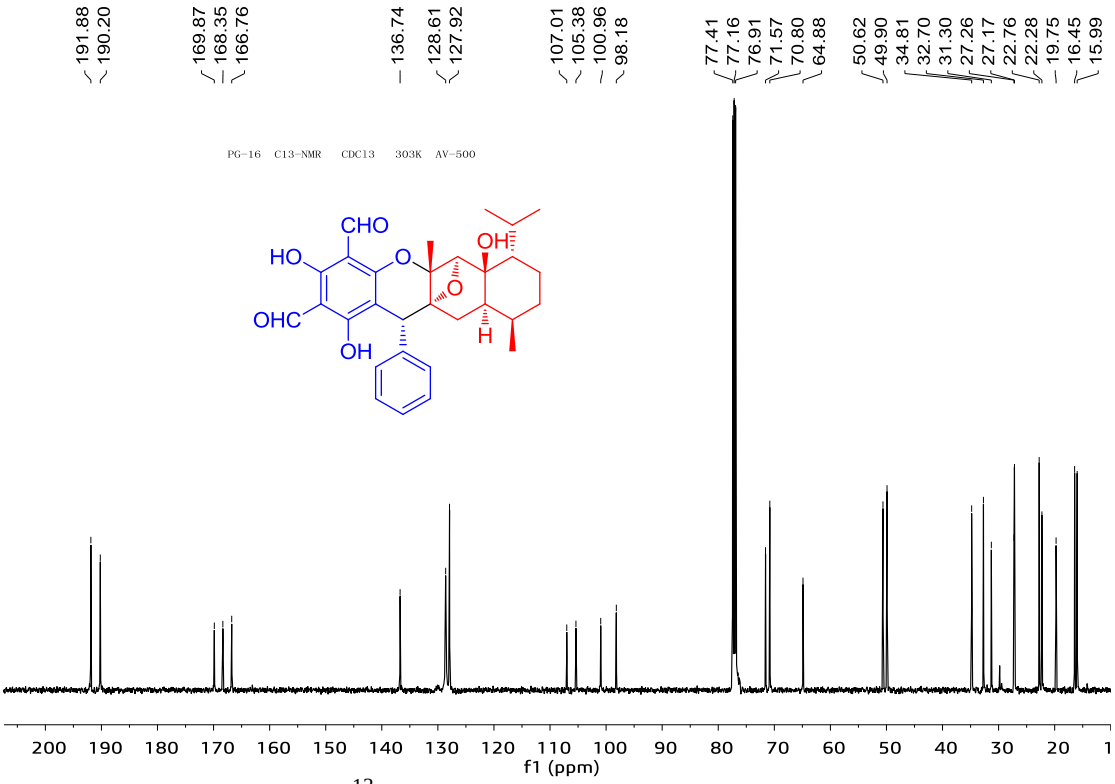

Figure S5-5. ^{13}C NMR spectrum of **5** in $CDCl_3$ (125 MHz)

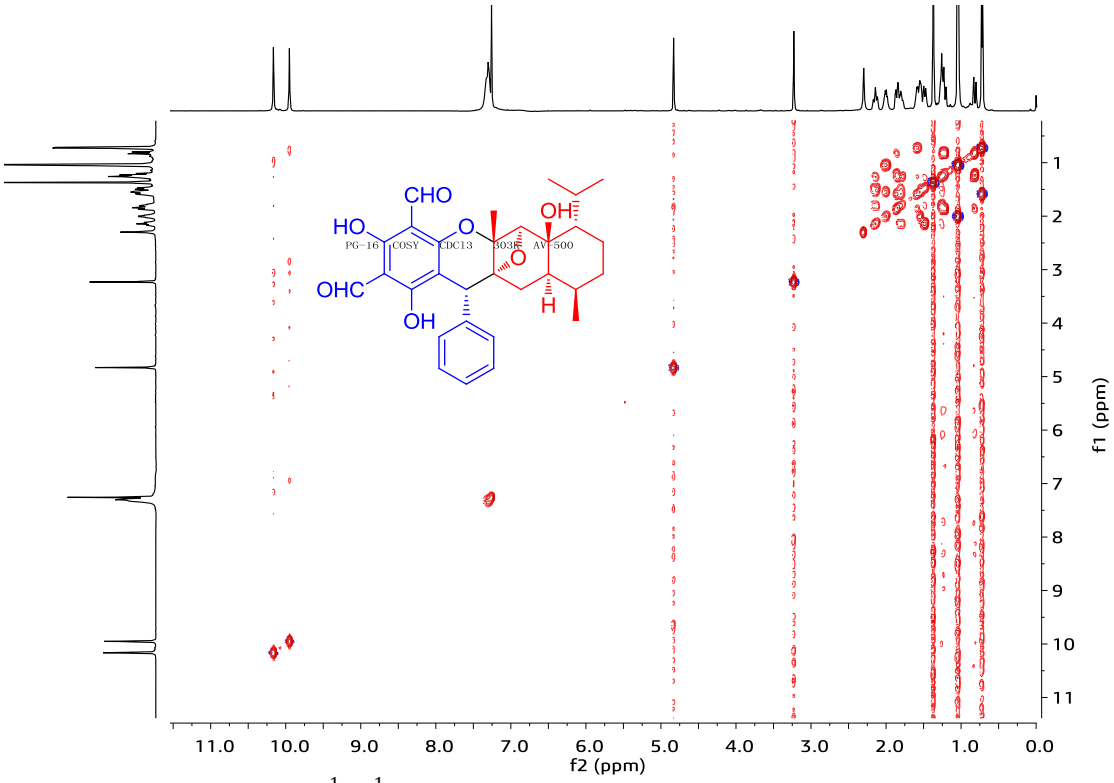

Figure S5-6. ^{1}H-^{1}H COSY spectrum of **5** in $CDCl_3$ (500 MHz)

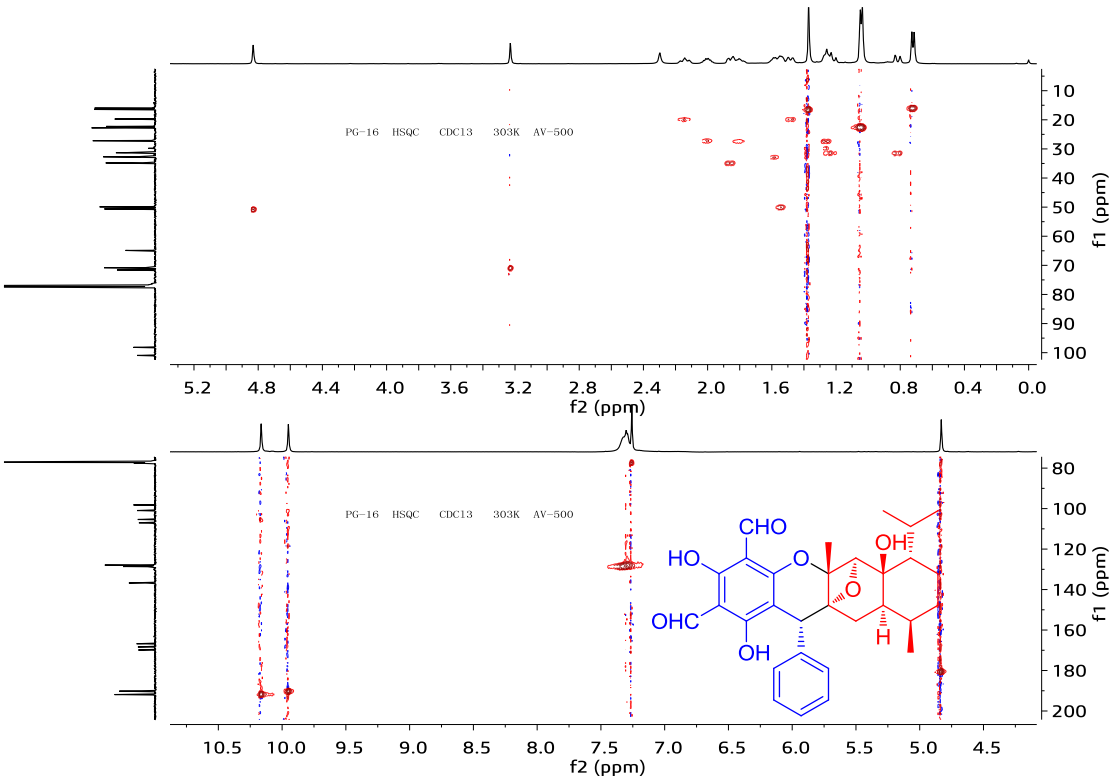

Figure S5-7. HSQC spectrum of **5** in $CDCl_3$ (500 MHz)

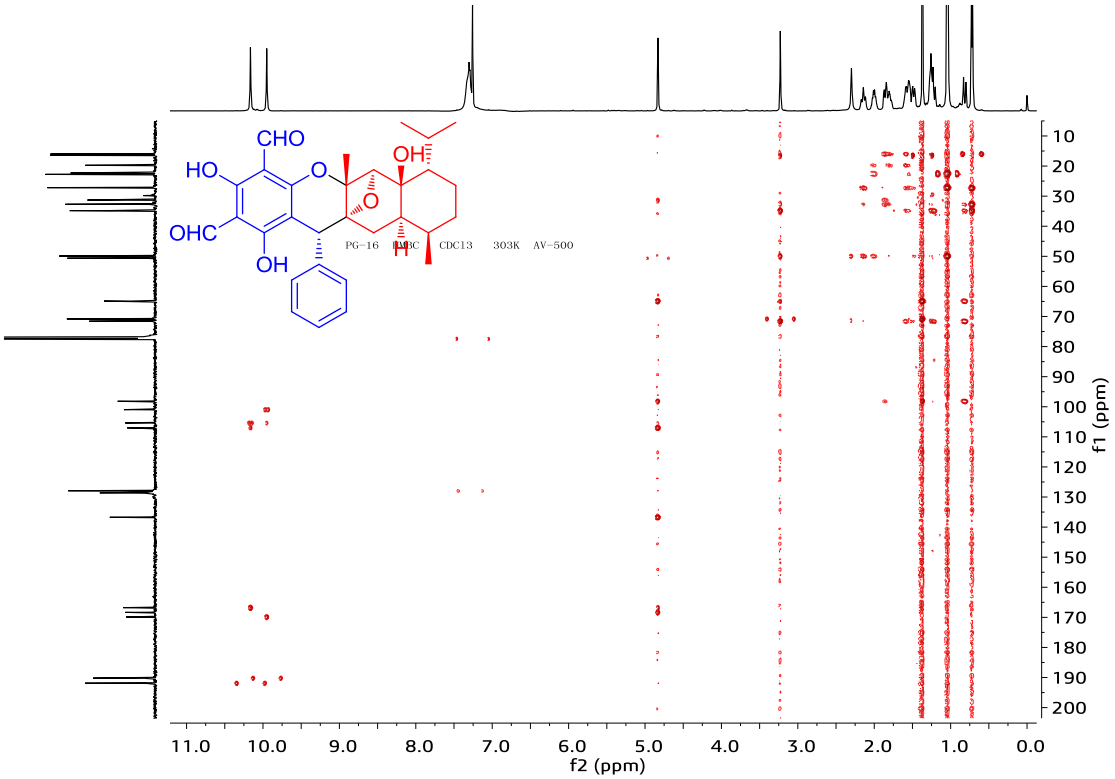

Figure S5-8. HMBC spectrum of **5** in $CDCl_3$ (500 MHz)

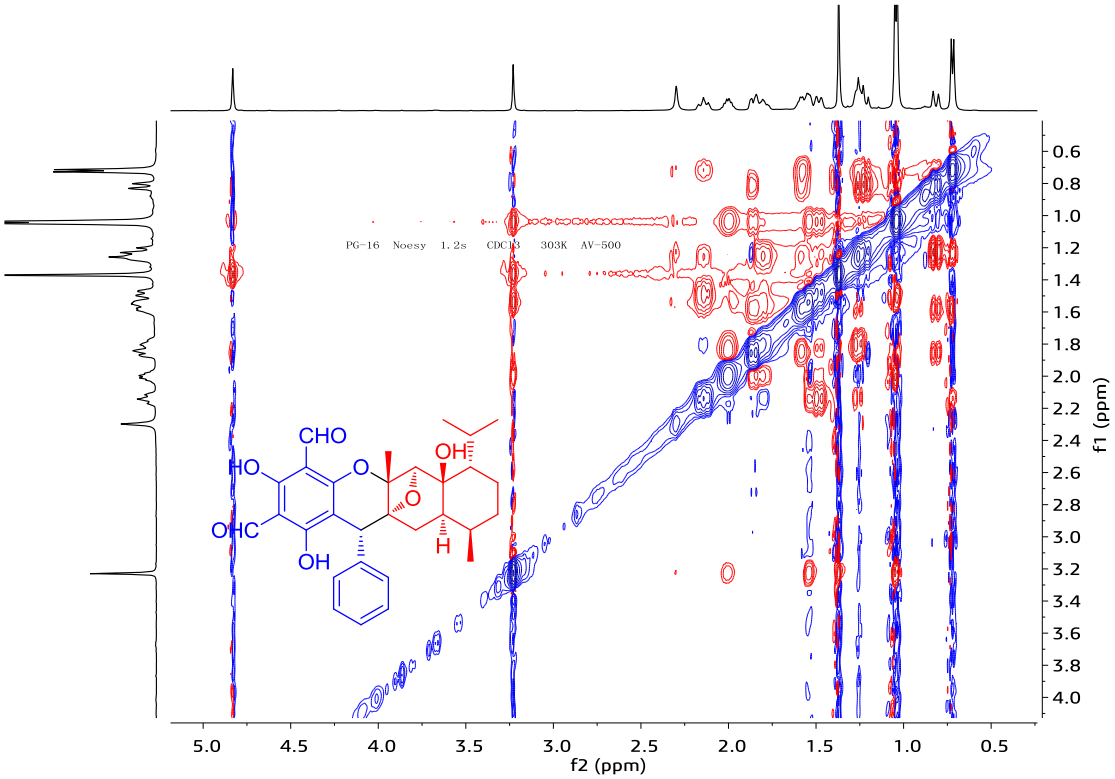

Figure S5-9. NOESY spectrum of **5** in $CDCl_3$ (500 MHz)

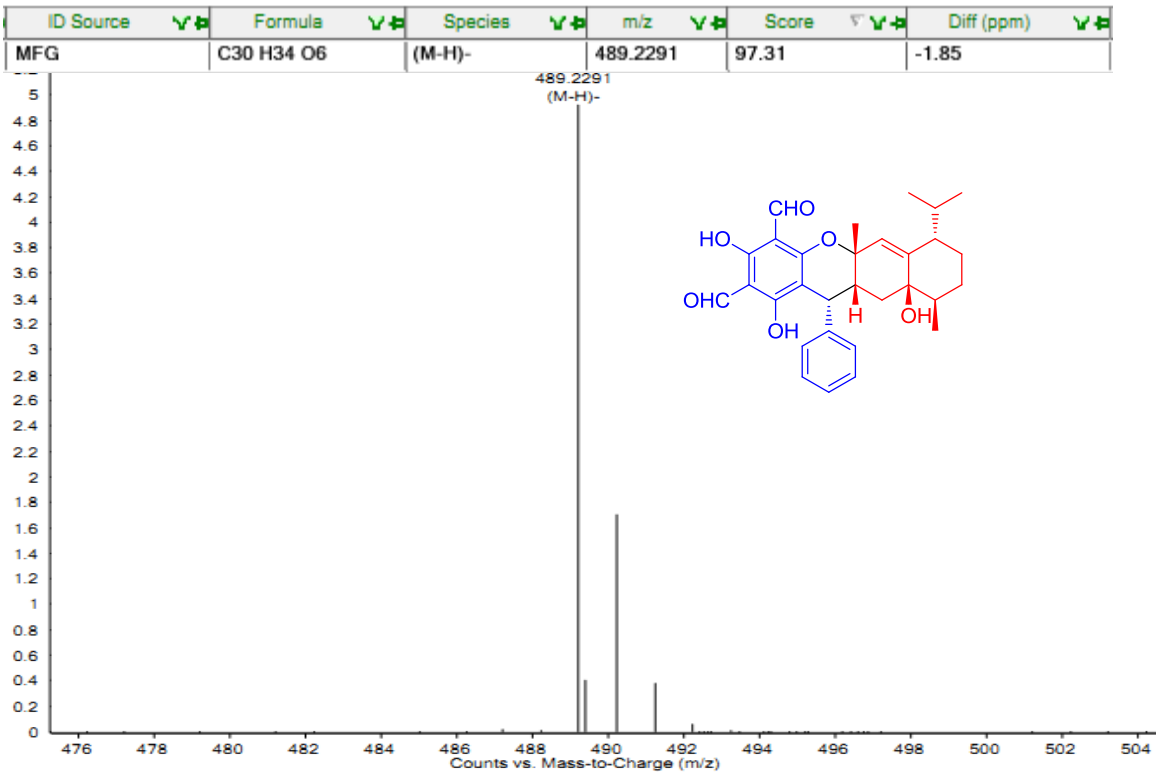

Figure S6-1. HR-ESI-MS spectrum of **6**

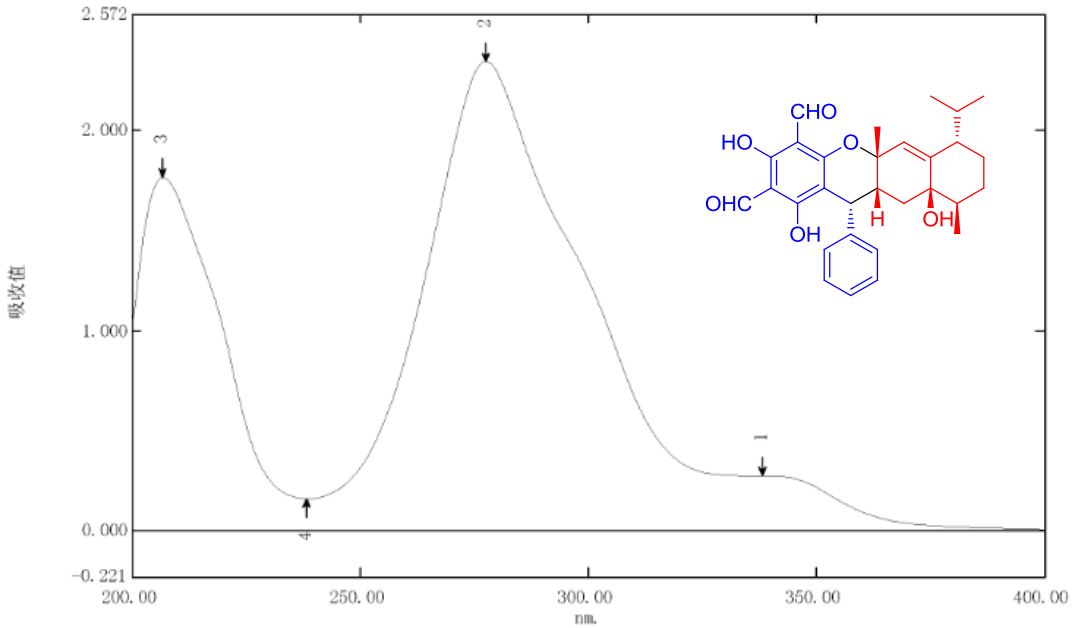

测定属性
波长范围 (nm.): 200.00 到 400.00
扫描速度: 中速
采样间隔: 0.2
自动采样间隔: 启用
扫描模式: 单个

No.	P/V	波长(nm)	吸收值
1	↑	338.20	0.278
2	↑	277.40	2.339
3	↑	206.80	1.762
4	↓	238.20	0.164

Figure S6-2. UV spectrum of **6** in MeOH

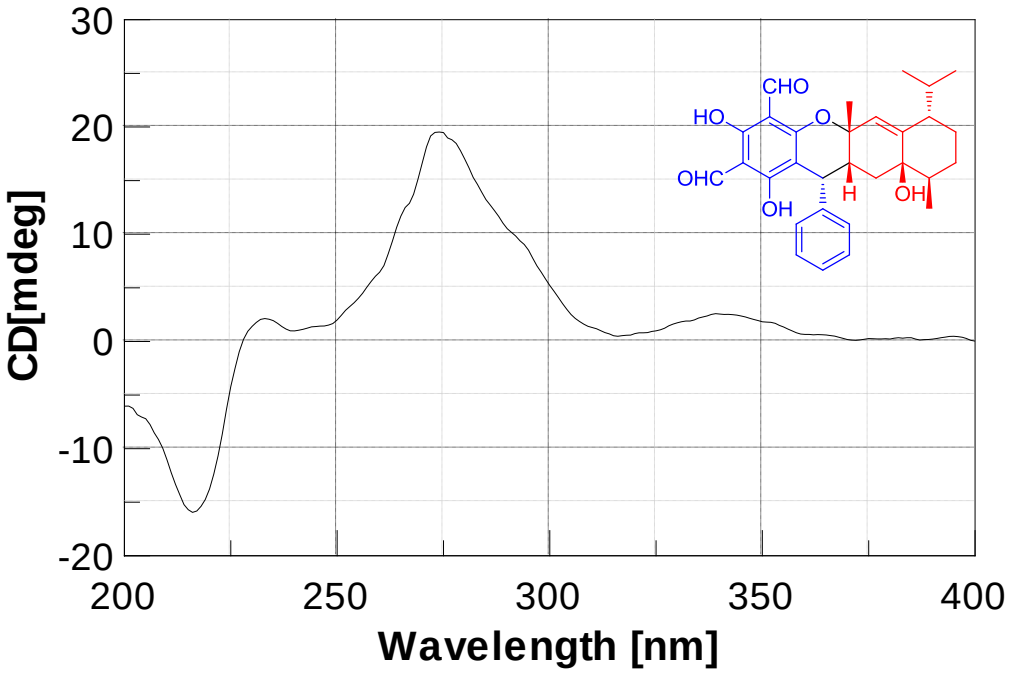

Figure S6-3. CD spectrum of **6** in MeOH

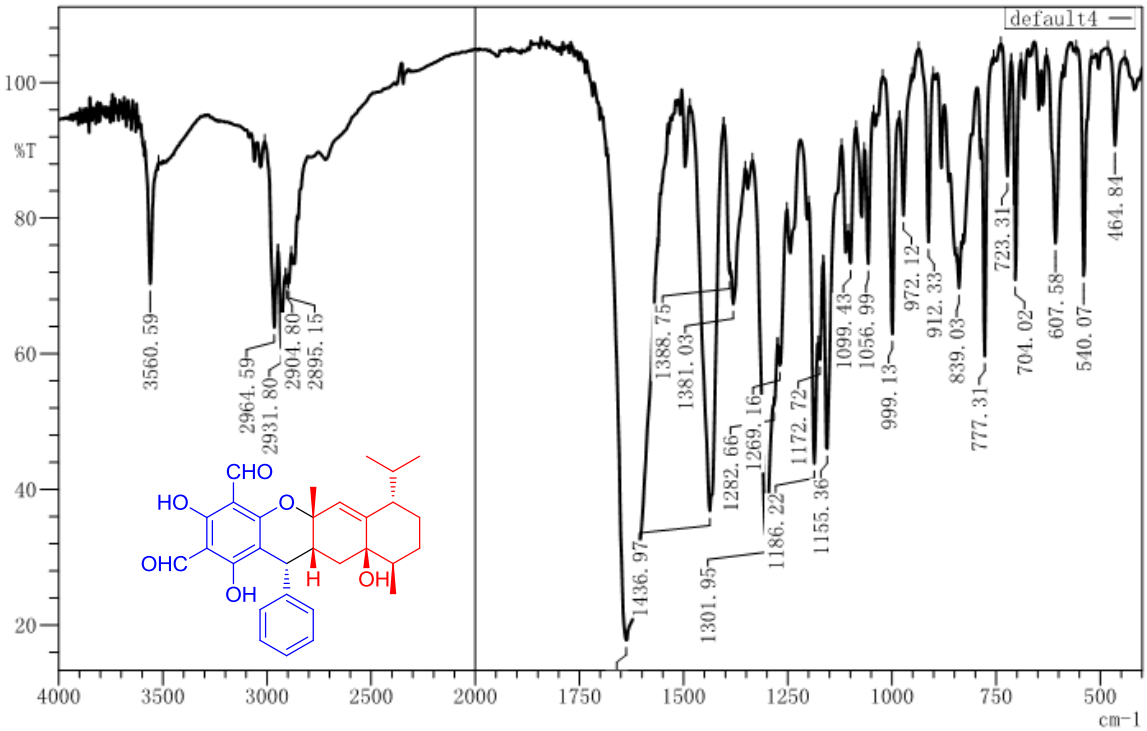

Figure S6-4. IR spectrum of **6**

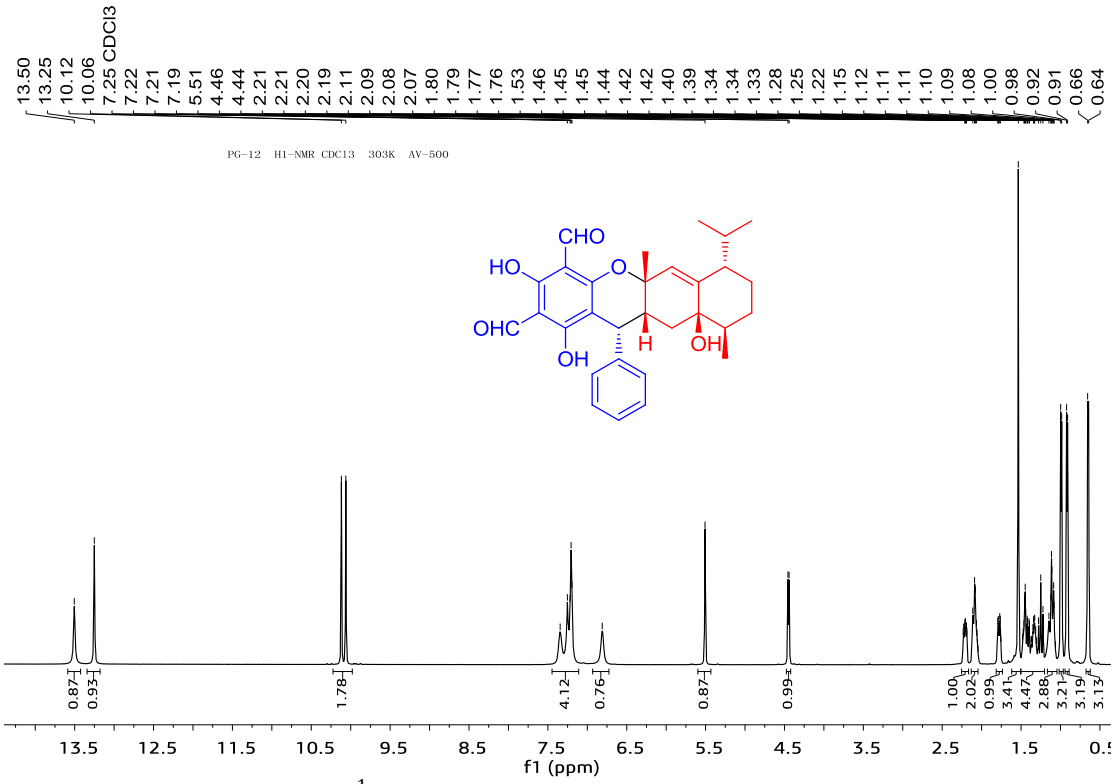

Figure S6-5. ^{1}H NMR spectrum of **6** in $CDCl_3$ (500 MHz)

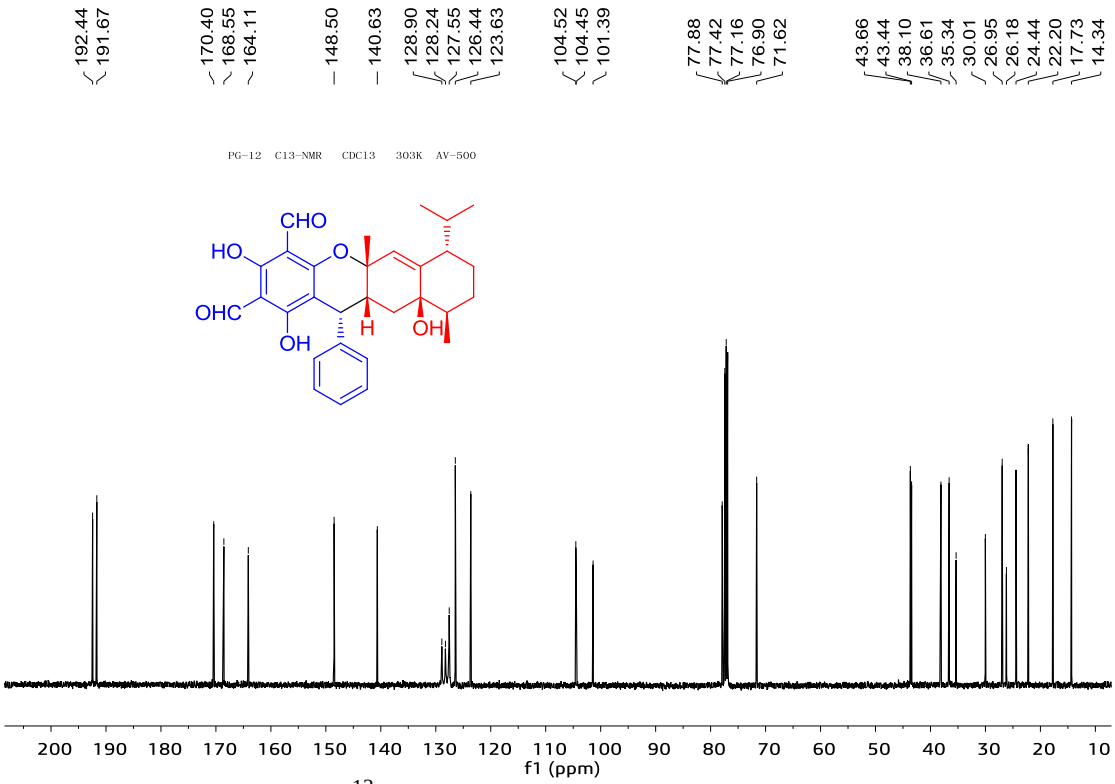

Figure S6-6. ^{13}C NMR spectrum of **6** in $CDCl_3$ (125 MHz)

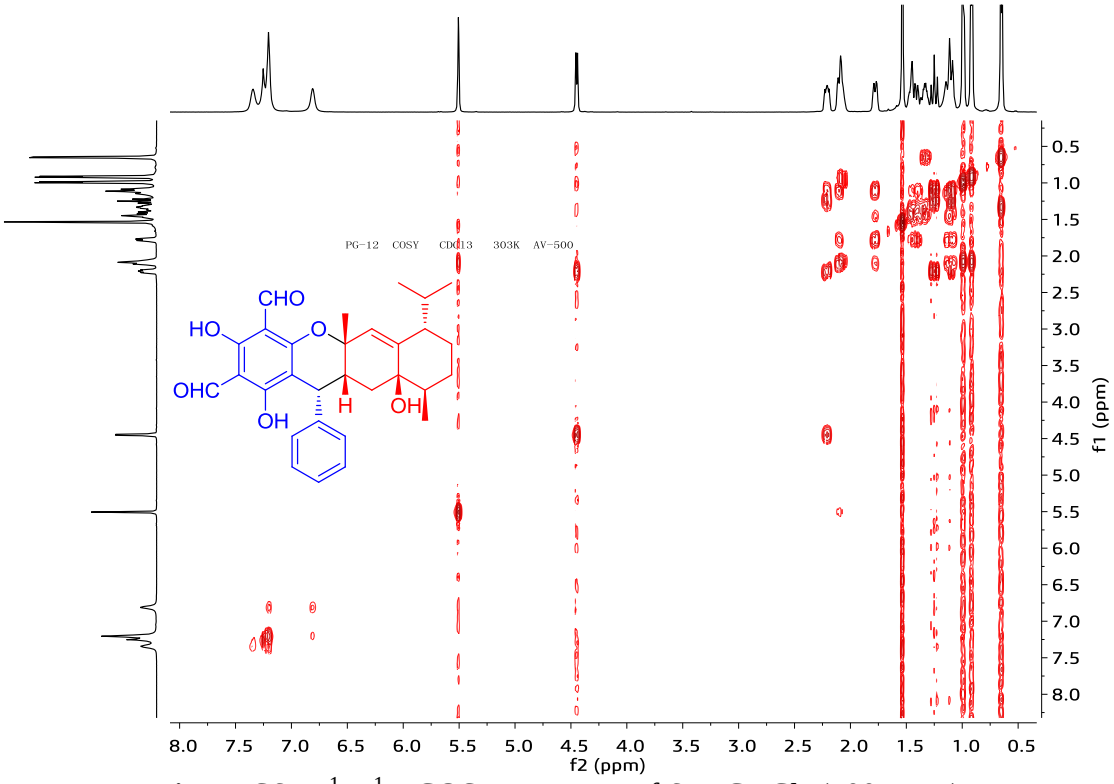

Figure S6-7. ^{1}H-^{1}H COSY spectrum of **6** in $CDCl_3$ (500 MHz)

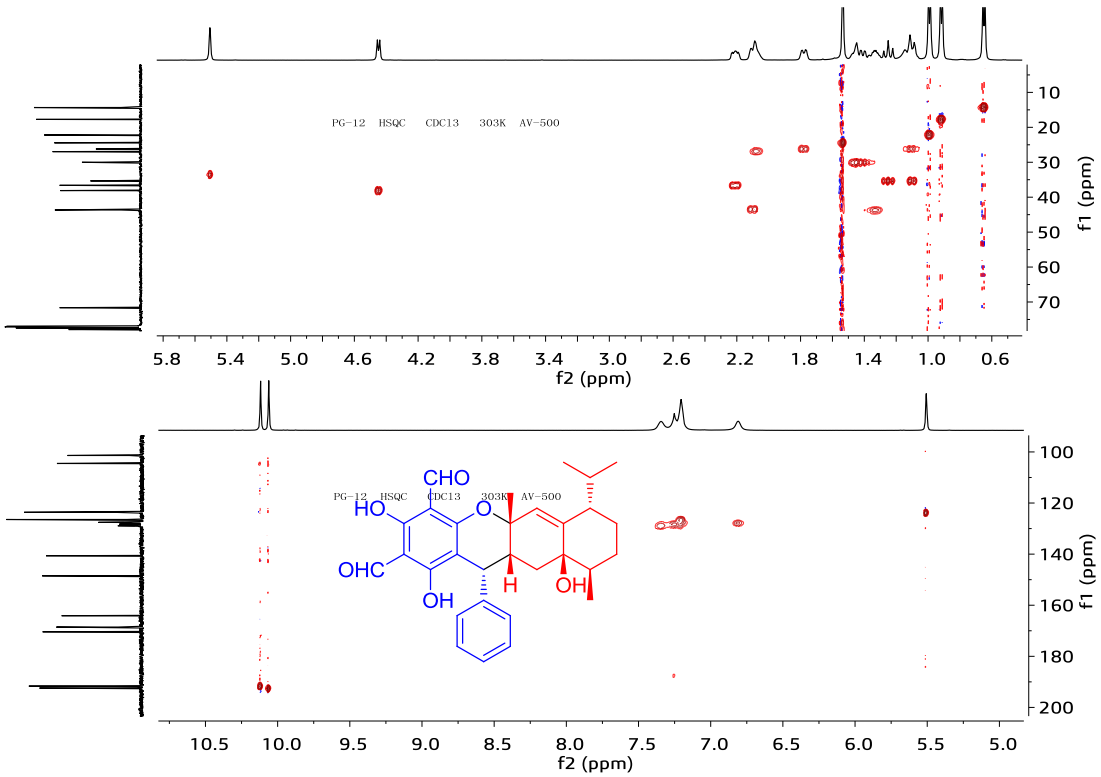

Figure S6-8. HSQC spectrum of **6** in $CDCl_3$ (500 MHz)

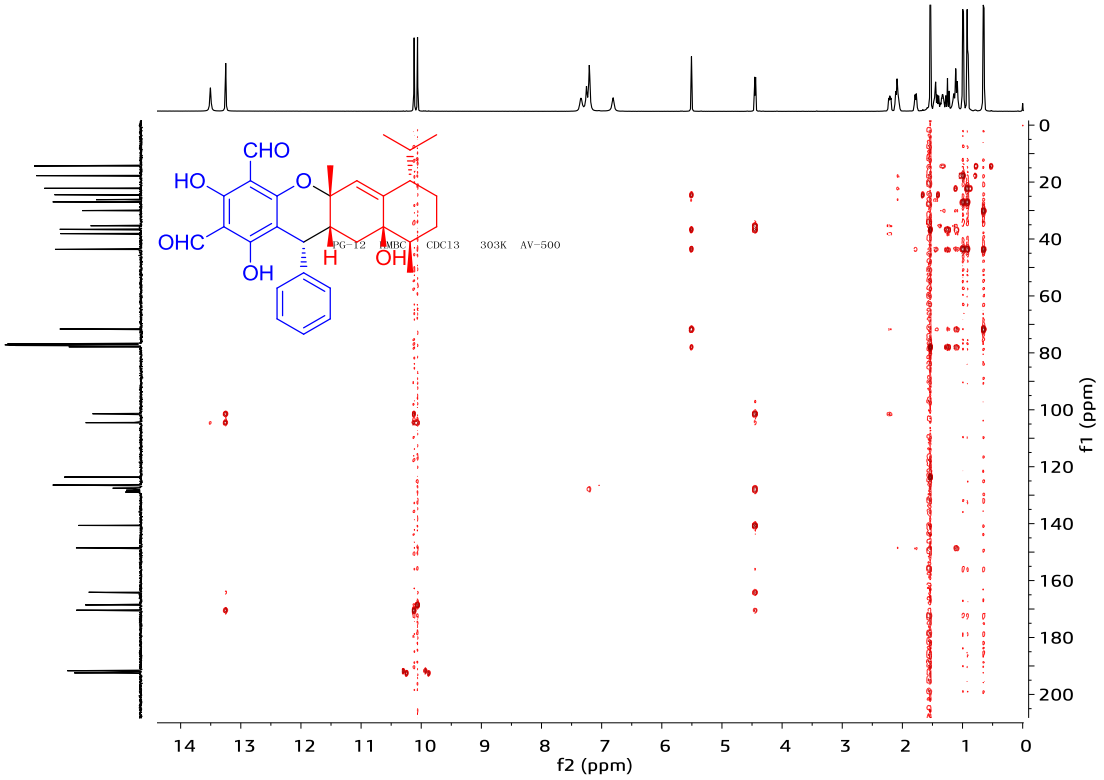

Figure S6-9. HMBC spectrum of **6** in $CDCl_3$ (500 MHz)

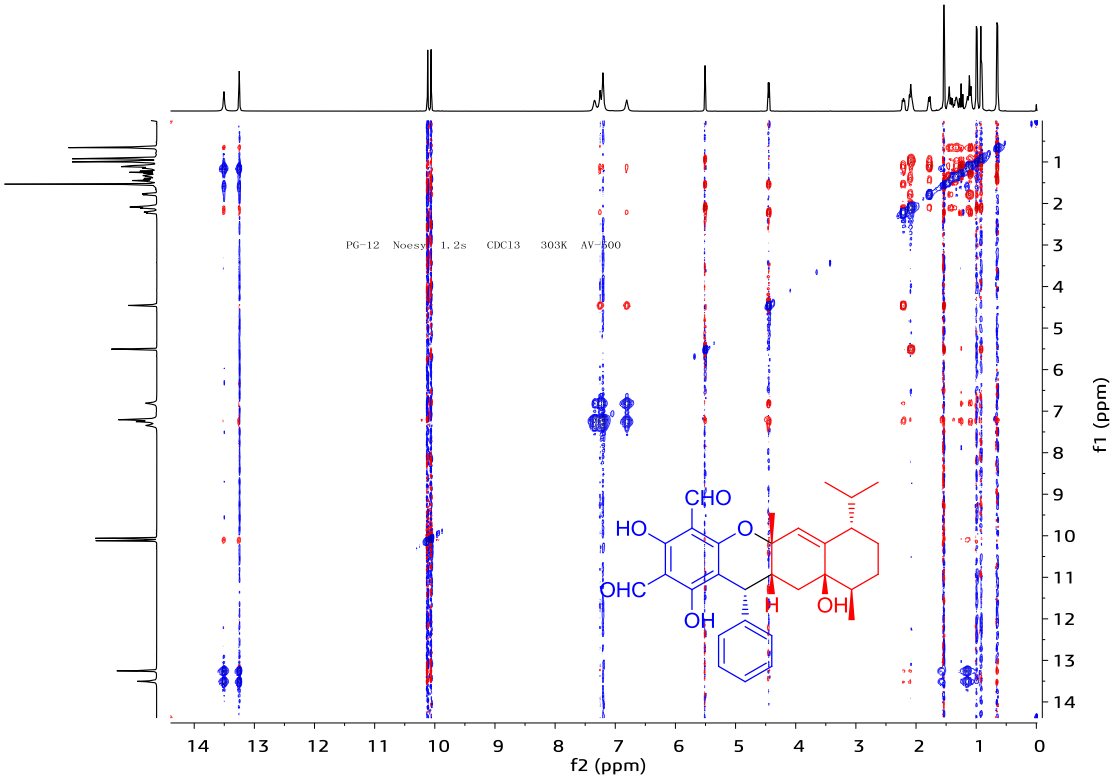

Figure S6-10. NOESY spectrum of **6** in $CDCl_3$ (500 MHz)

ID Source	Formula	Species	m/z	Score	Diff (ppm)
MFG	C30 H34 O6	(M-H)-	489.2273	87.15	1.15

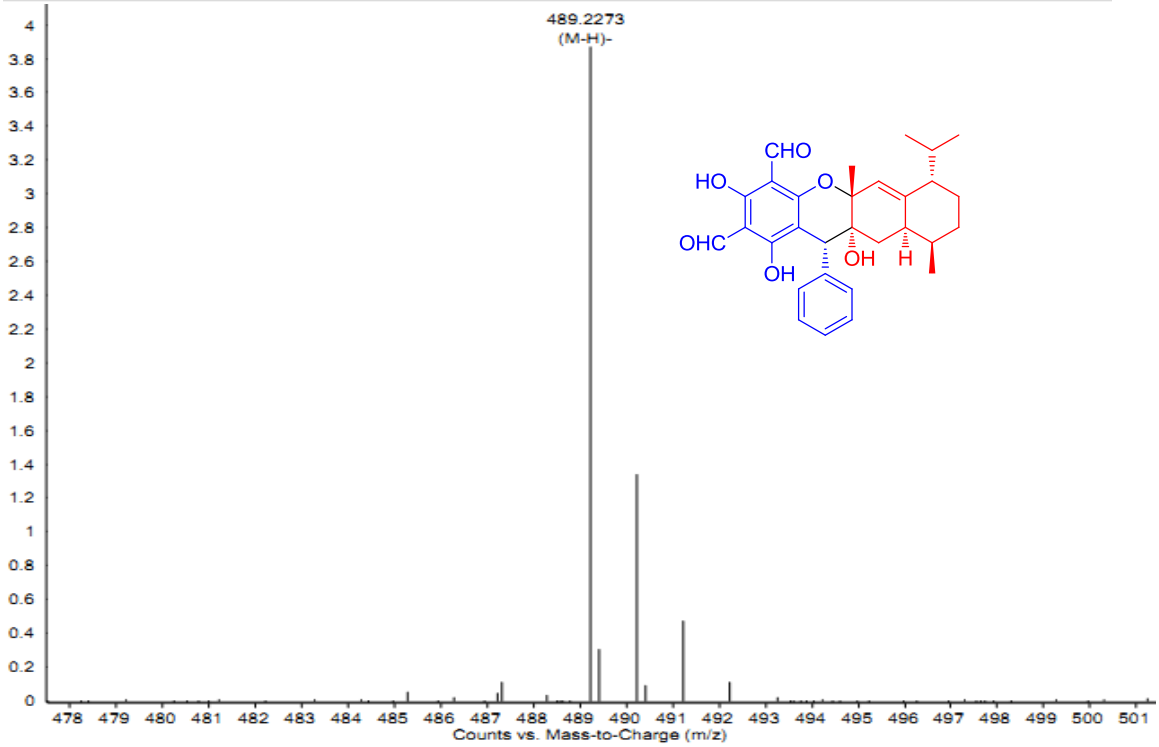

Figure S7-1. HR-ESI-MS spectrum of **7**

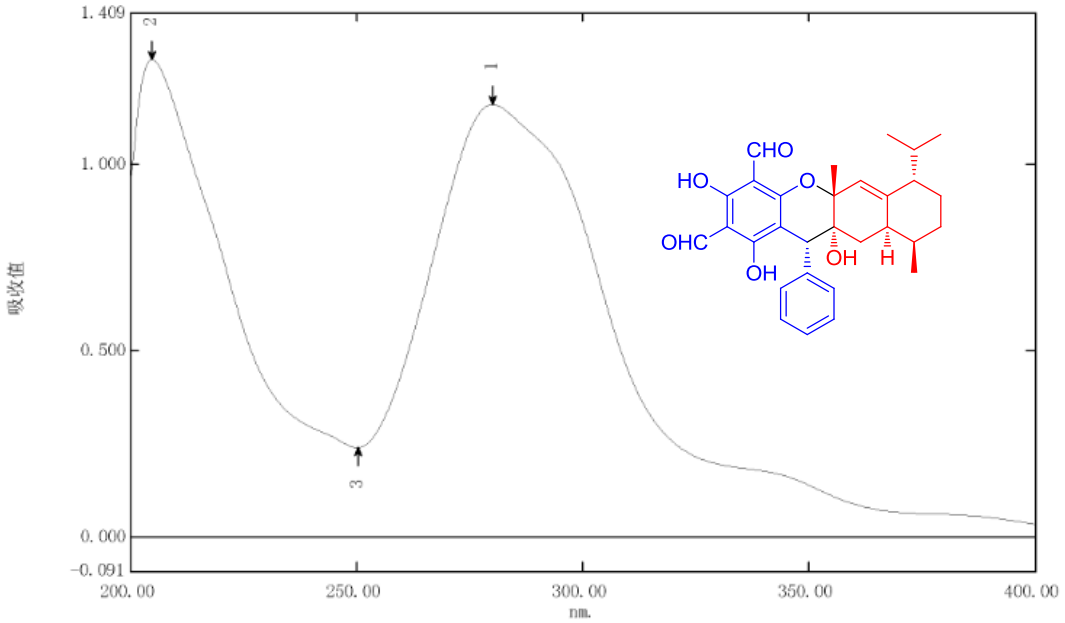

测定属性
波长范围 (nm.): 200.00 到 400.00
扫描速度: 中速
采样间隔: 0.2
自动采样间隔: 启用

No.	P/V	波长(nm)	吸收值
1	↑	280.00	1.163
2	↑	204.80	1.284
3	↓	250.20	0.239

Figure S7-2. UV spectrum of **7** in MeOH

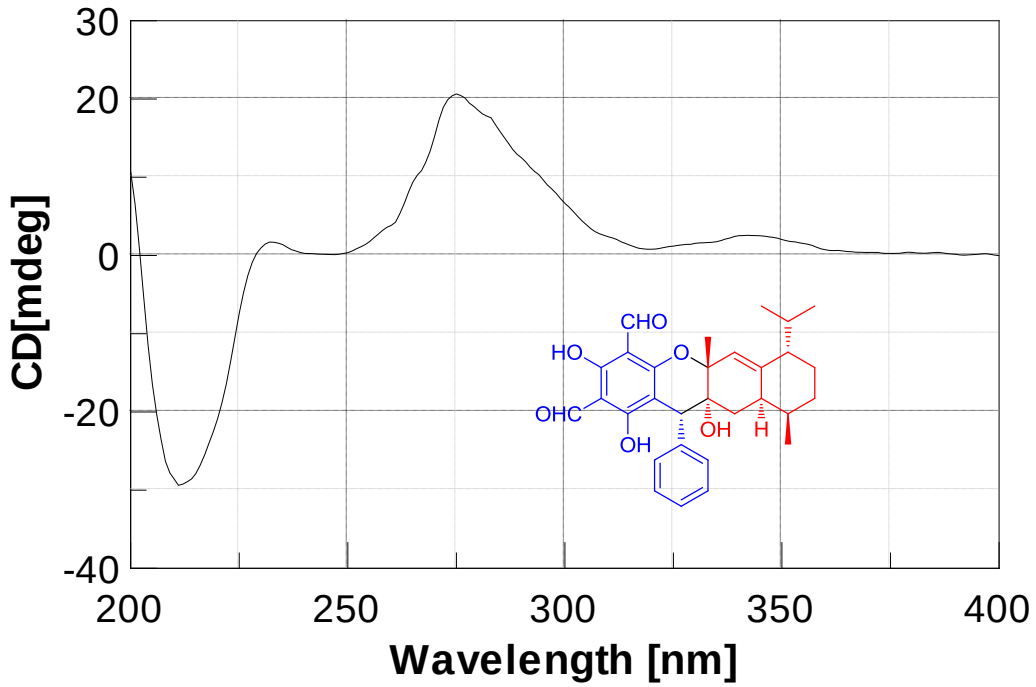

Figure S7-3. CD spectrum of **7** in MeOH

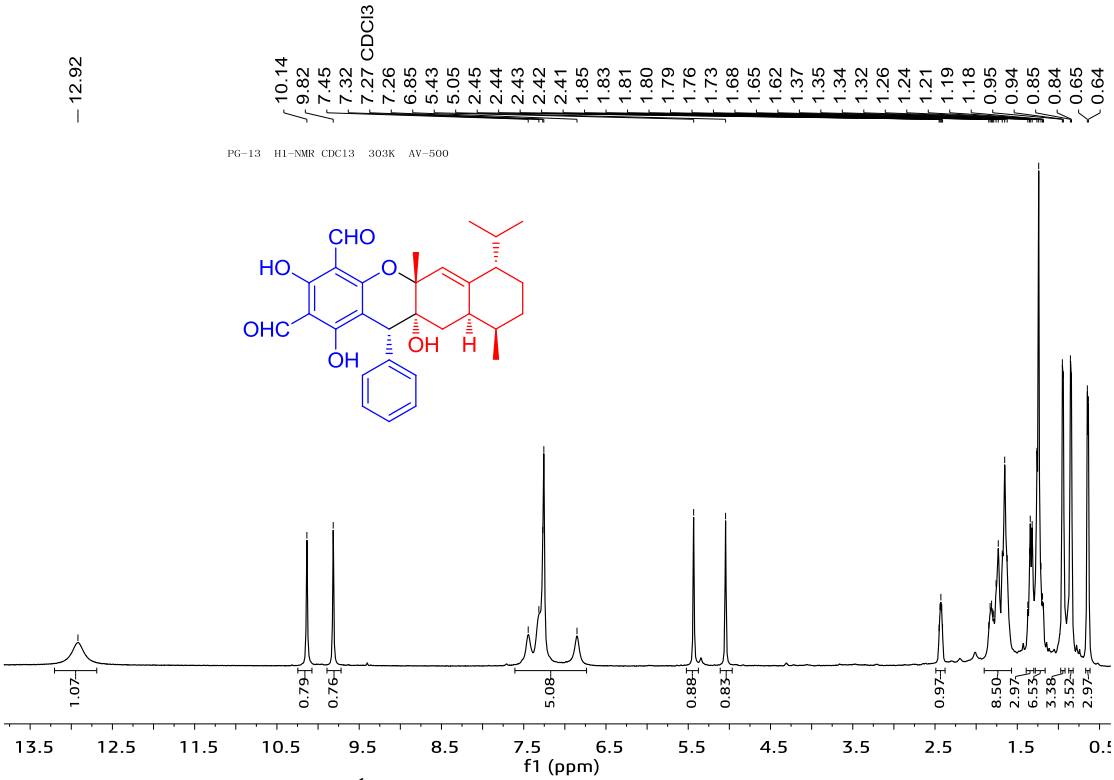

Figure S7-4. ^{1}H NMR spectrum of **7** in $CDCl_3$ (500 MHz)

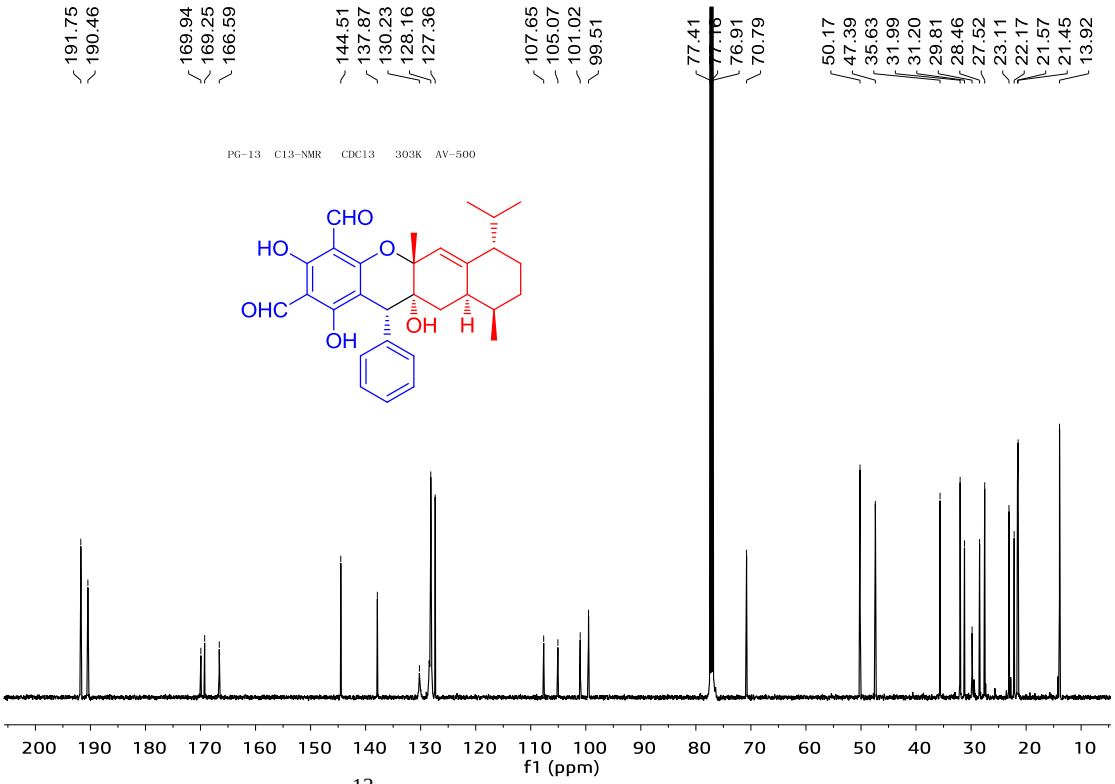

Figure S7-5. ^{13}C NMR spectrum of **7** in $CDCl_3$ (125 MHz)

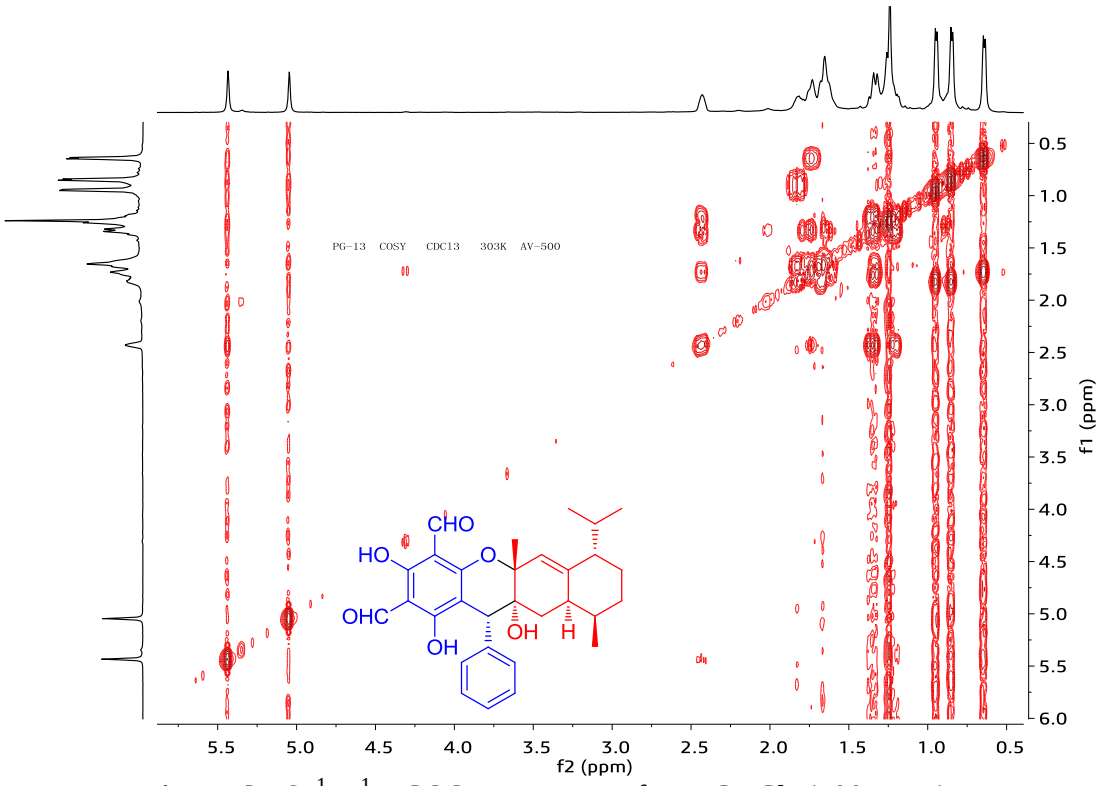

Figure S7-6. ^{1}H-^{1}H COSY spectrum of **7** in $CDCl_3$ (500 MHz)

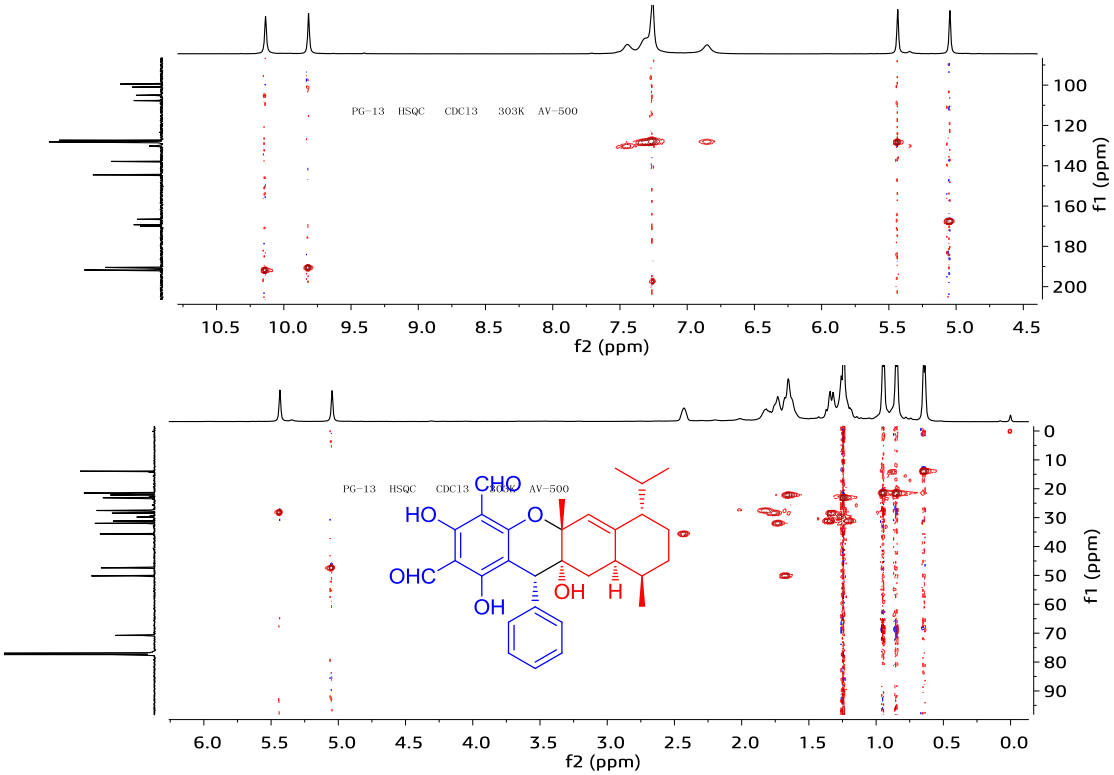

Figure S7-7. HSQC spectrum of **7** in $CDCl_3$ (500 MHz)

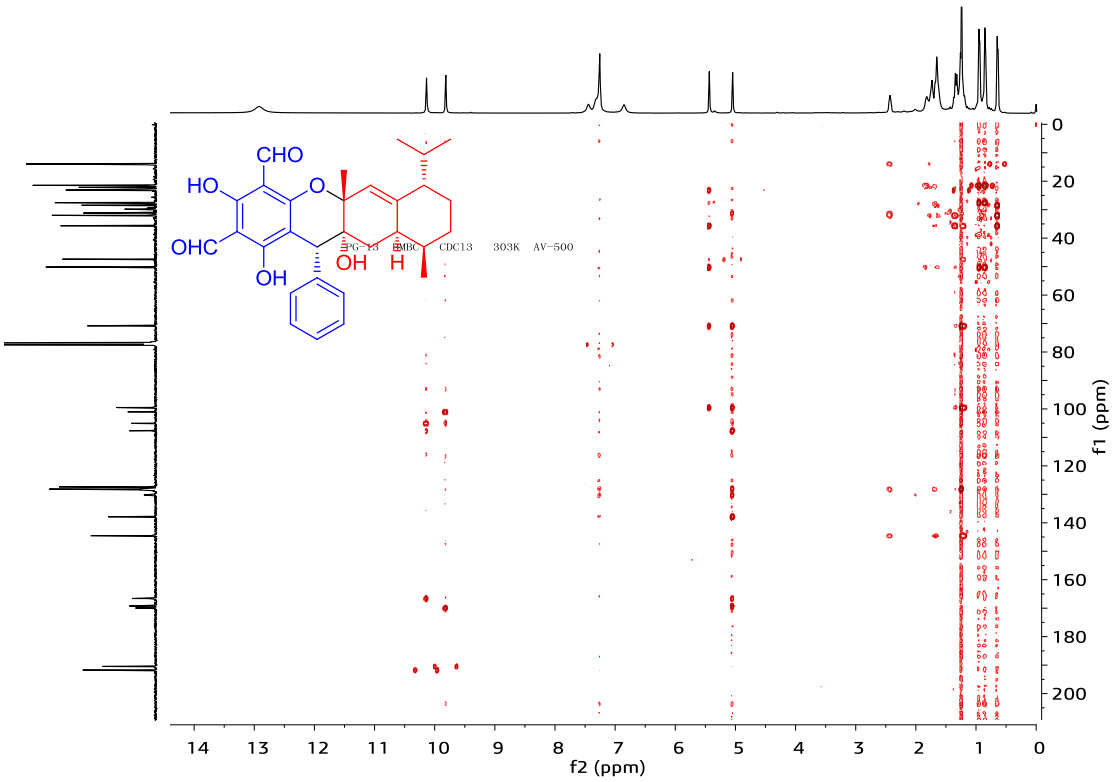

Figure S7-8. HMBC spectrum of **7** in $CDCl_3$ (500 MHz)

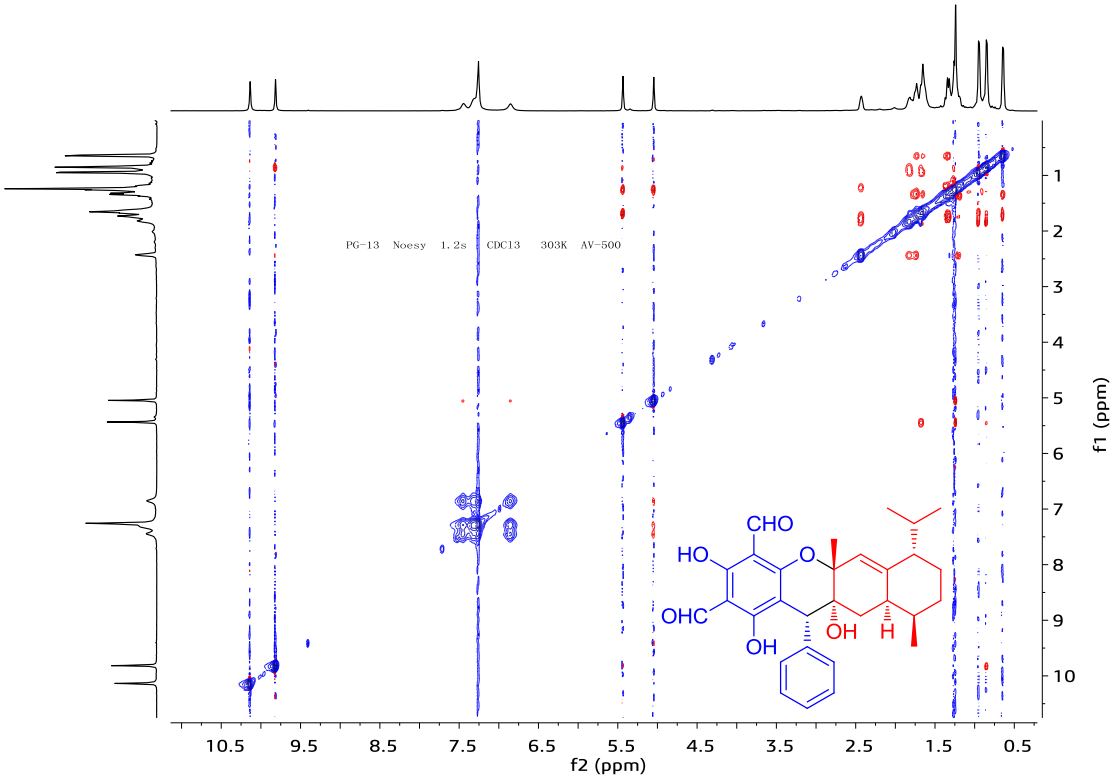

Figure S7-9. NOESY spectrum of **7** in $CDCl_3$ (500 MHz)

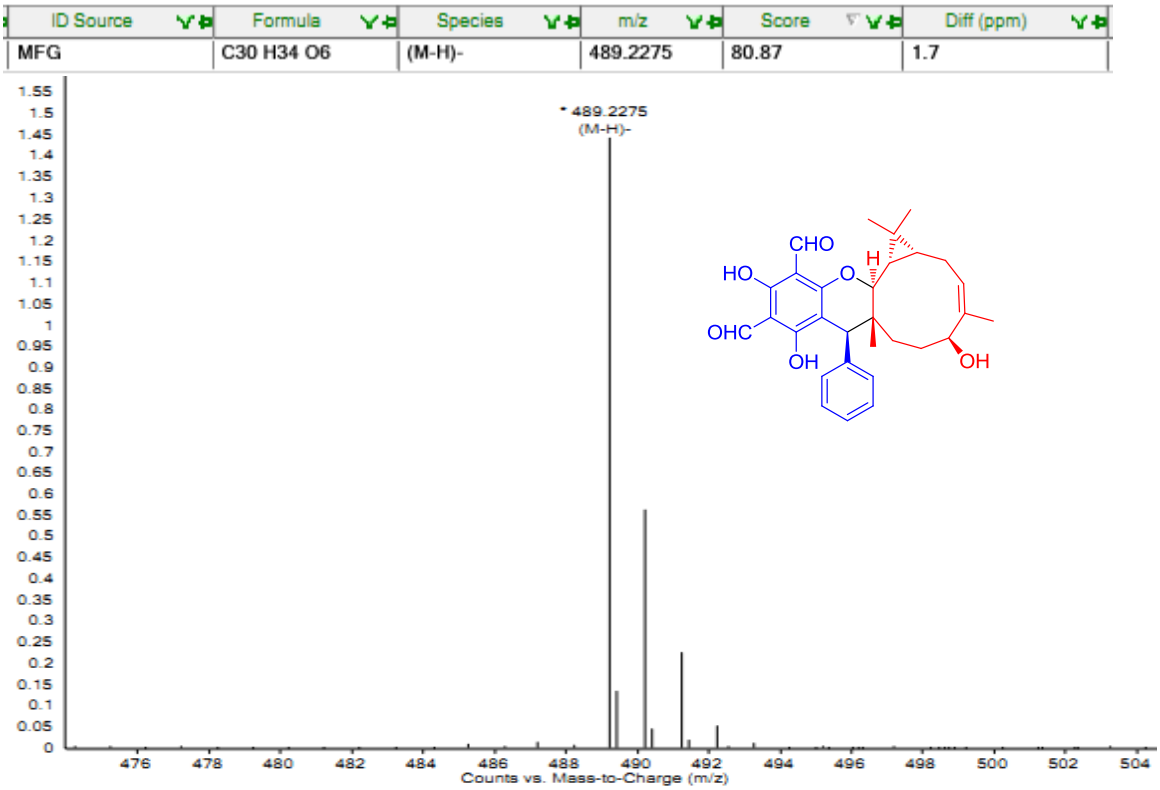

Figure S8-1. HR-ESI-MS spectrum of **8**

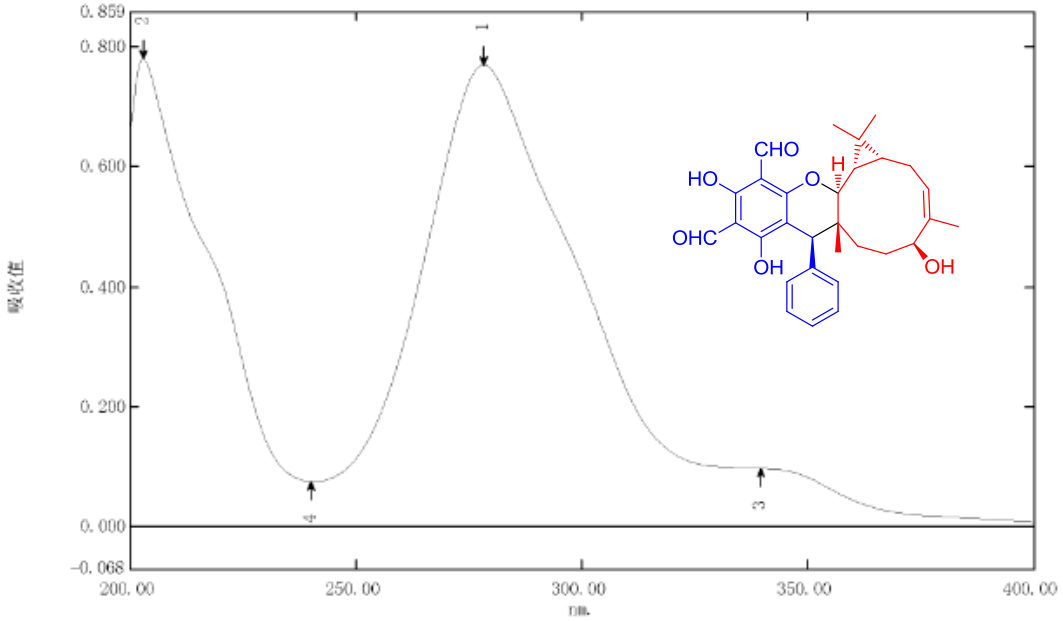

测定属性
波长范围 (nm.): 200.00 到 400.00
扫描速度: 中速
采样间隔: 0.2
自动采样间隔: 启用
扫描模式: 单个

No.	P/V	波长(nm)	吸收值
1	↑	278.20	0.771
2	↑	202.80	0.781
3	↓	339.60	0.098
4	↓	240.20	0.076

Figure S8-2. UV spectrum of **8** in MeOH

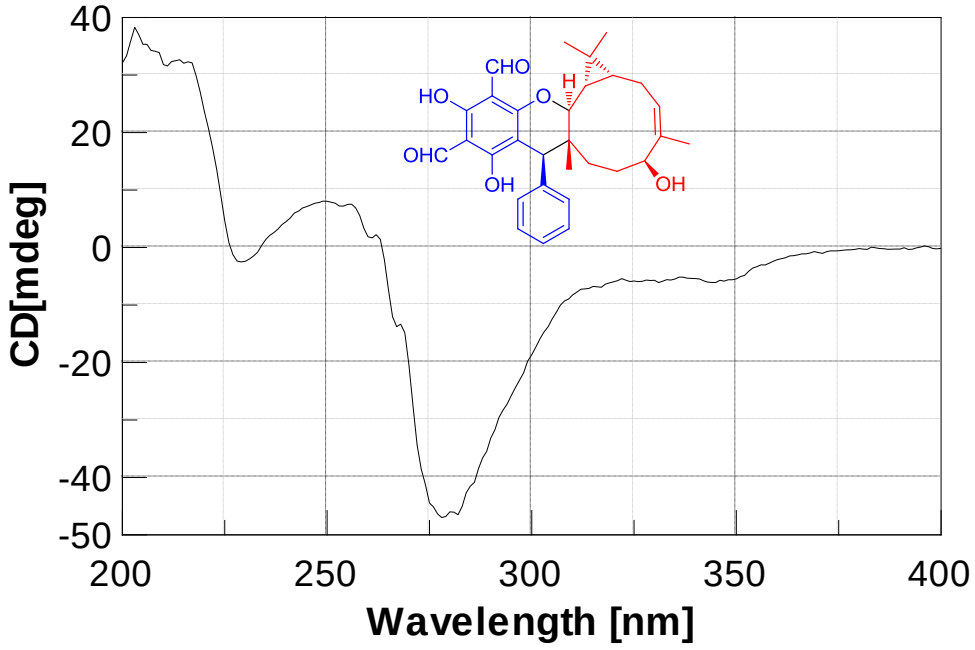

Figure S8-3. CD spectrum of **8** in MeOH

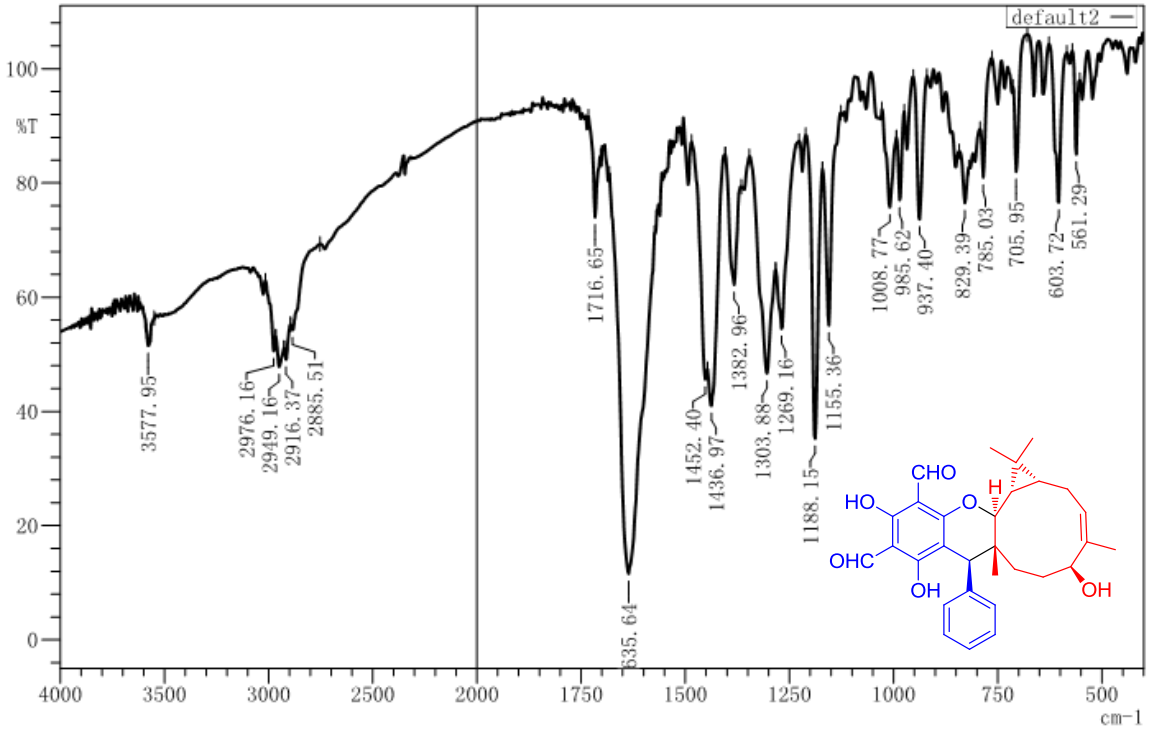

Figure S8-4. IR spectrum of **8**

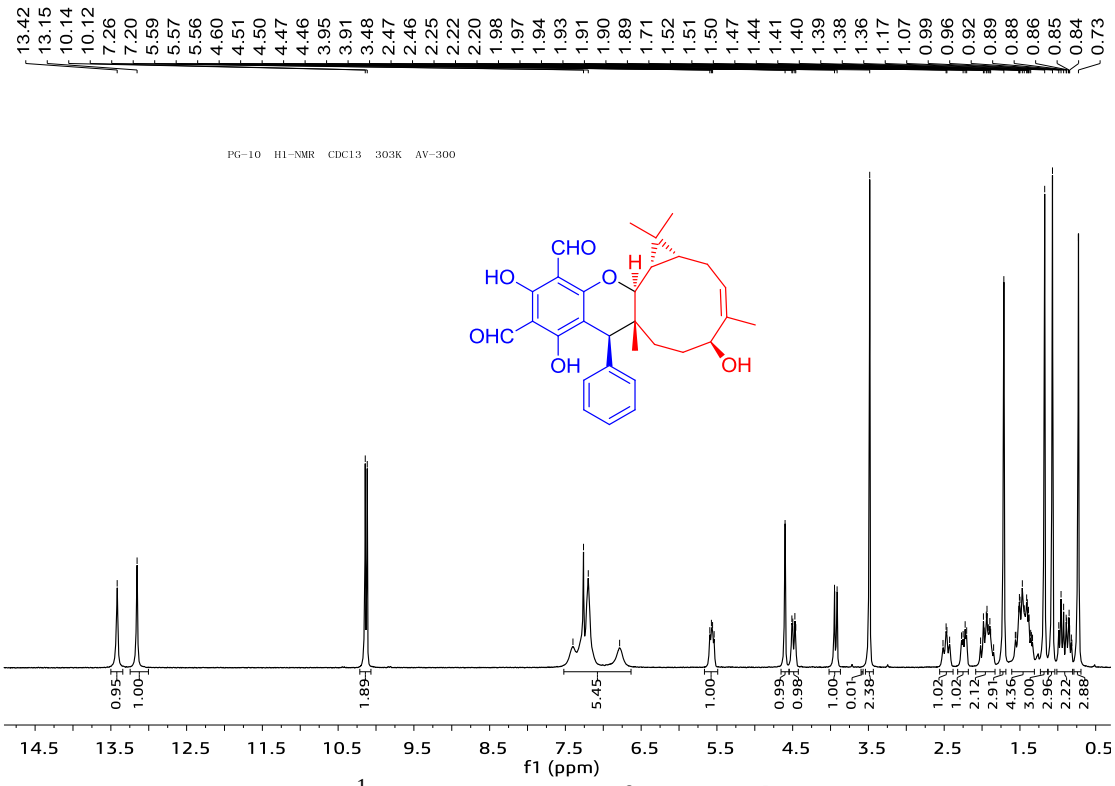

Figure S8-5. ^{1}H NMR spectrum of **8** in $CDCl_3$ (500 MHz)

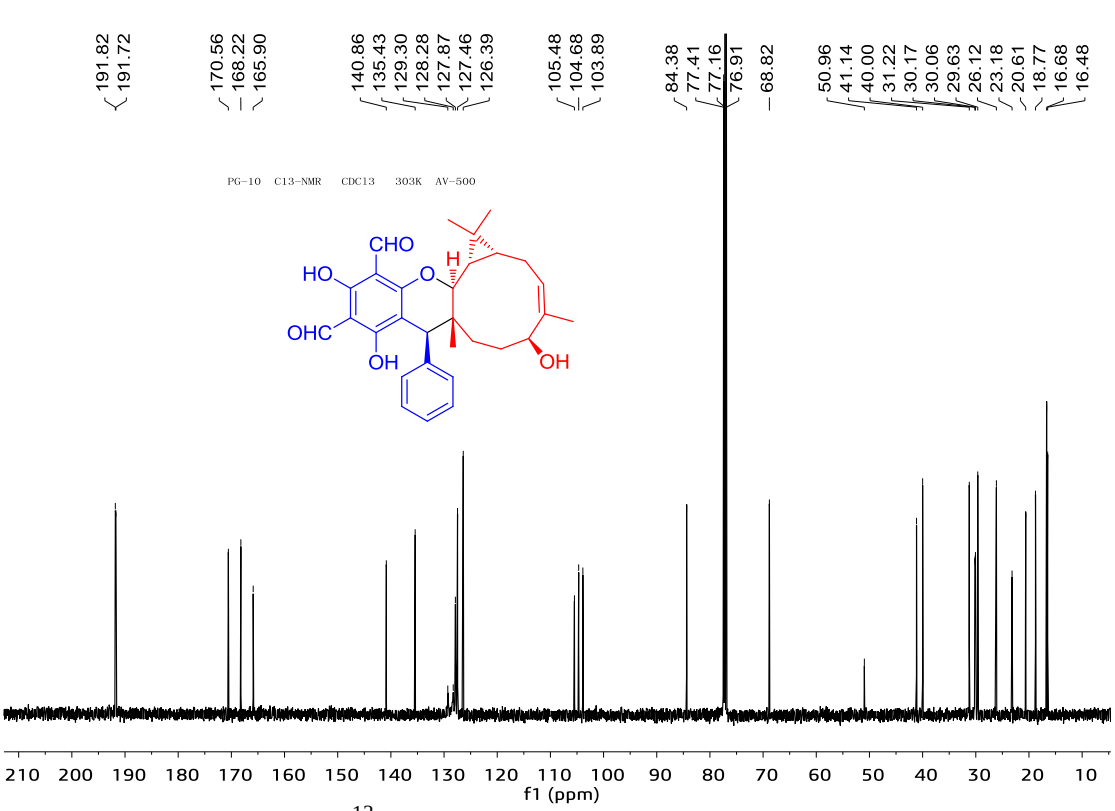

Figure S8-6. ^{13}C NMR spectrum of **8** in $CDCl_3$ (125 MHz)

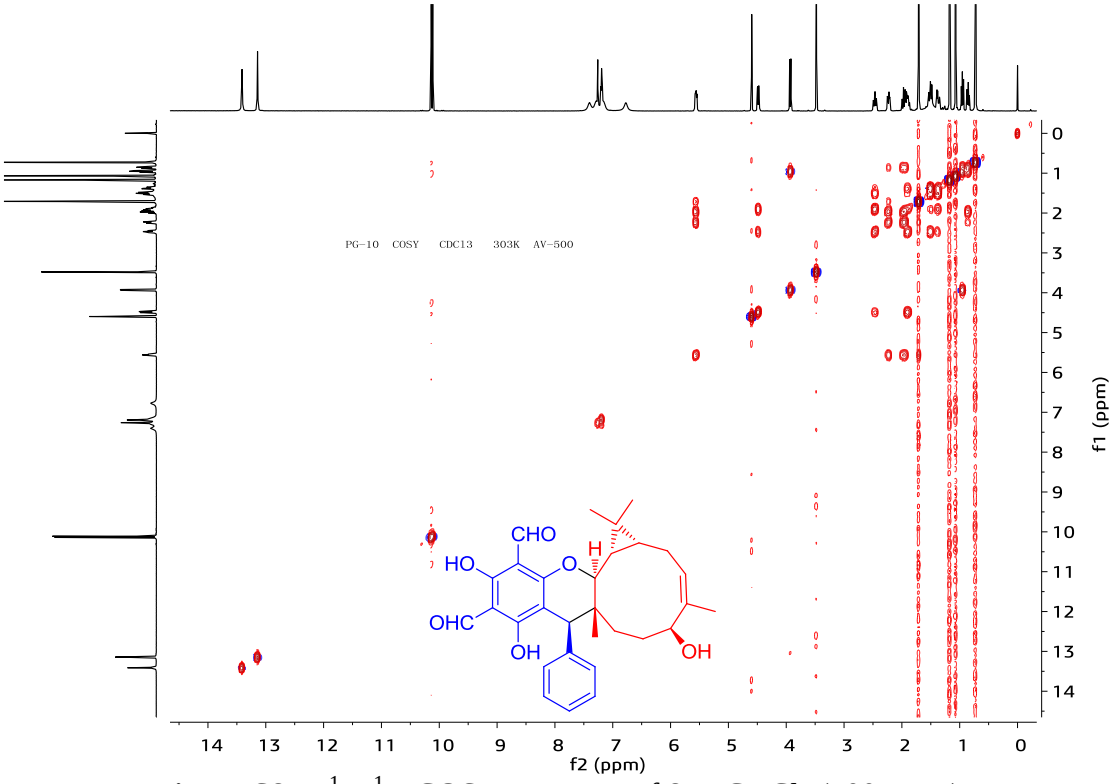

Figure S8-7. ^{1}H-^{1}H COSY spectrum of **8** in $CDCl_3$ (500 MHz)

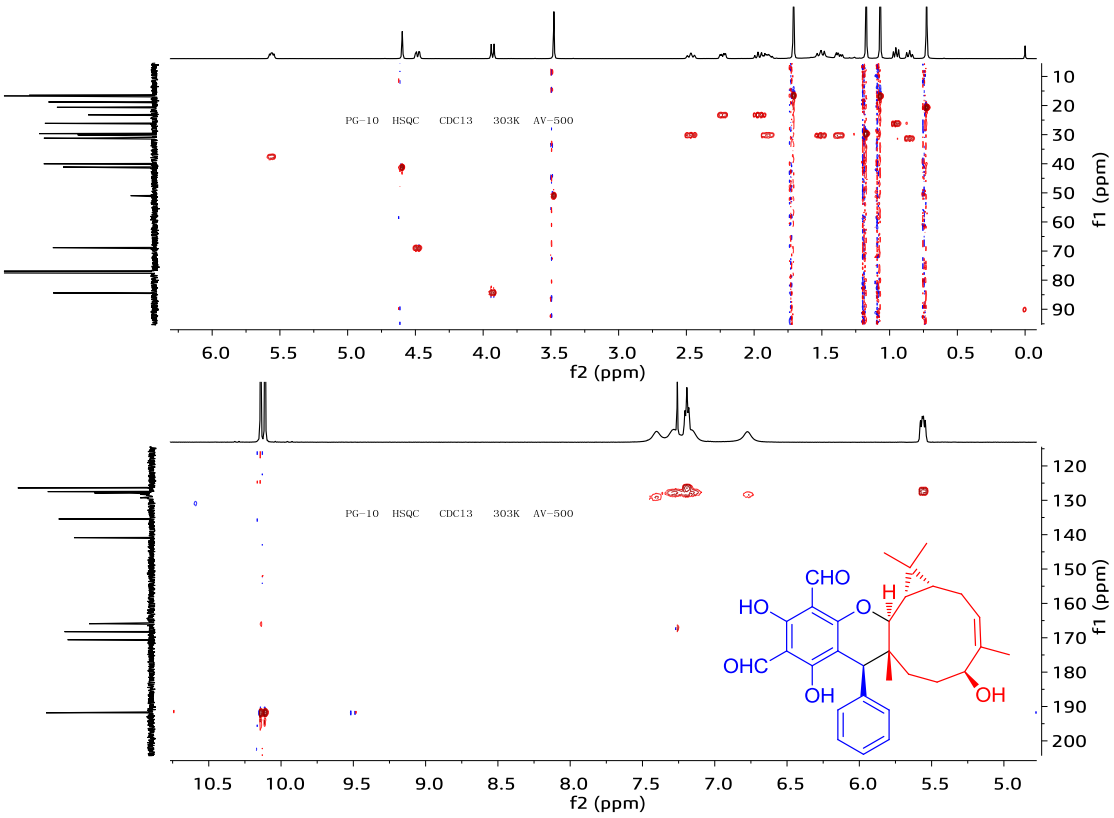

Figure S8-8. HSQC spectrum of **8** in $CDCl_3$ (500 MHz)

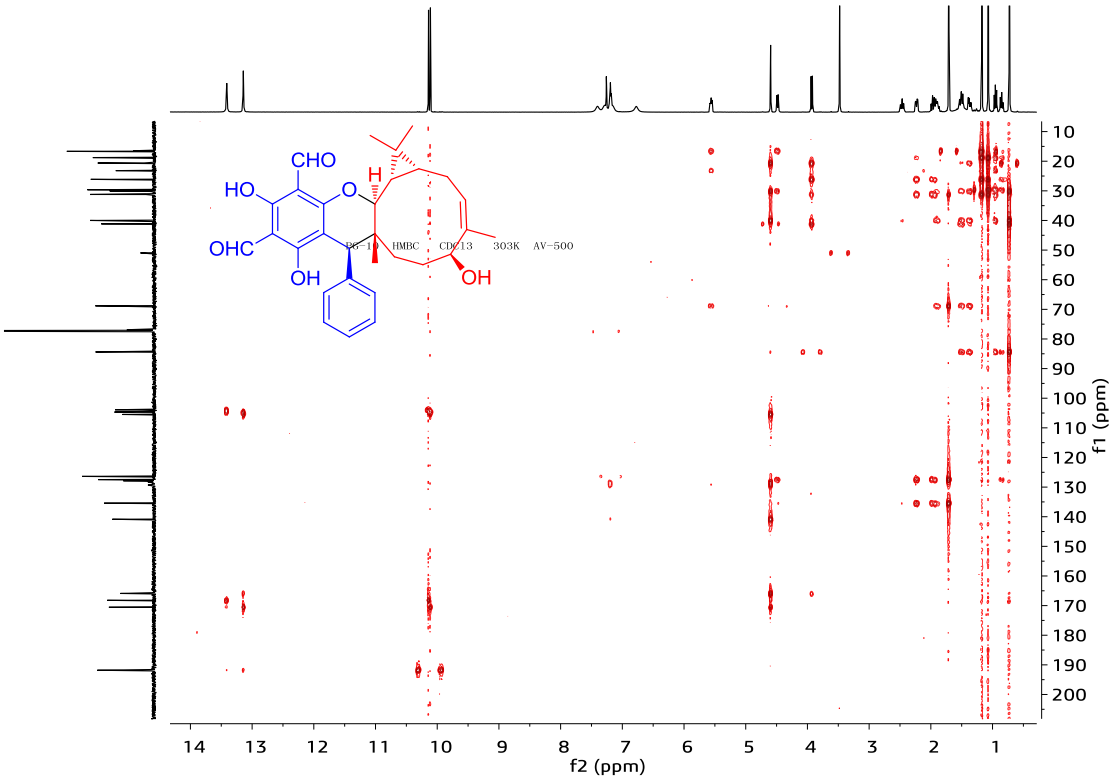

Figure S8-9. HMBC spectrum of **8** in $CDCl_3$ (500 MHz)

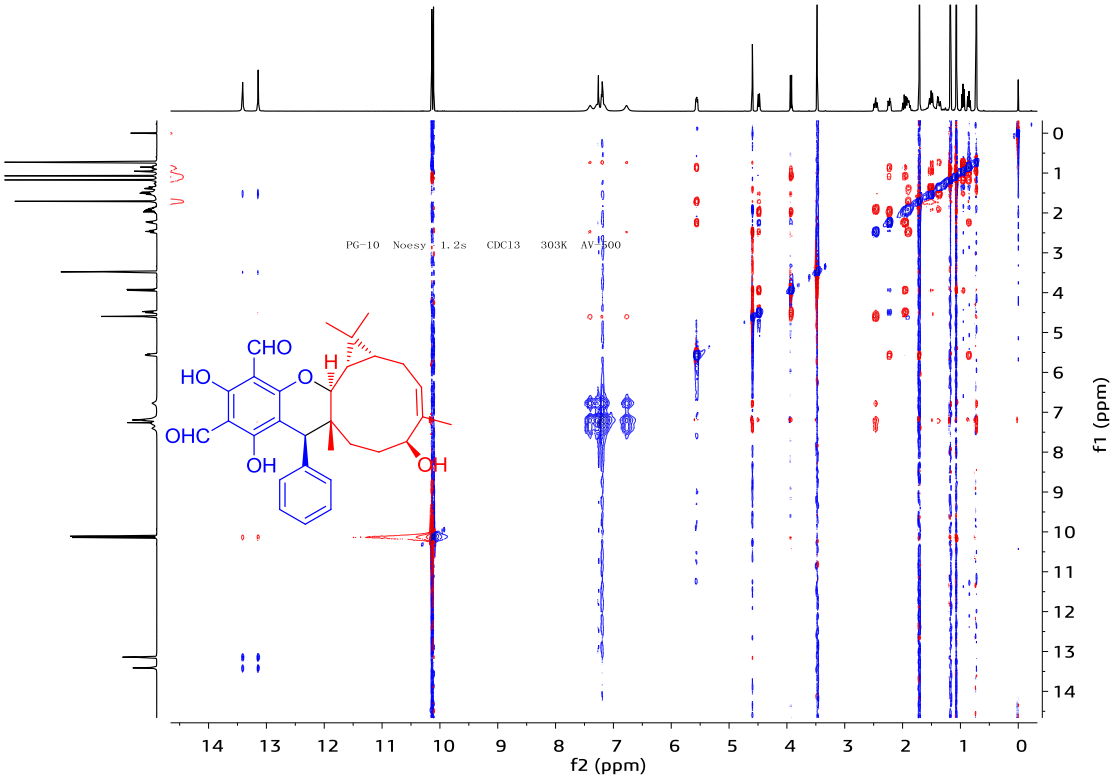

Figure S8-10. NOESY spectrum of **8** in $CDCl_3$ (500 MHz)

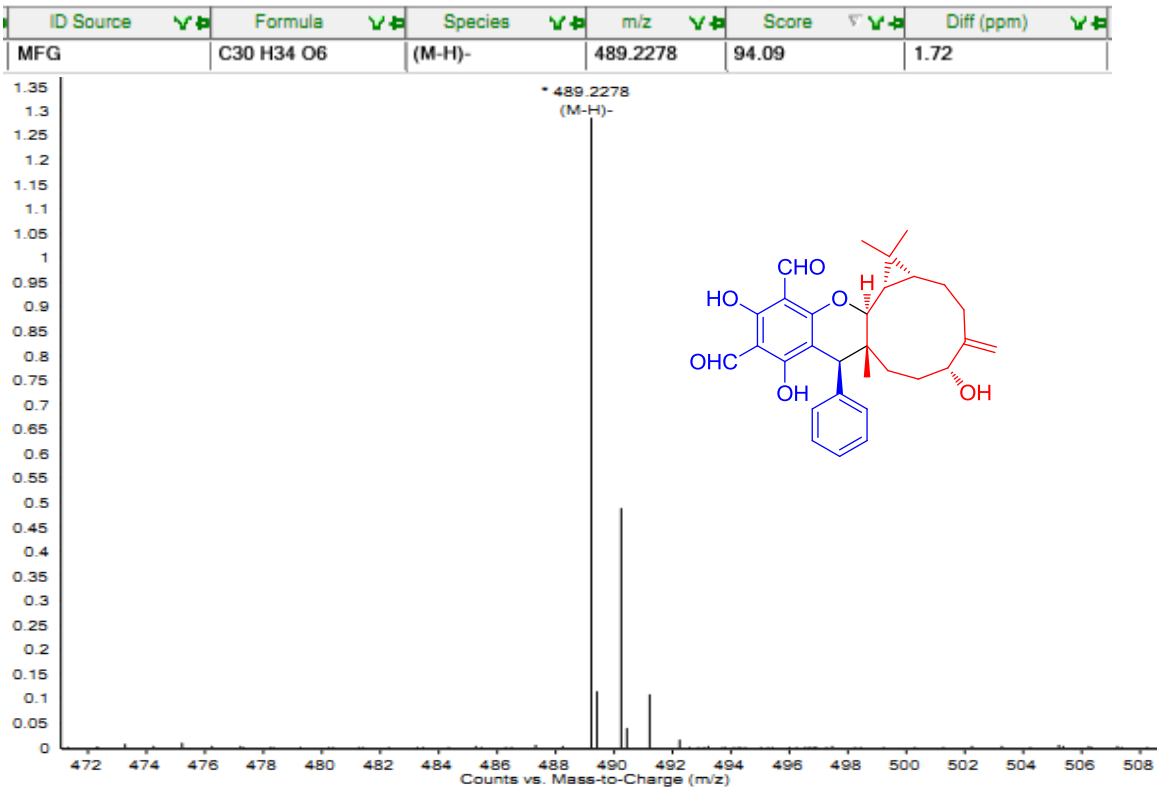

Figure S9-1. HR-ESI-MS spectrum of **9**

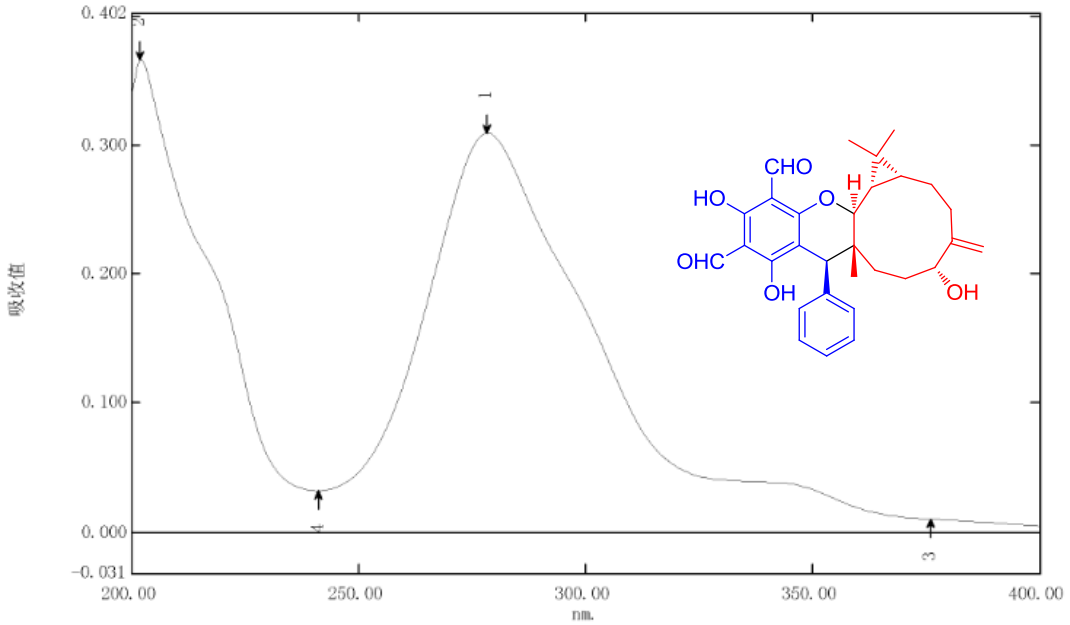

测定属性
波长范围 (nm.): 200.00 到 400.00
扫描速度: 中速
采样间隔: 0.2
自动采样间隔: 启用
扫描模式: 单个

No.	P/V	波长(nm)	吸收值
1	↑	278.40	0.310
2	↑	202.00	0.366
3	↓	376.20	0.010
4	↓	241.20	0.032

Figure S9-2. UV spectrum of **9** in MeOH

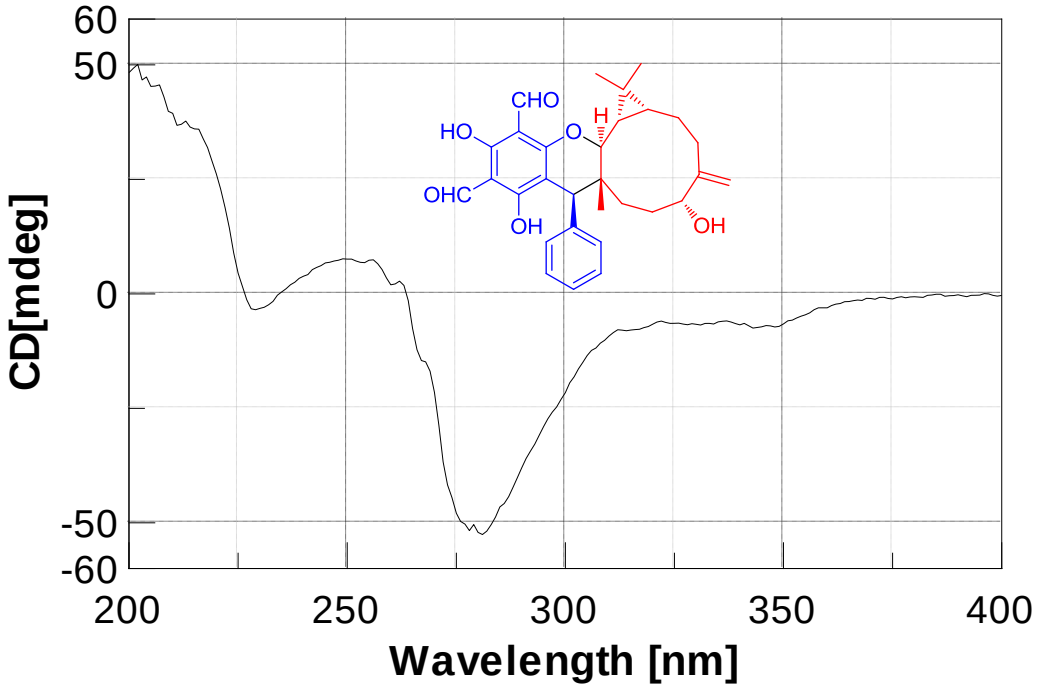

Figure S9-3. CD spectrum of **9** in MeOH

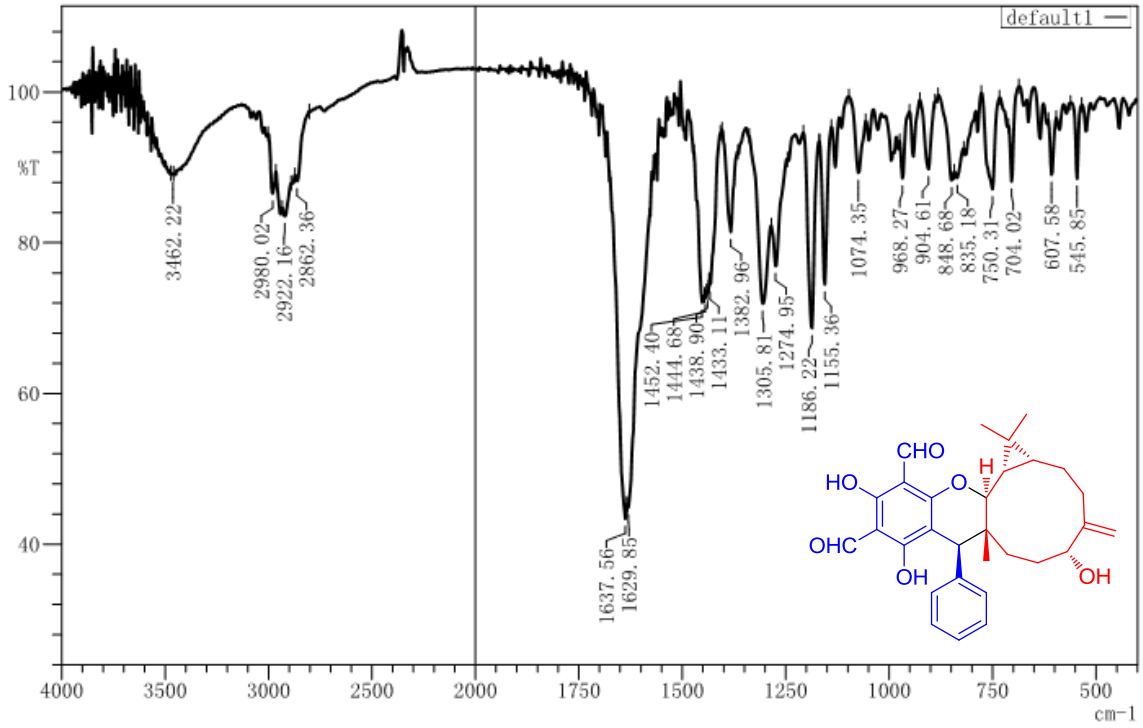

Figure S9-4. IR spectrum of **9**

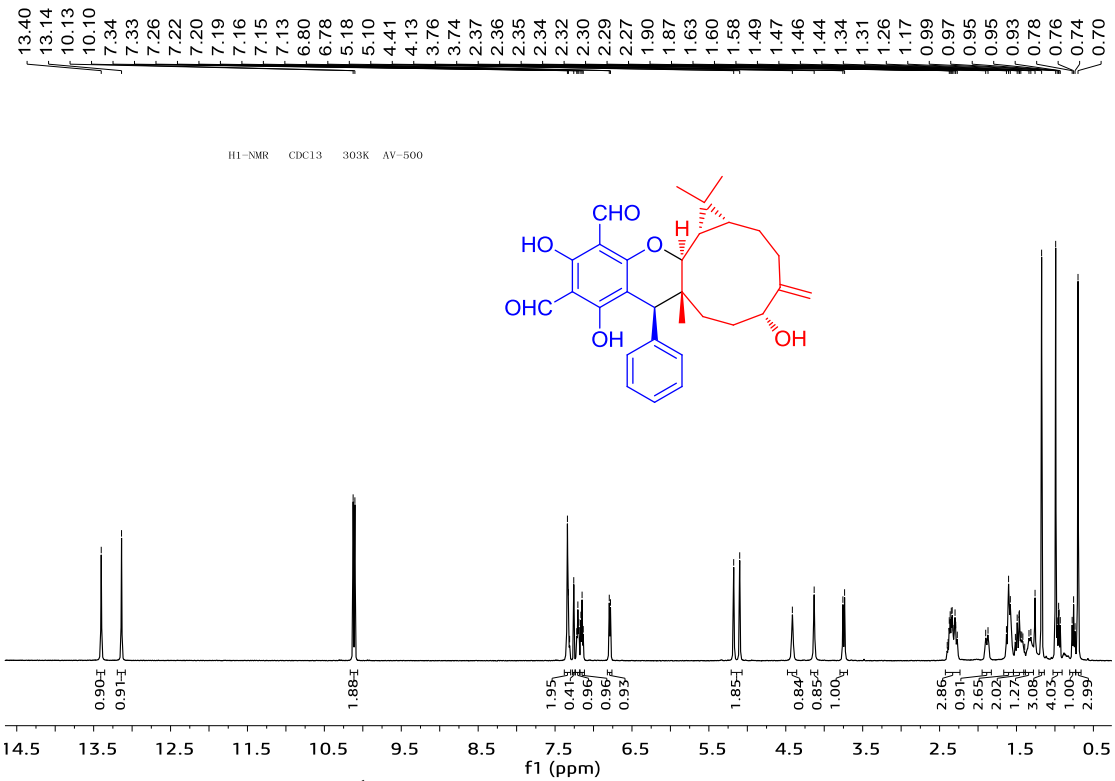

Figure S9-5. ^{1}H NMR spectrum of **9** in $CDCl_3$ (500 MHz)

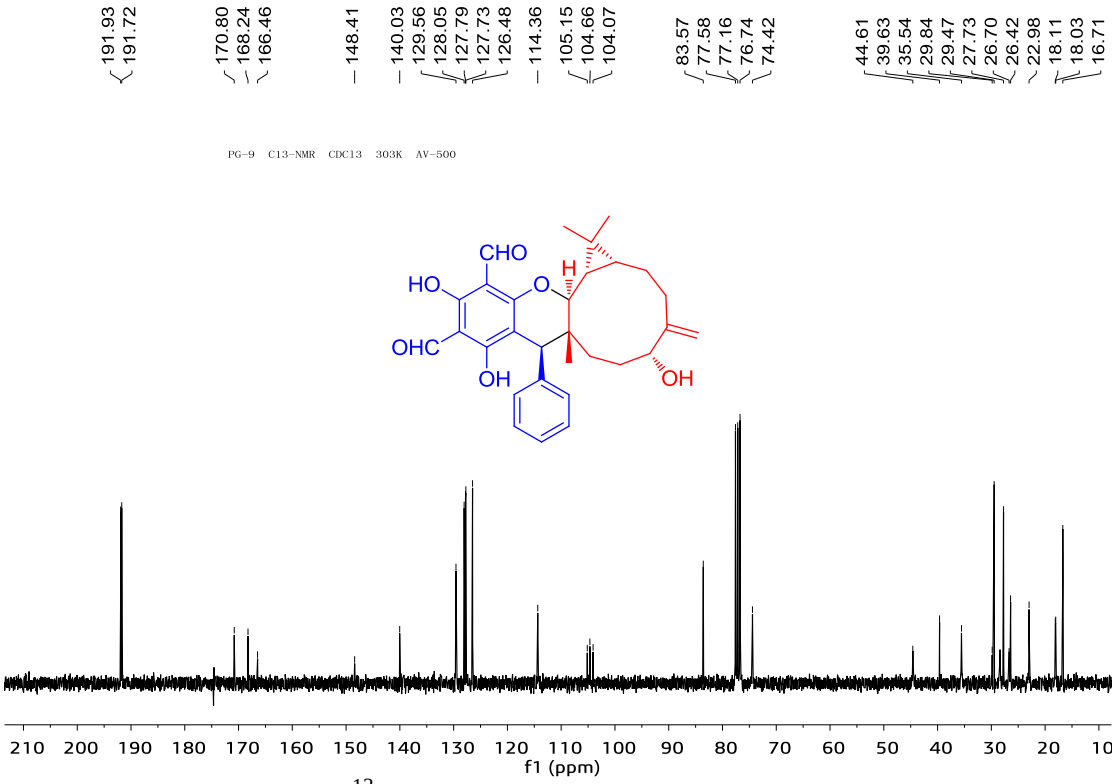

Figure S9-6. ^{13}C NMR spectrum of **9** in $CDCl_3$ (125 MHz)

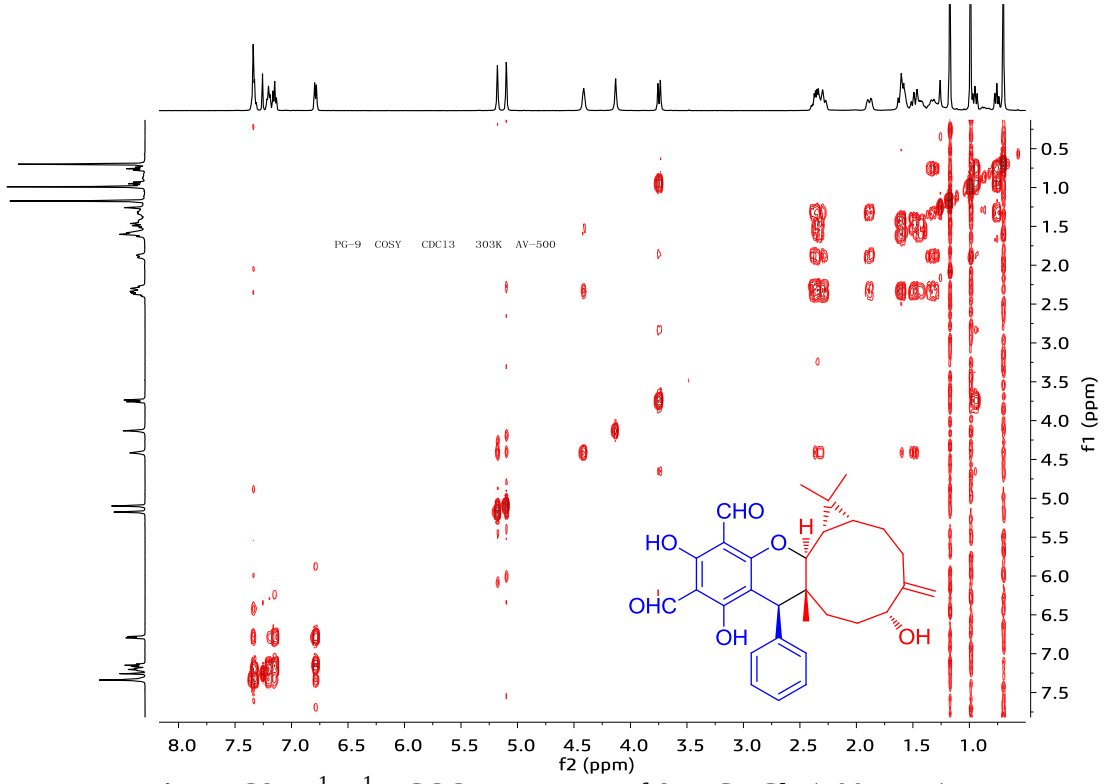

Figure S9-7. ^{1}H-^{1}H COSY spectrum of **9** in $CDCl_3$ (500 MHz)

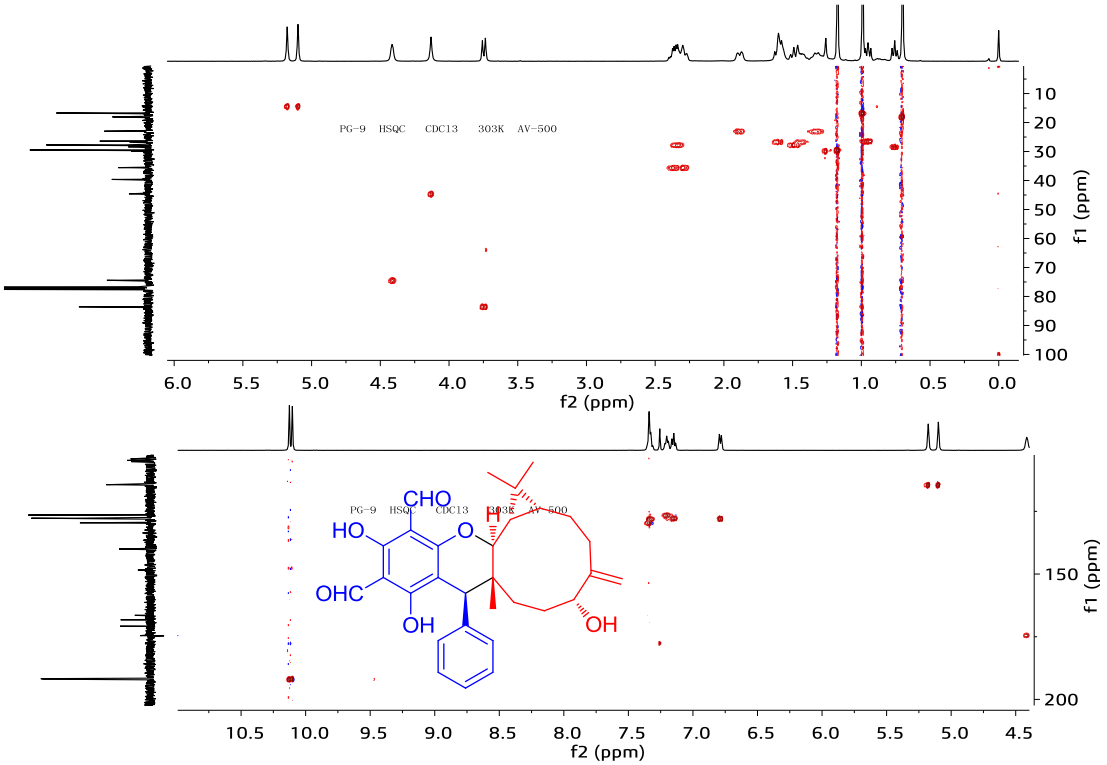

Figure S9-8. HSQC spectrum of **9** in $CDCl_3$ (500 MHz)

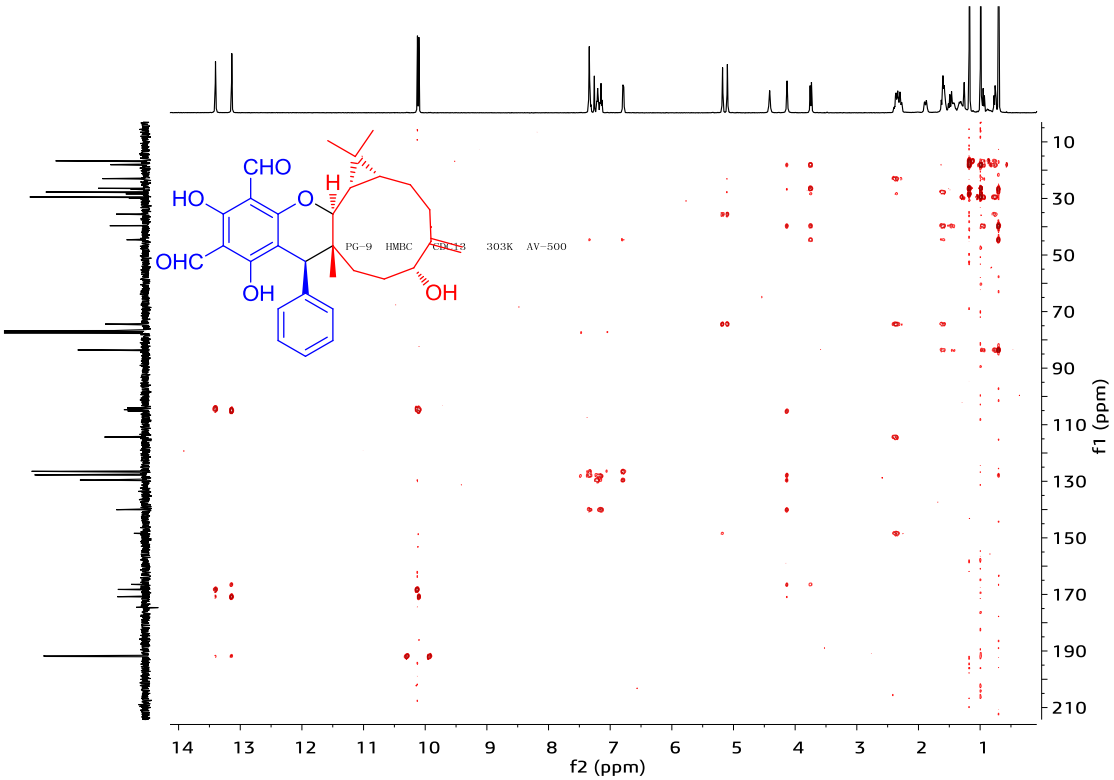

Figure S9-9. HMBC spectrum of **9** in $CDCl_3$ (500 MHz)

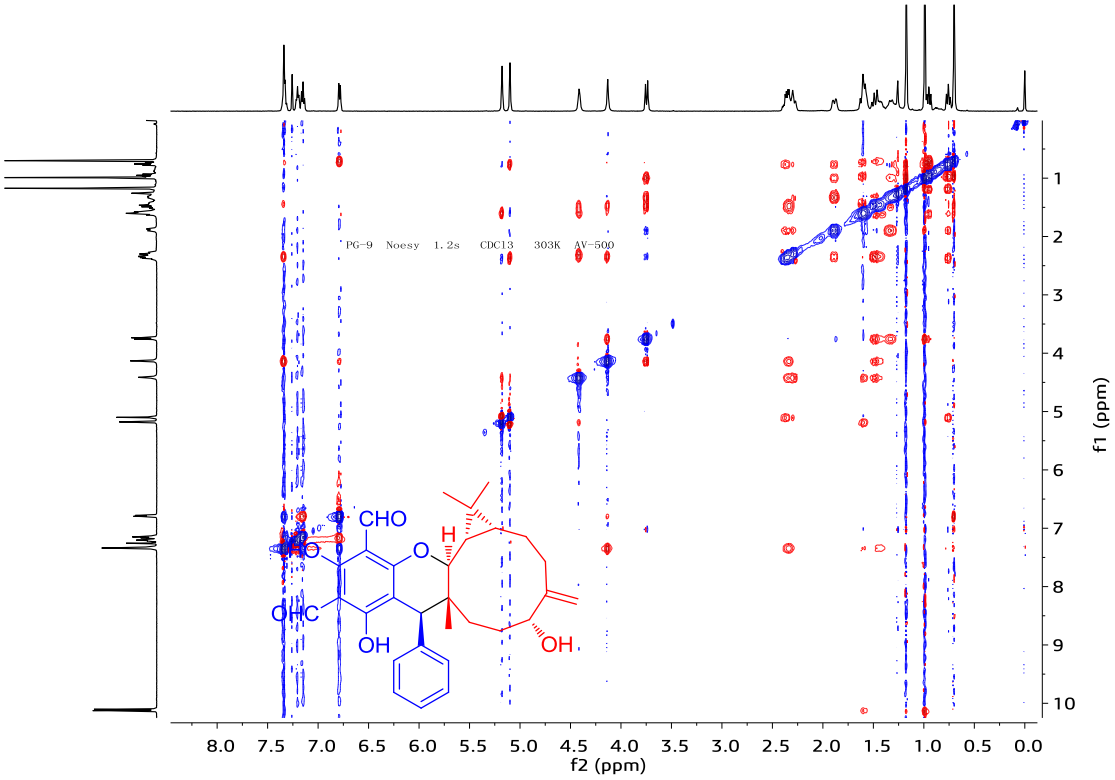

Figure S9-10. NOESY spectrum of **9** in $CDCl_3$ (500 MHz)

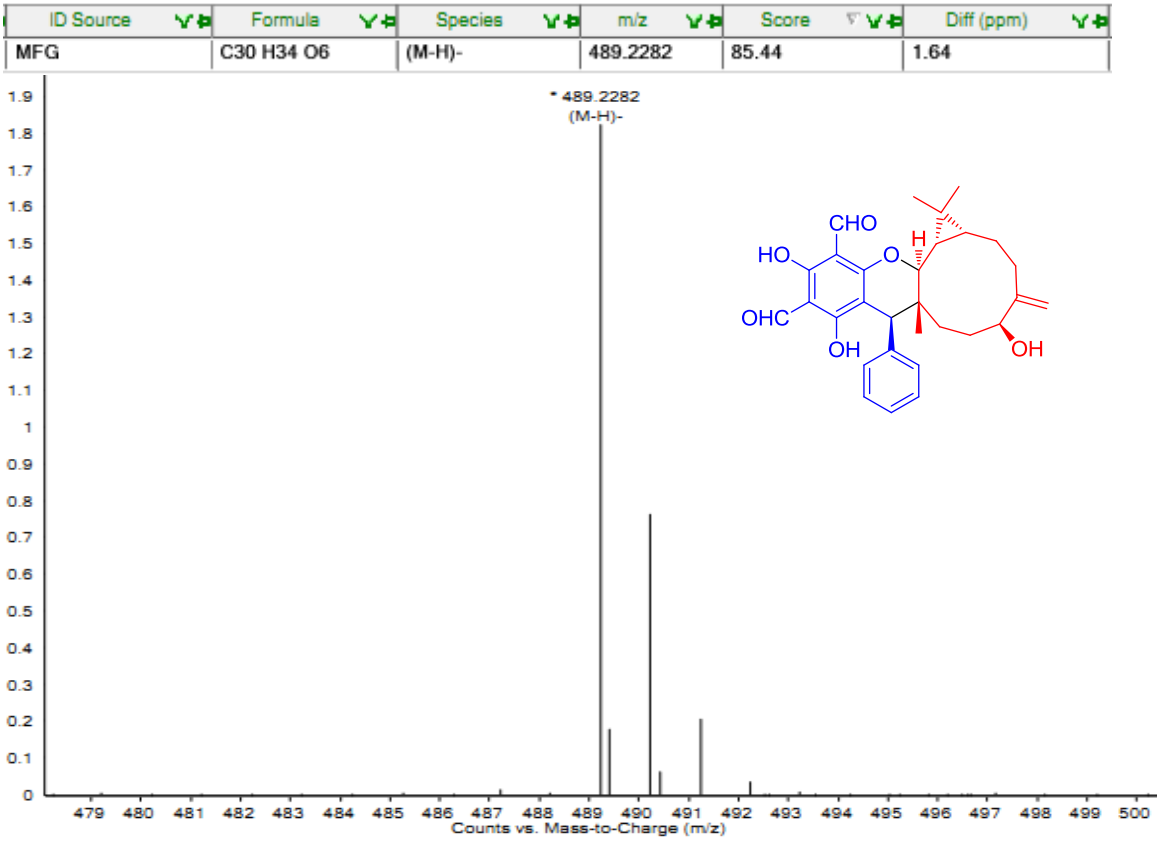

Figure S10-1. HR-ESI-MS spectrum of **10**

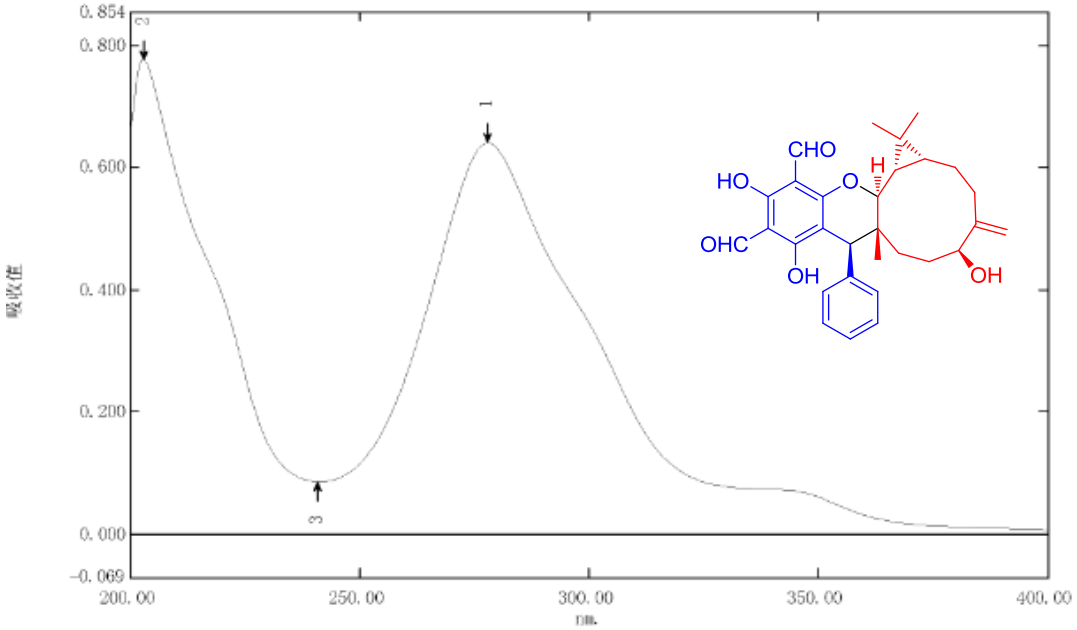

测定属性
波长范围（nm.）：200.00 到 400.00
扫描速度：中速
采样间隔：0.2
自动采样间隔：启用

No.	P/V	波长(nm)	吸收值
1	↑	278.00	0.640
2	↑	202.80	0.777
3	↓	240.80	0.087

Figure S10-2. UV spectrum of **10** in MeOH

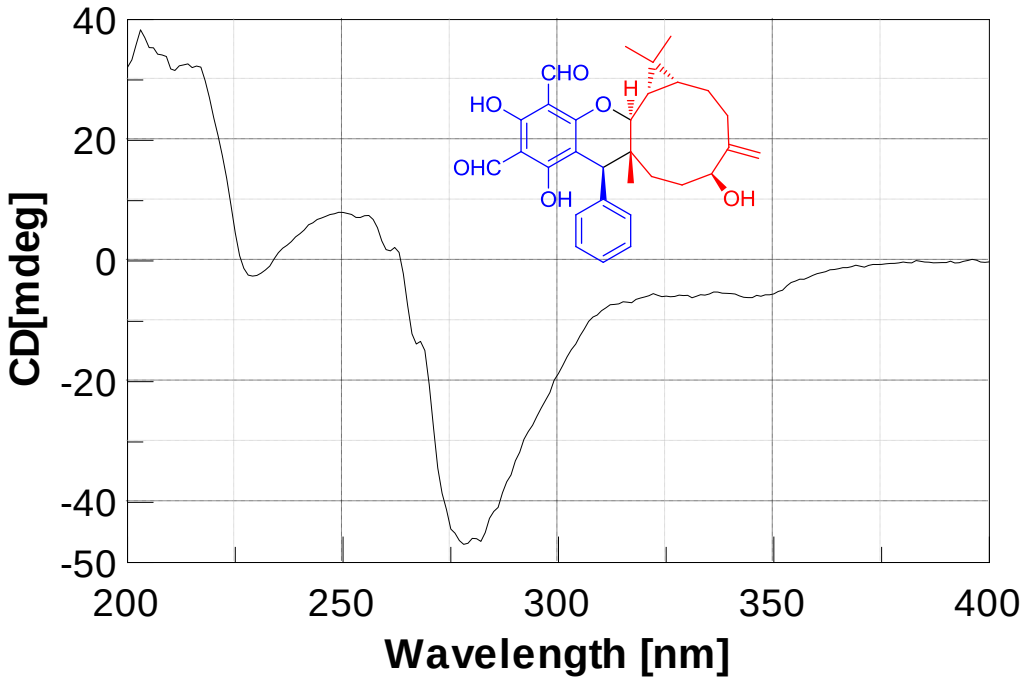

Figure S10-3. CD spectrum of **10** in MeOH

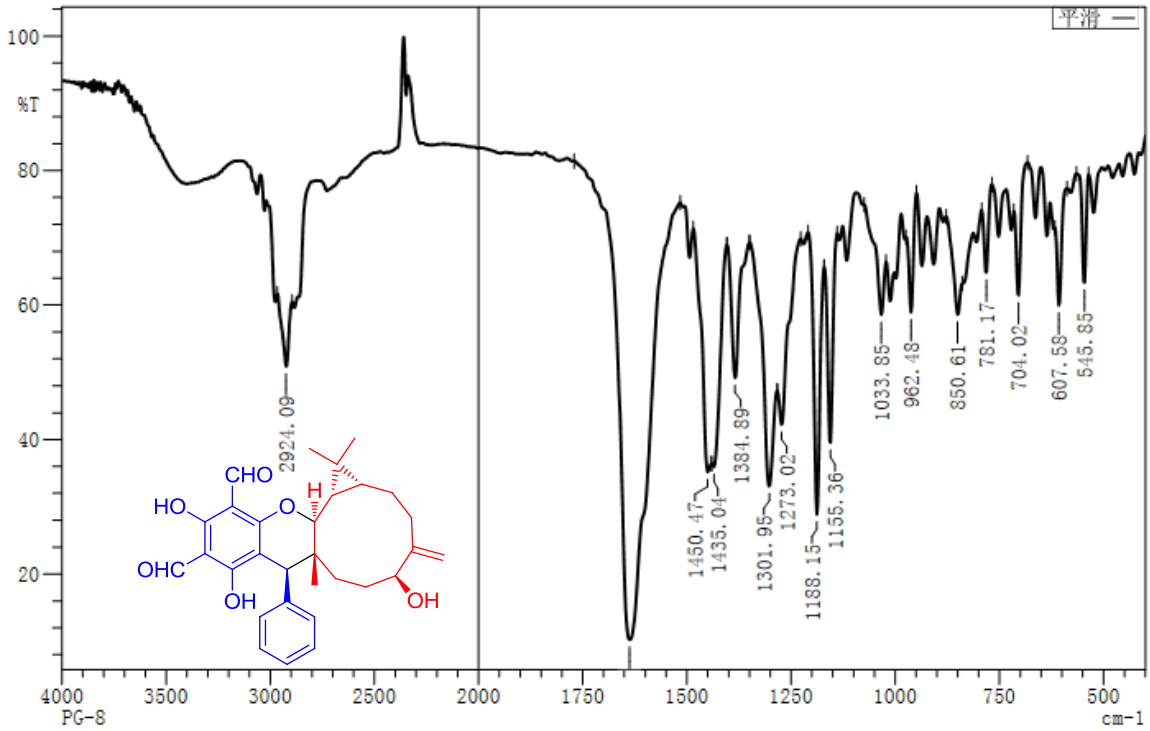

Figure S10-4. IR spectrum of **10**

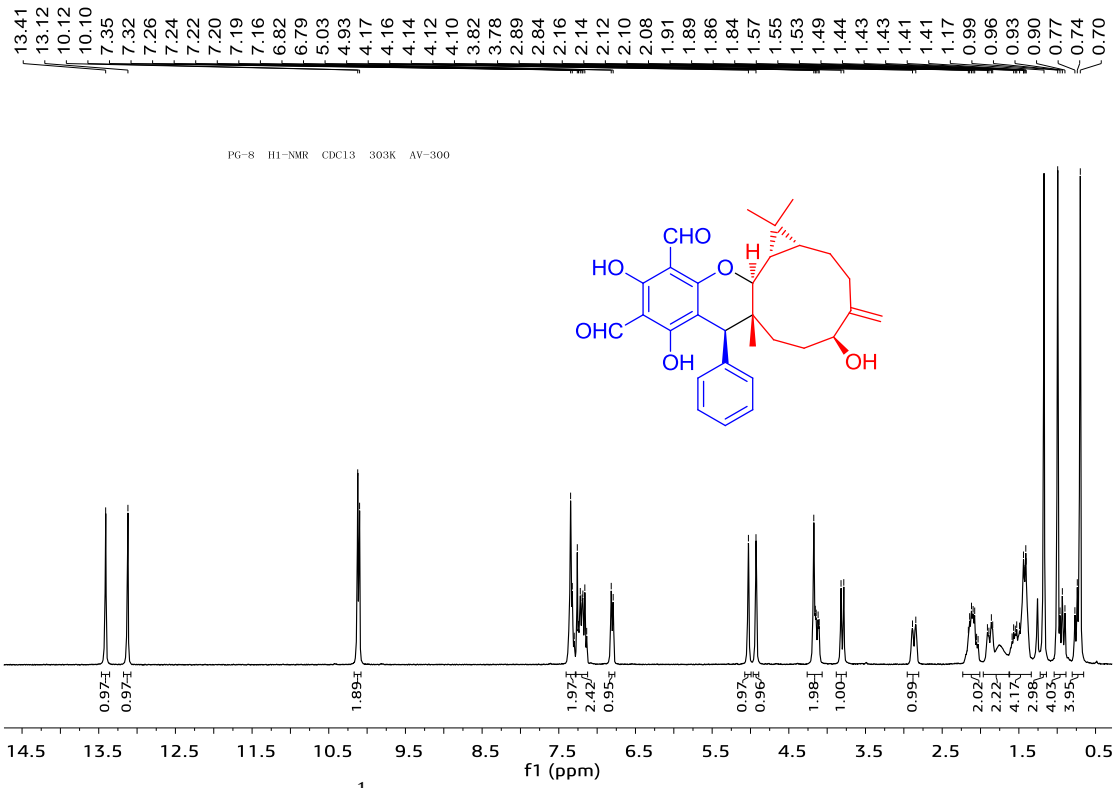

Figure S10-5. ^{1}H NMR spectrum of **10** in $CDCl_3$ (300 MHz)

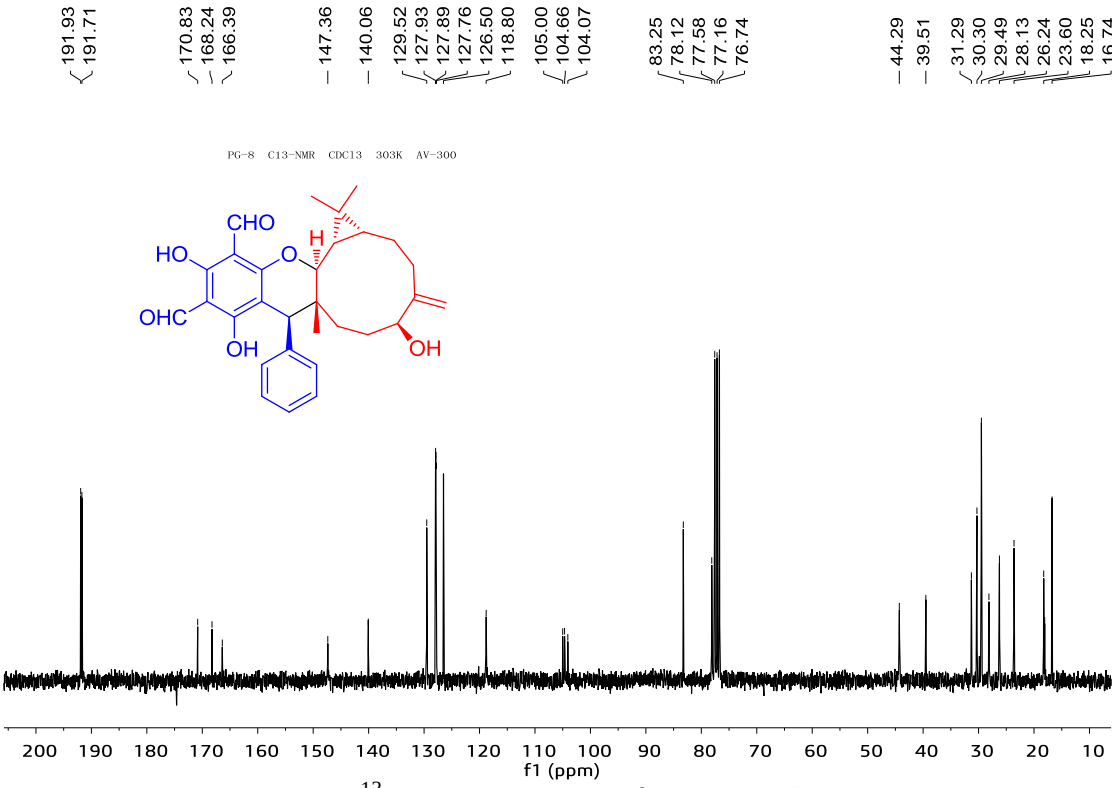

Figure S10-6. ^{13}C NMR spectrum of **10** in $CDCl_3$ (75 MHz)

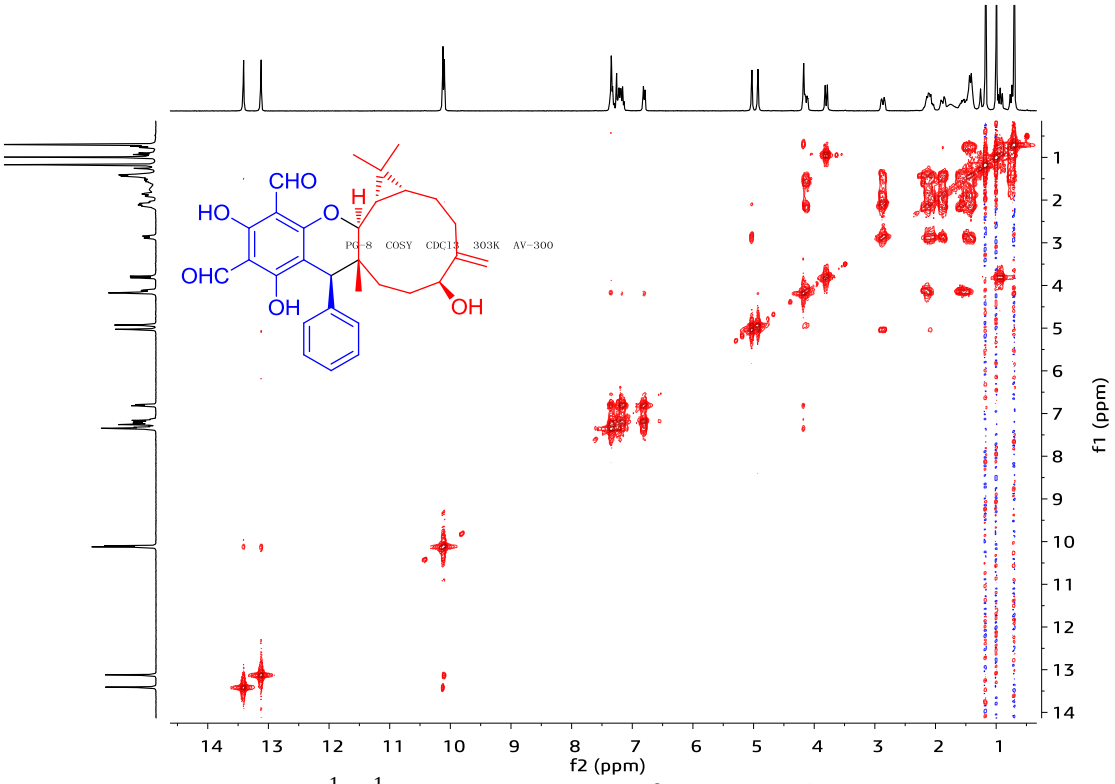

Figure S10-7. ^{1}H-^{1}H COSY spectrum of **10** in $CDCl_3$ (300 MHz)

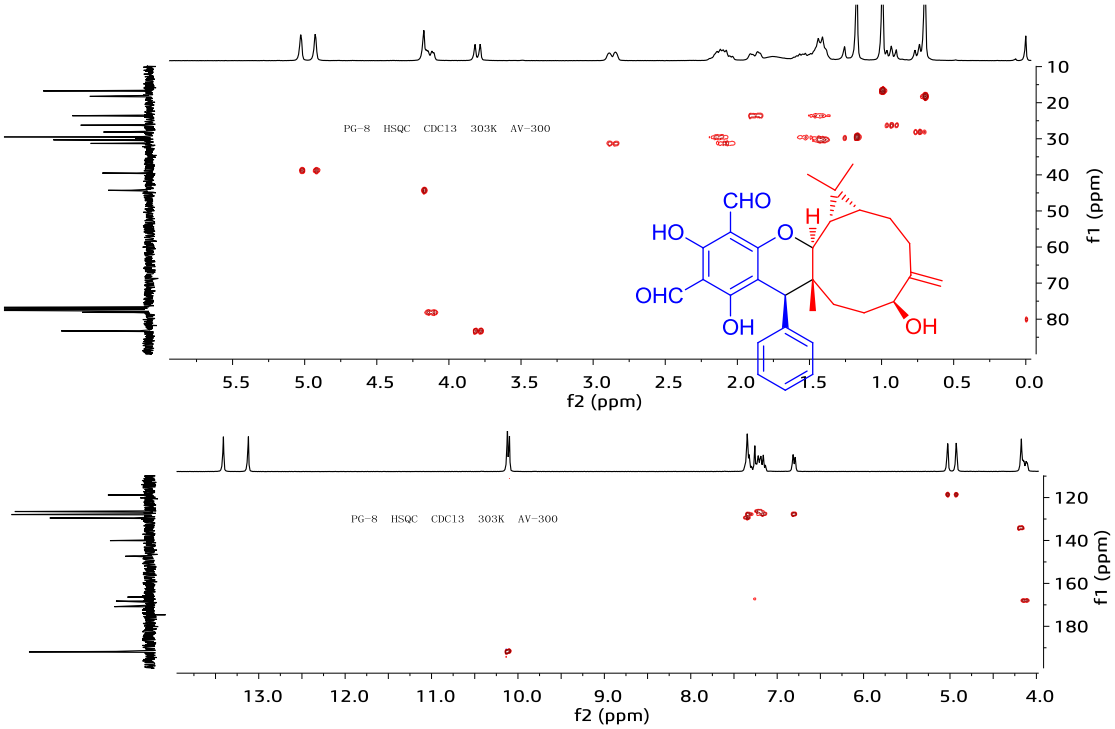

Figure S10-8. HSQC spectrum of **10** in $CDCl_3$ (300 MHz)

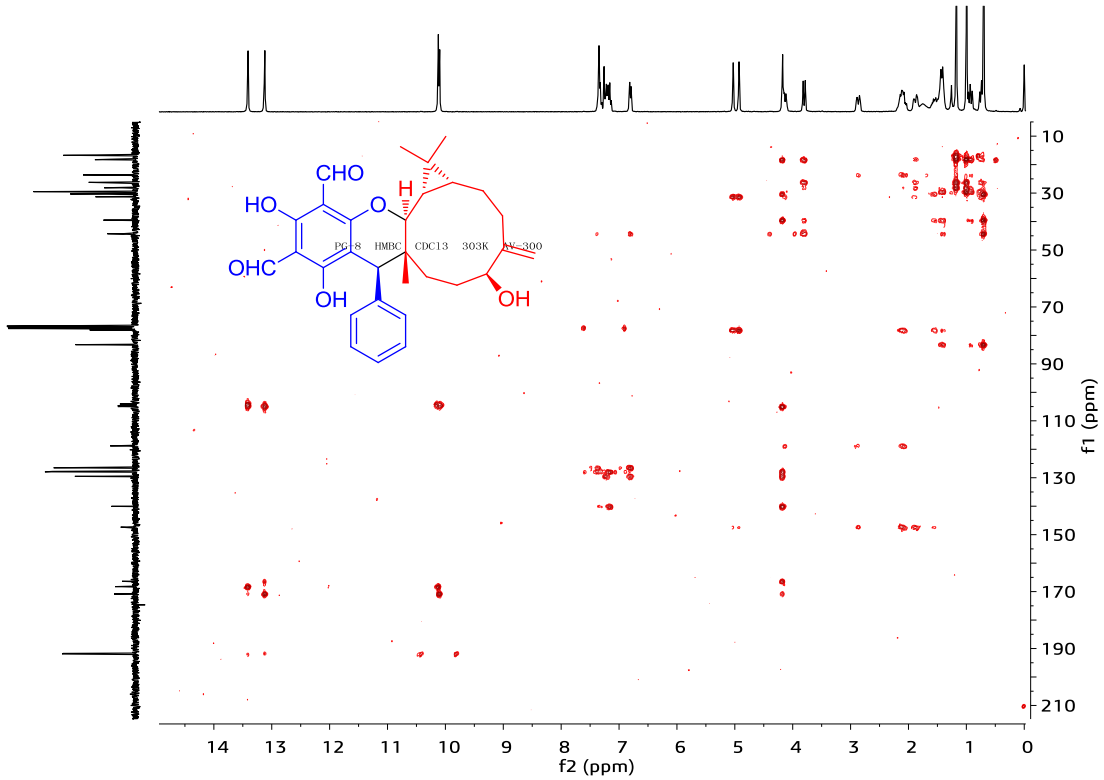

Figure S10-9. HMBC spectrum of **10** in $CDCl_3$ (300 MHz)

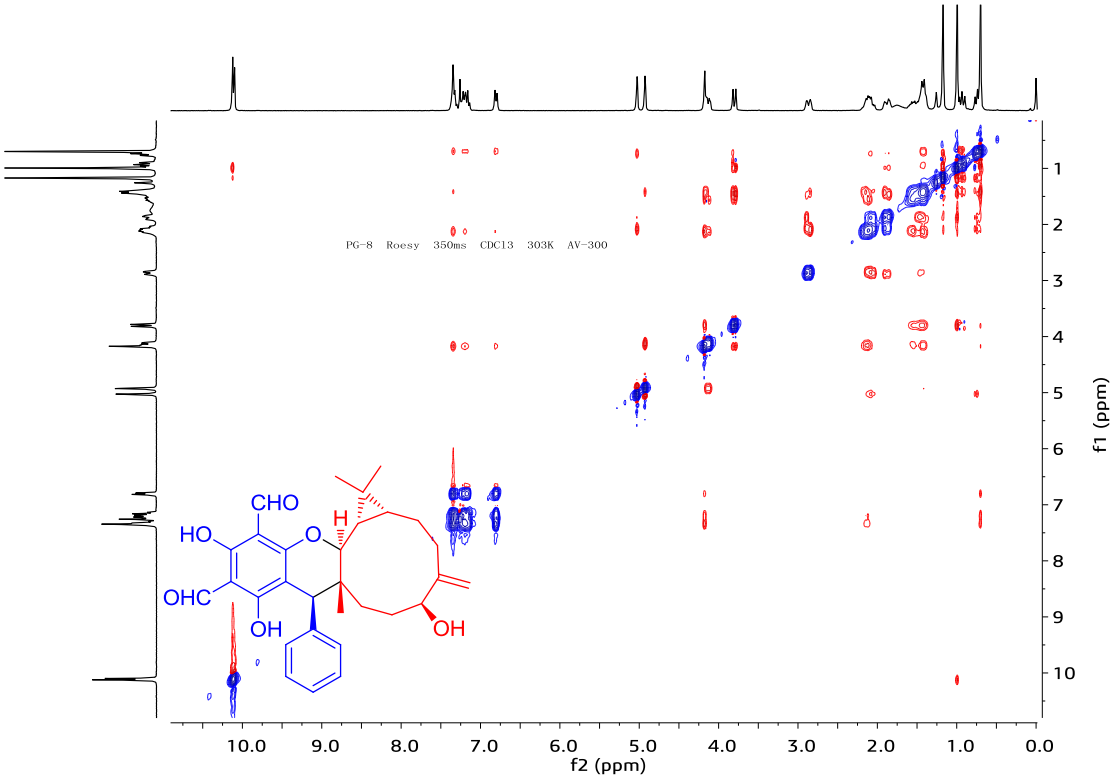

Figure S10-10. NOESY spectrum of **10** in $CDCl_3$ (300 MHz)

Quantum chemical ECD calculation for **1**, **4**, **5**, **7**, and **8**

The systematic random conformational analysis of the enantiomers of compounds (1'*R*, 1*R*, 5*R*, 8*R*, 9*S*)-**1**, (1'*S*, 1*S*, 5*S*, 8*S*, 9*R*)-**1**; (1*β*, 6*β*-epoxy)-/(1'*R*, 1*R*, 3*R*, 4*S*, 5*R*, 6*R*, 7*S*, 10*R*)-**4**, (1*α*, 6*α*-epoxy)-/(1'*R*, 1*S*, 3*R*, 4*S*, 5*R*, 6*S*, 7*S*, 10*R*-**4**); (3*β*,5*β*-epoxy-6*β*-OH)-/(1'*R*, 1*R*, 3*S*, 4*R*, 5*S*, 6*S*, 7*S*, 10*R*)-**5**, (3*β*,5*β*-epoxy-6*α*-OH)-/(1'*R*, 1*R*, 3*S*, 4*R*, 5*S*, 6*R*, 7*S*, 10*R*)-**5**, (3*α*,5*α*-epoxy-6*α*-OH)-/(1'*R*, 1*R*, 3*R*, 4*R*, 5*R*, 6*R*, 7*S*, 10*R*)-**5**, (3*α*,5*α*-epoxy-6*β*-OH)-/(1'*R*, 1*R*, 3*R*, 4*R*, 5*R*, 6*S*, 7*S*, 10*R*)-**5**; (1'*R*, 1*R*, 3*R*, 4*R*, 7*S*, 10*R*)-**7**, (1'*R*, 1*R*, 3*S*, 4*R*, 7*S*, 10*R*)-**7**; (1'*R*, 1*S*, 4*R*, 5*S*, 6*S*, 7*R*)-**8**, and (1'*S*, 1*R*, 4*S*, 5*R*, 6*R*, 7*S*)-**8**, were performed in the SYBYL 8.1 program by using the Monte Carlo protocol at the MMFF94s level. Considering a cutoff of 10 kcal/mol, 3, 3, 4, 6, 2, 3, 3, 3, 2, 4, 5, and 5 minimum energy conformers for **1**, **4**, **5**, **7**, and **8**, respectively, were inferred to the global minima. All the obtained conformers were optimized using DFT at the B3LYP/6-31+G(d) level in gas phase, and 2, 2, 4, 4, 2, 2, 2, 3, 1, 2, 4, and 4 most stable conformers for **1**, **4**, **5**, **7**, and **8** respectively, were selected. All of the optimized stable conformers were used for TDDFT computation of the excited stats at the same levels, with the consideration of the first 50 excitations. The overall ECD curves were weighted by Boltzmann distribution of each conformer (with a half-bandwidth of 0.3eV) derived from their relative free energy values. The ECD spectra were produced by SpecDis 1.6 software.

Computational data of **1**

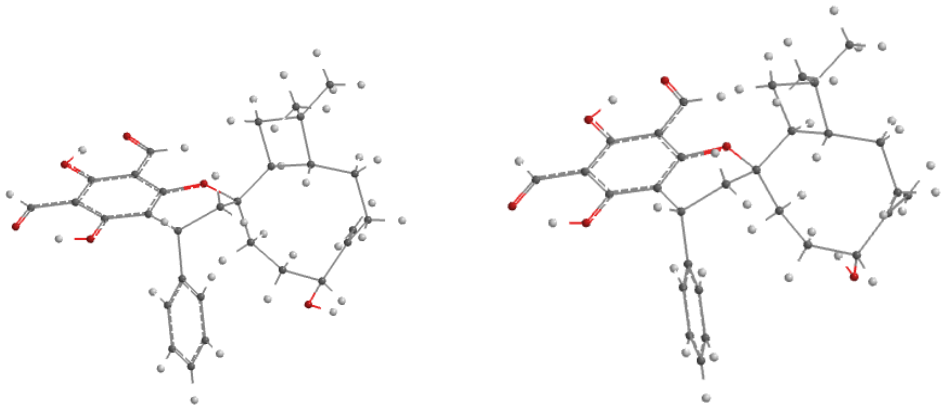

Conf. 1
Δε (kcal/mol)=0
(64.3%)

Conf. 2
Δε (kcal/mol)=+0.58
(35.6%)

Figure S11-1. DFT-optimized structures for low-energy conformers of (1'*R*, 1*R*, 5*R*, 8*R*, 9*S*)-**1** at B3LYP/6-31+G(d) level in methanol (PCM), with zero-point corrected free energies calculated at the same level (and Boltzmann population at 298K estimated thereof).

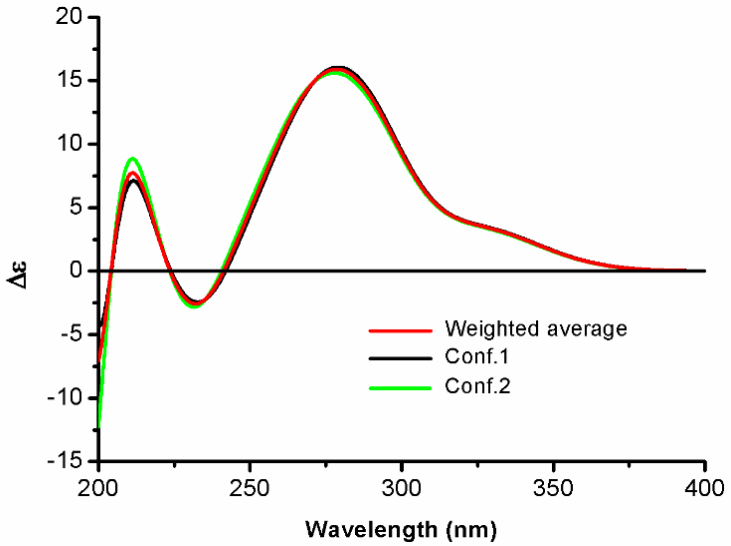

Figure S11-2. TDDFT-calculated spectra at B3LYP/6-31+G(d) level in methanol (PCM) for the low energy structures of (1'*R*, 1*R*, 5*R*, 8*R*, 9*S*)-**1**, and their weighted average using Boltzmann populations at 298K. Gaussian band-shape with 0.3 eV applied to generate the spectra.

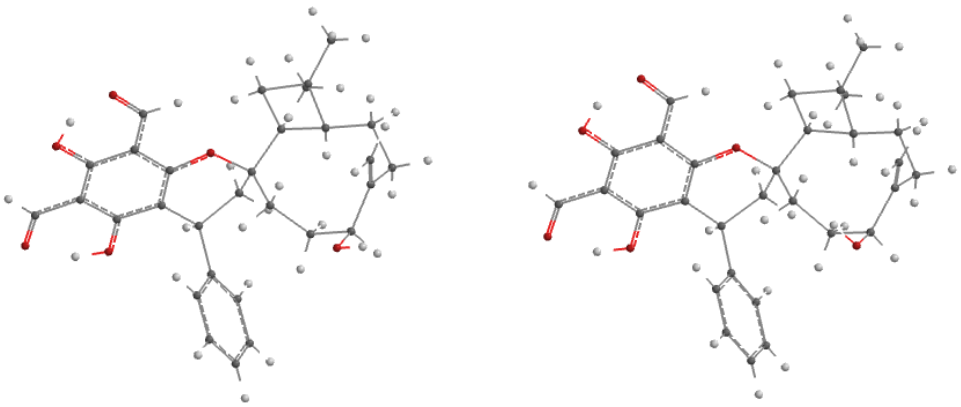

Conf. 1
Δε (kcal/mol)=0
(64.3%)

Conf. 2
Δε (kcal/mol)=+0.58
(35.6%)

Figure S11-3. DFT-optimized structures for low-energy conformers of (1'*S*, 1*S*, 5*S*, 8*S*, 9*R*)-**1** at B3LYP/6-31+G(d) level in methanol (PCM), with zero-point corrected free energies calculated at the same level (and Boltzmann population at 298K estimated thereof).

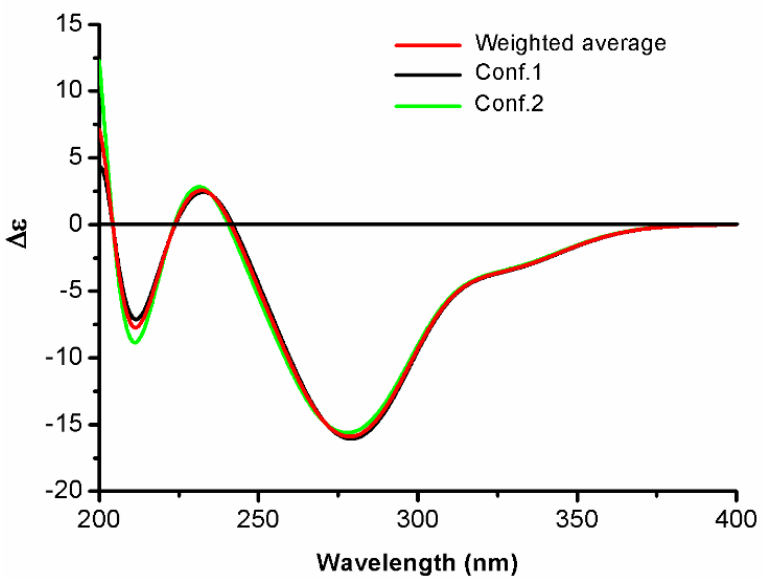

Figure S11-4. TDDFT-calculated spectra at B3LYP/6-31+G(d) level in methanol (PCM) for the low energy structures of (1'*S*, 1*S*, 5*S*, 8*S*, 9*R*)-**1**, and their weighted average using Boltzmann populations at 298K. Gaussian band-shape with 0.3 eV applied to generate the spectra.

Computational data of **4**

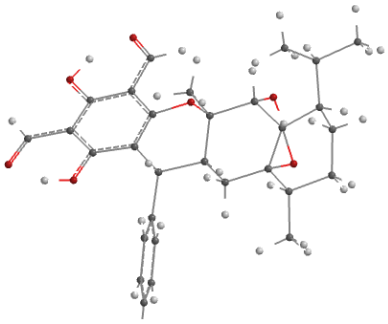

Conf. 1
Δε (kcal/mol)=0
(74.3%)

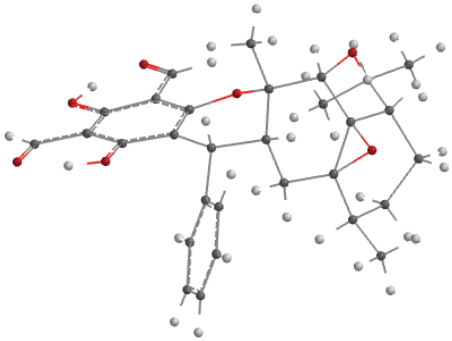

Conf. 2
Δε (kcal/mol)=+1.63
(14.5%)

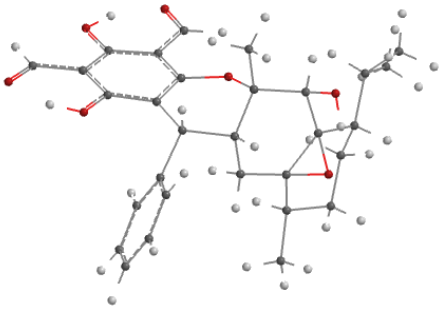

Conf. 3
Δε (kcal/mol)=+2.11
(8.9%)

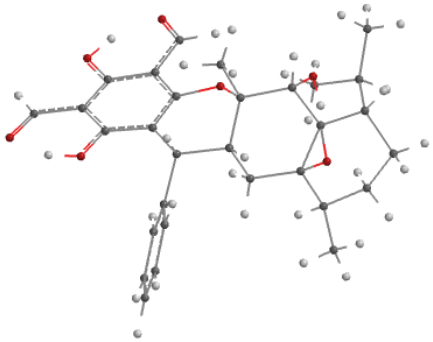

Conf. 4
Δε (kcal/mol)=+3.51
(2.2%)

Figure S12-1. DFT-optimized structures for low-energy conformers of (1*β*, 6*β*-epoxy)-/(1'*R*, 1*R*, 3*R*, 4*S*, 5*R*, 6*R*, 7*S*, 10*R*)-**4** at B3LYP/6-31+G(d) level in methanol (PCM), with zero-point corrected free energies calculated at the same level (and Boltzmann population at 298K estimated thereof).

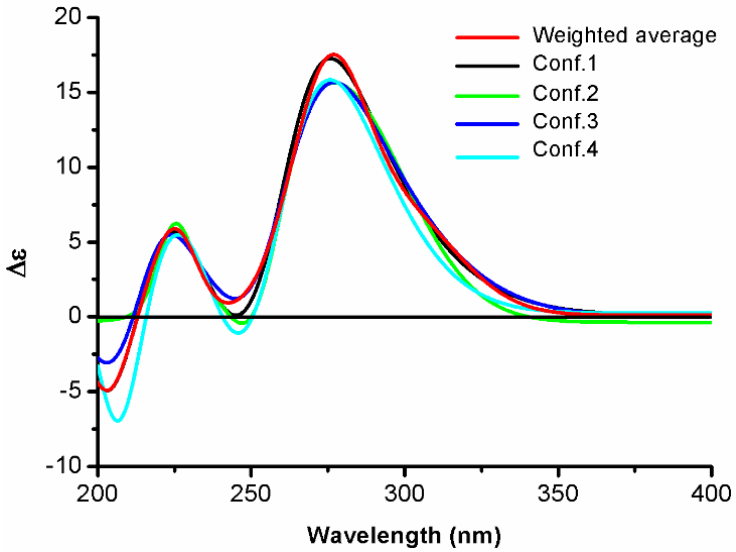

Figure S12-2. TDDFT-calculated spectra at B3LYP/6-31+G(d) level in methanol (PCM) for the low energy structures of (1*β*, 6*β*-epoxy)-/(1'*R*, 1*R*, 3*R*, 4*S*, 5*R*, 6*R*, 7*S*, 10*R*)-**4**, and their weighted average using Boltzmann populations at 298K. Gaussian band-shape with 0.3 eV applied to generate the spectra.

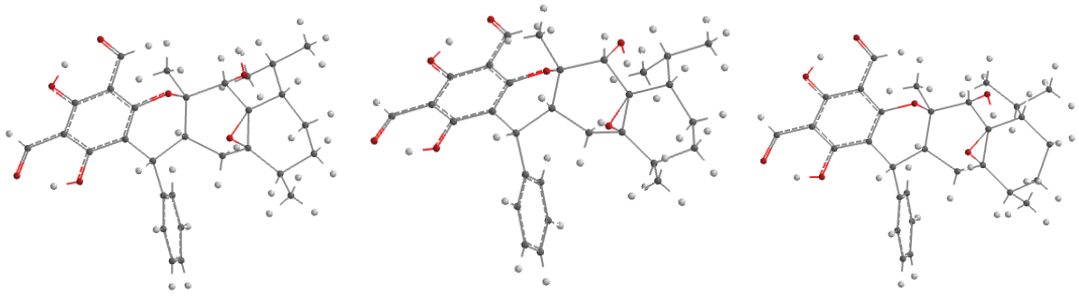

Conf. 1
Δε (kcal/mol)=0
(27.8%)

Conf. 2
Δε (kcal/mol)=+0.37
(19.1%)

Conf. 3
Δε (kcal/mol)=+0.55
(15.9%)

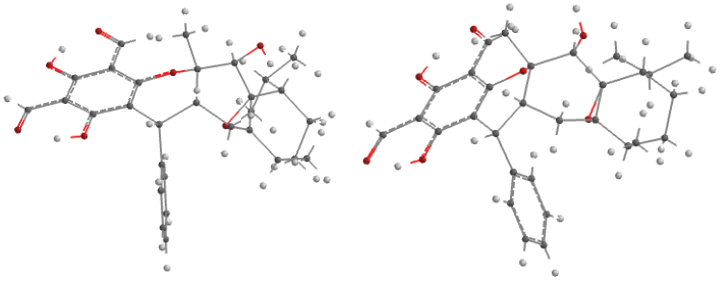

Conf. 4
Δε (kcal/mol)=+0.71
(13.7%)

Conf. 5
Δε (kcal/mol)=+0.86
(11.7%)

Figure S12-3. DFT-optimized structures for low-energy conformers of (1*α*, 6*α*-epoxy)-/(1'*R*, 1*S*, 3*R*, 4*S*, 5*R*, 6*S*, 7*S*, 10*R*-**4**) at B3LYP/6-31+G(d) level in methanol (PCM), with zero-point corrected free energies calculated at the same level (and Boltzmann population at 298K estimated thereof).

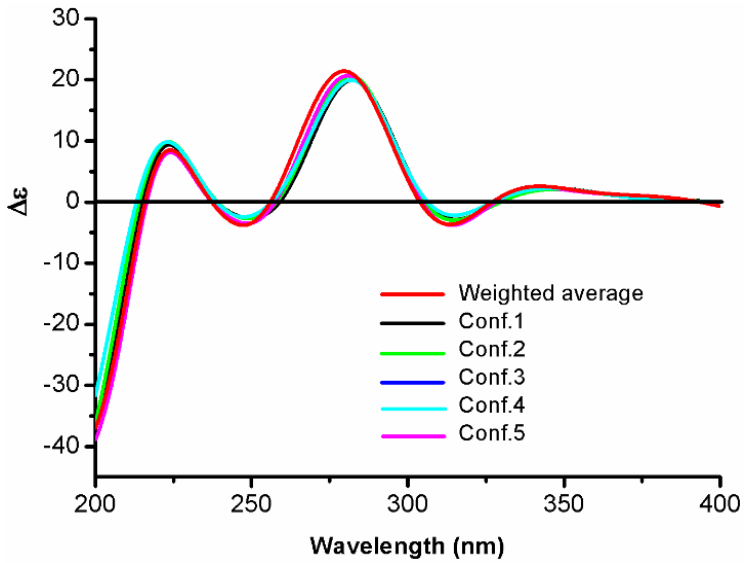

Figure S12-4. TDDFT-calculated spectra at B3LYP/6-31+G(d) level in methanol (PCM) for the low energy structures of (1*α*, 6*α*-epoxy)-/(1'*R*, 1*S*, 3*R*, 4*S*, 5*R*, 6*S*, 7*S*, 10*R*-**4**), and their weighted average using Boltzmann populations at 298K. Gaussian band-shape with 0.3 eV applied to generate the spectra.

Computational data of **5**

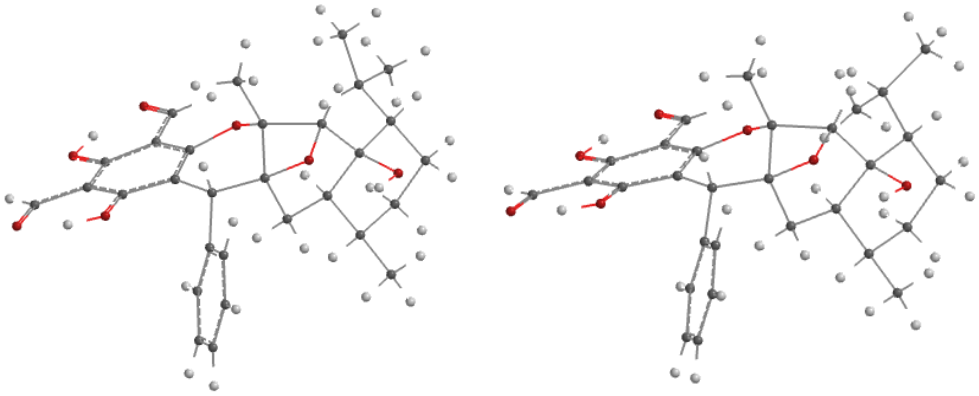

Conf. 1
Δε (kcal/mol)=0
(70.4%)

Conf. 2
Δε (kcal/mol)=+0.86
(29.6%)

Figure S13-1. DFT-optimized structures for low-energy conformers of (3*β*,5*β*-epoxy-6*β*-OH)-/(1'*R*, 1*R*, 3*S*, 4*R*, 5*S*, 6*S*, 7*S*, 10*R*)-**5** at B3LYP/6-31+G(d) level in methanol (PCM), with zero-point corrected free energies calculated at the same level (and Boltzmann population at 298K estimated thereof).

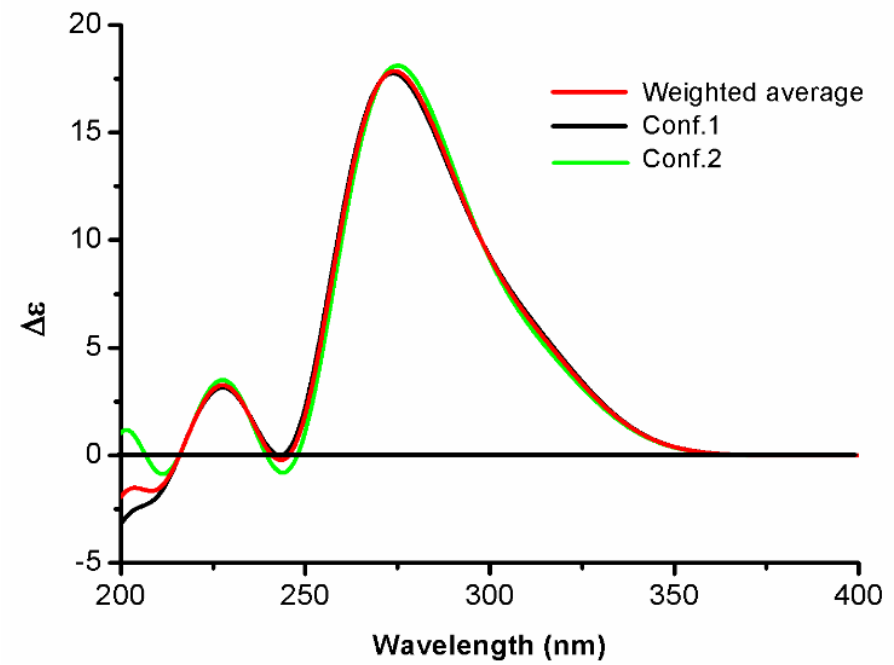

Figure S13-2. DFT-optimized structures for low-energy conformers of (3*β*,5*β*-epoxy-6*β*-OH)-/(1'*R*, 1*R*, 3*S*, 4*R*, 5*S*, 6*S*, 7*S*, 10*R*)-**5** at B3LYP/6-31+G(d) level in methanol (PCM), with zero-point corrected free energies calculated at the same level (and Boltzmann population at 298K estimated thereof).

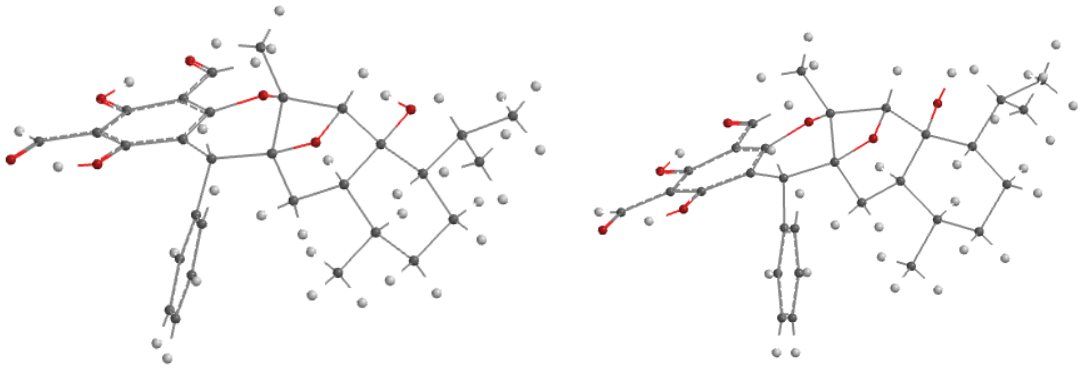

Conf. 1
Δε (kcal/mol)=0
(68.1%)

Conf. 2
Δε (kcal/mol)=+0.76
(31.9%)

Figure S13-3. DFT-optimized structures for low-energy conformers of (3*β*,5*β*-epoxy-6*α*-OH)-/(1'*R*, 1*R*, 3*S*, 4*R*, 5*S*, 6*R*, 7*S*, 10*R*)-**5** at B3LYP/6-31+G(d) level in methanol (PCM), with zero-point corrected free energies calculated at the same level (and Boltzmann population at 298K estimated thereof).

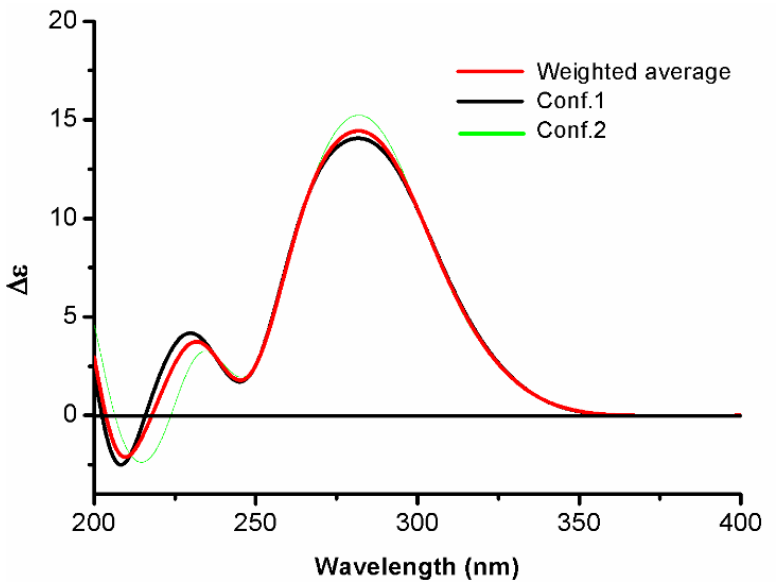

Figure S13-4. DFT-optimized structures for low-energy conformers of (3*β*,5*β*-epoxy-6*α*-OH)-/(1'*R*, 1*R*, 3*S*, 4*R*, 5*S*, 6*R*, 7*S*, 10*R*)-**5** at B3LYP/6-31+G(d) level in methanol (PCM), with zero-point corrected free energies calculated at the same level (and Boltzmann population at 298K estimated thereof).

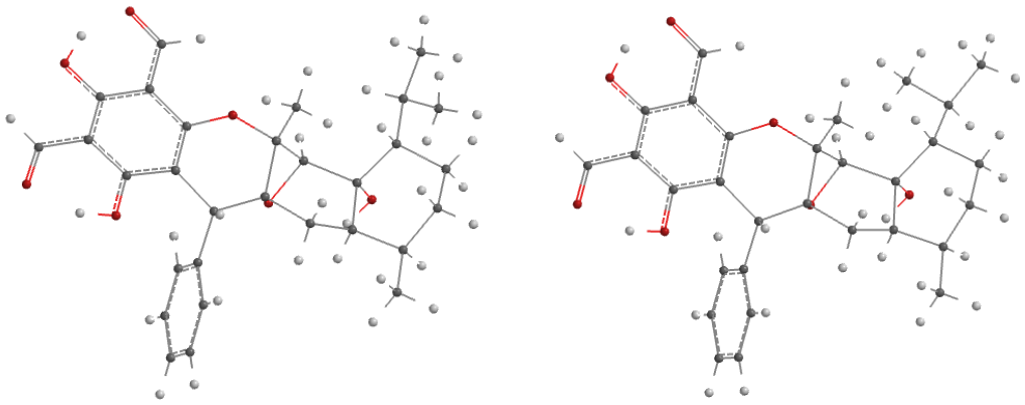

Conf. 1
Δε (kcal/mol)=0
(90.8%)

Conf. 2
Δε (kcal/mol)=+2.29
(9.2%)

Figure S13-5. DFT-optimized structures for low-energy conformers of (3*α*,5*α*-epoxy-6*α*-OH)-/(1'*R*, 1*R*, 3*R*, 4*R*, 5*R*, 6*R*, 7*S*, 10*R*)-**5** at B3LYP/6-31+G(d) level in methanol (PCM), with zero-point corrected free energies calculated at the same level (and Boltzmann population at 298K estimated thereof).

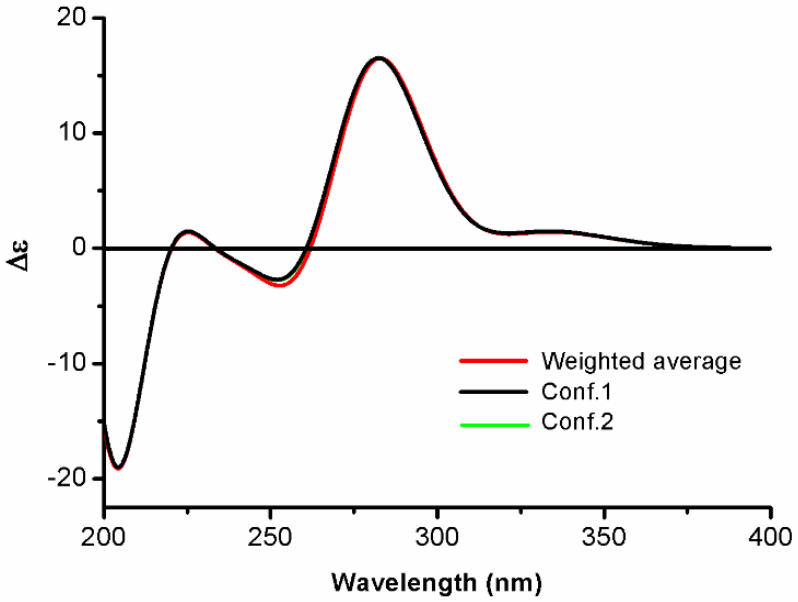

Figure S13-6. DFT-optimized structures for low-energy conformers of (3*α*,5*α*-epoxy-6*α*-OH)-/(1'*R*, 1*R*, 3*R*, 4*R*, 5*R*, 6*R*, 7*S*, 10*R*)-**5** at B3LYP/6-31+G(d) level in methanol (PCM), with zero-point corrected free energies calculated at the same level (and Boltzmann population at 298K estimated thereof).

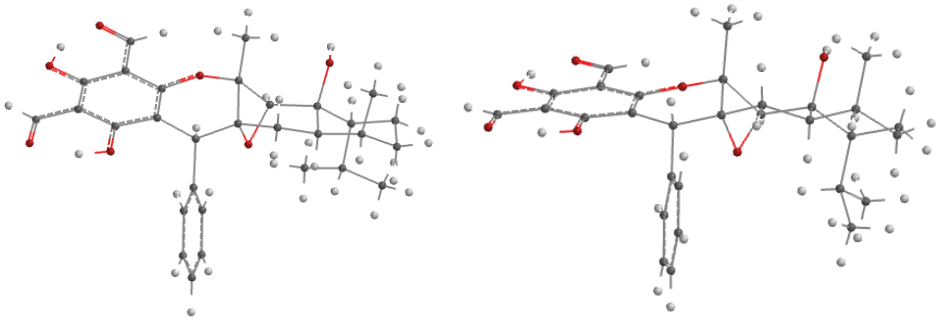

Conf. 1
Δε (kcal/mol)=0
(54.5%)

Conf. 2
Δε (kcal/mol)=+0.61
(29.6%)

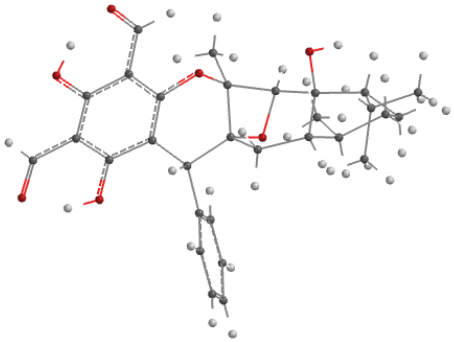

Conf. 3
Δε (kcal/mol)=+1.23
(15.8%)

Figure S13-7. DFT-optimized structures for low-energy conformers of (3*α*,5*α*-epoxy-6*β*-OH)-/(1'*R*, 1*R*, 3*R*, 4*R*, 5*R*, 6*S*, 7*S*, 10*R*)-**5** at B3LYP/6-31+G(d) level in methanol (PCM), with zero-point corrected free energies calculated at the same level (and Boltzmann population at 298K estimated thereof).

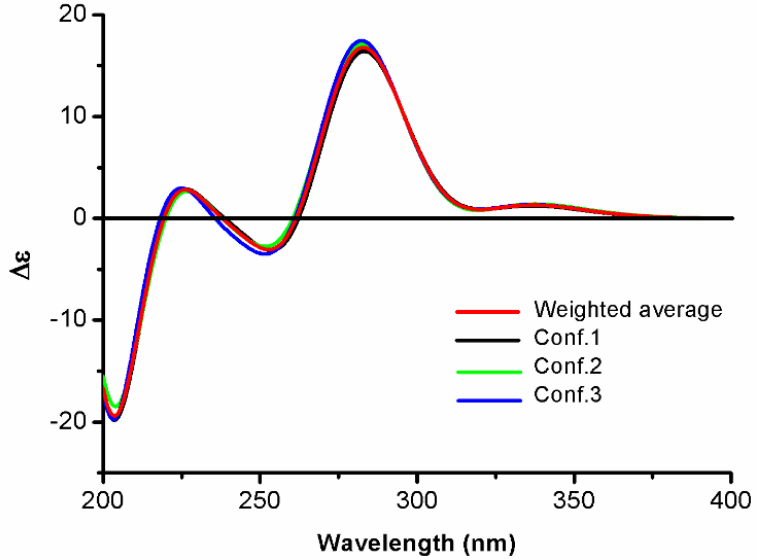

Figure S13-8. TDDFT-calculated spectra at B3LYP/6-31+G(d) level in methanol (PCM) for the low energy structures of (3*α*,5*α*-epoxy-6*β*-OH)-/(1'*R*, 1*R*, 3*R*, 4*R*, 5*R*, 6*S*, 7*S*, 10*R*)-**5**, and their weighted average using Boltzmann populations at 298K. Gaussian band-shape with 0.3 eV applied to generate the spectra.

Computational data of **7**

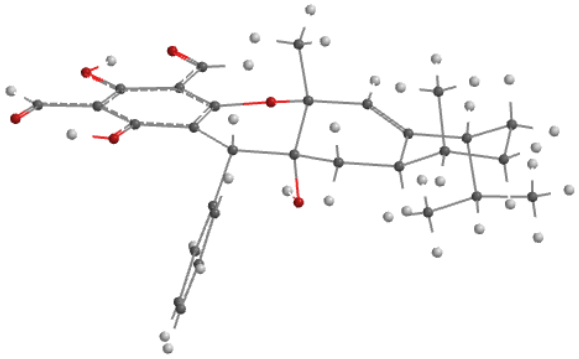

Conf. 1
Δε (kcal/mol)=0
(100%)

Figure S14-1. DFT-optimized structures for low-energy conformers of (1'*R*, 1*R*, 3*R*, 4*R*, 7*S*, 10*R*)-**7** at B3LYP/6-31+G(d) level in methanol (PCM), with zero-point corrected free energies calculated at the same level (and Boltzmann population at 298K estimated thereof).

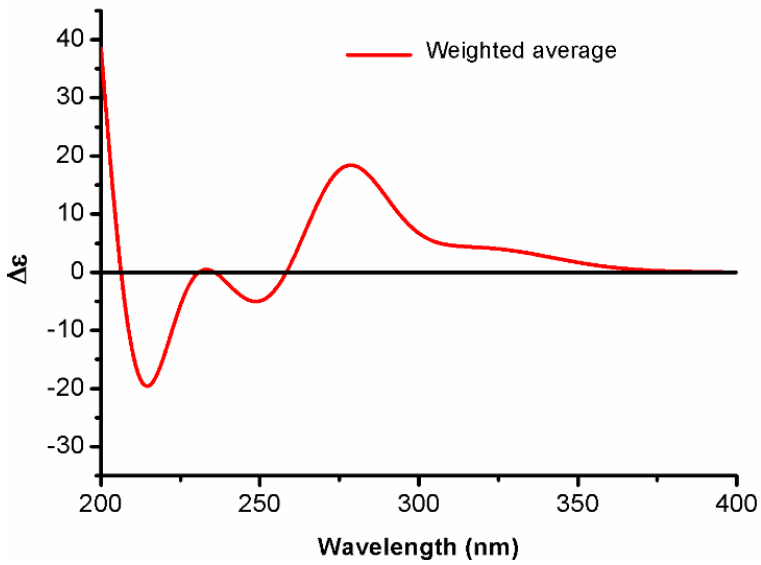

Figure S14-2. TDDFT-calculated spectra at B3LYP/6-31+G(d) level in methanol (PCM) for the low energy structures of (1'*R*, 1*R*, 3*R*, 4*R*, 7*S*, 10*R*)-**7**, and the weighted average using Boltzmann populations at 298K. Gaussian band-shape with 0.3 eV applied to generate the spectra.

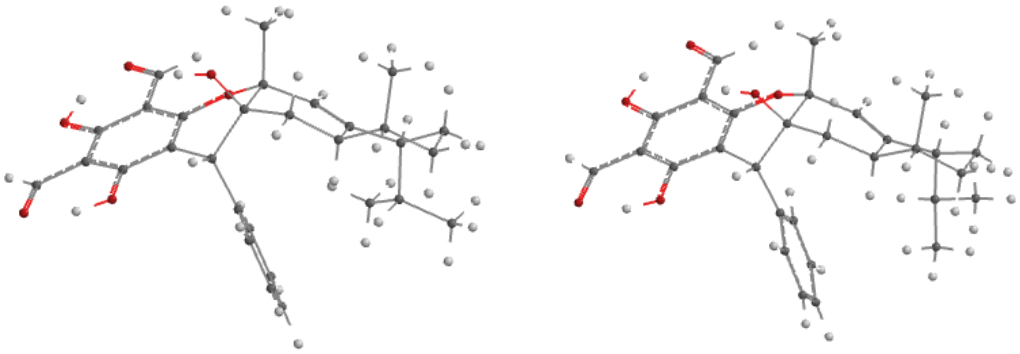

Conf. 1
Δε (kcal/mol)=+0
(75.1%)

Conf. 2
Δε (kcal/mol)=+1.1
(24.8%)

Figure S14-3. TDDFT-calculated spectra at B3LYP/6-31+G(d) level in methanol (PCM) for the low energy structures of (1'*R*, 1*R*, 3*S*, 4*R*, 7*S*, 10*R*)-**7**, and the weighted average using Boltzmann populations at 298K. Gaussian band-shape with 0.3 eV applied to generate the spectra.

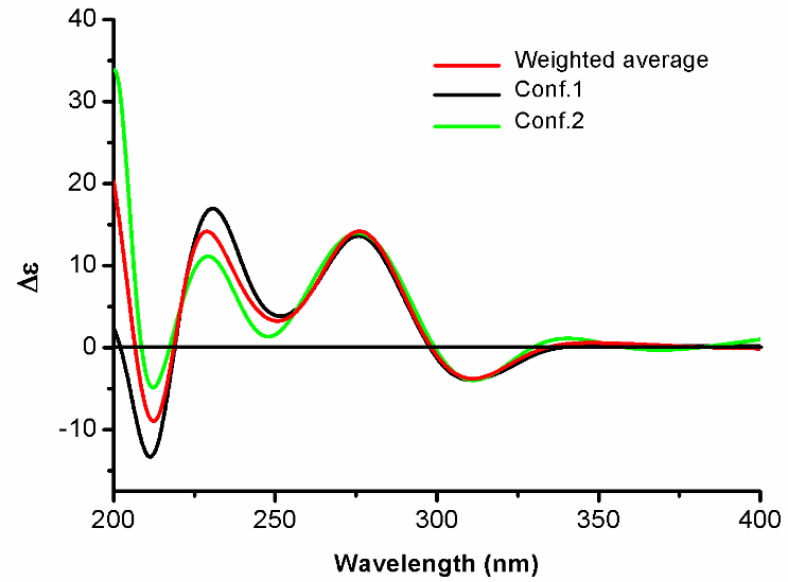

Figure S14-4. TDDFT-calculated spectra at B3LYP/6-31+G(d) level in methanol (PCM) for the low energy structures of (1'*R*, 1*R*, 3*S*, 4*R*, 7*S*, 10*R*)-**7**, and the weighted average using Boltzmann populations at 298K. Gaussian band-shape with 0.3 eV applied to generate the spectra.

Computational data of **8**

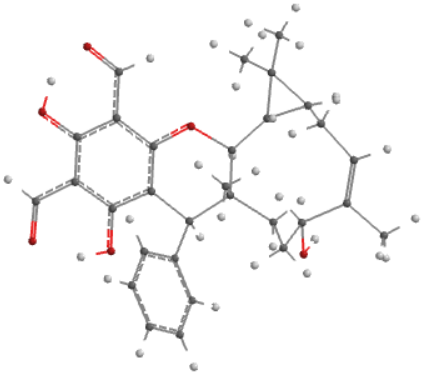

Conf. 1
Δε (kcal/mol)=0
(51.3%)

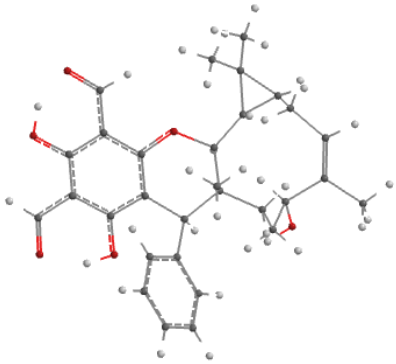

Conf. 2
Δε (kcal/mol)=+0.89
(20.8%)

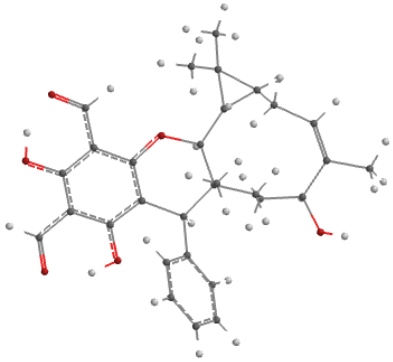

Conf. 3
Δε (kcal/mol)=+1.23
(14.8%)

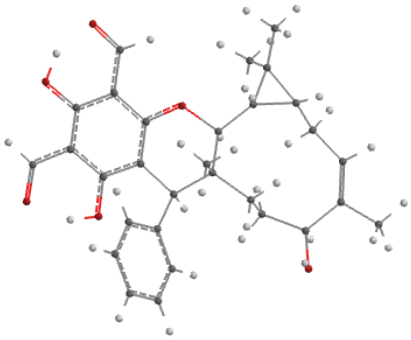

Conf. 4
Δε (kcal/mol)=+1.37
(12.9%)

Figure S15-1. TDDFT-calculated spectra at B3LYP/6-31+G(d) level in methanol (PCM) for the low energy structures of (1'*R*, 1*S*, 4*R*, 5*S*, 6*S*, 7*R*)-**8**, and the weighted average using Boltzmann populations at 298K. Gaussian band-shape with 0.3 eV applied to generate the spectra.

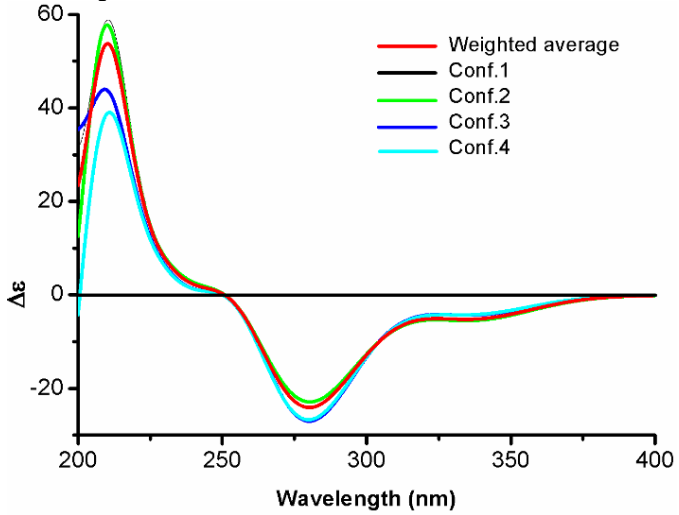

Figure S15-2. TDDFT-calculated spectra at B3LYP/6-31+G(d) level in methanol (PCM) for the low energy structures of (1'*R*, 1*S*, 4*R*, 5*S*, 6*S*, 7*R*)-**8**, and the weighted average using Boltzmann populations at 298K. Gaussian band-shape with 0.3 eV applied to generate the spectra.

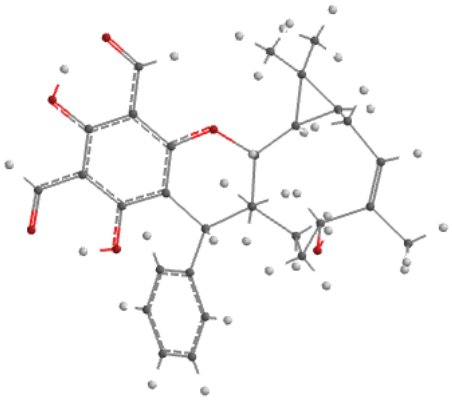

Conf. 1
Δε (kcal/mol)=0
(51.3%)

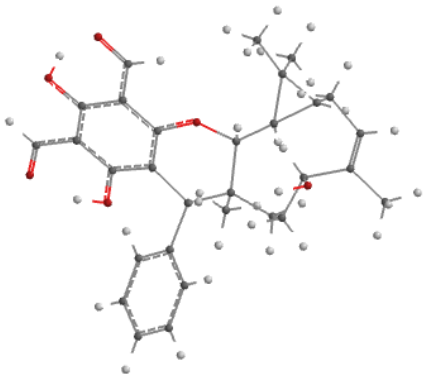

Conf. 2
Δε (kcal/mol)=+0.89
(20.8%)

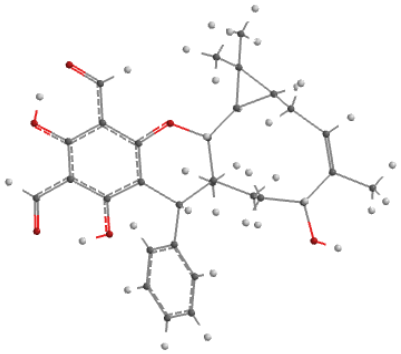

Conf. 3
Δε (kcal/mol)=+1.23
(14.8%)

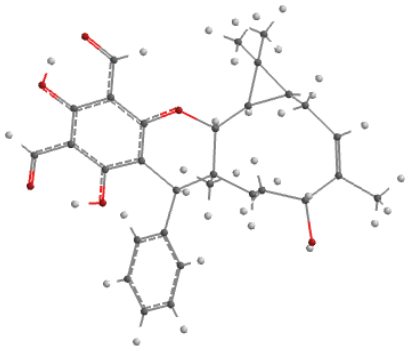

Conf. 4
Δε (kcal/mol)=+1.37
(12.9%)

Figure S15-3. TDDFT-calculated spectra at B3LYP/6-31+G(d) level in methanol (PCM) for the low energy structures of (1'*S*, 1*R*, 4*S*, 5*R*, 6*R*, 7*S*)-**8**, and the weighted average using Boltzmann populations at 298K. Gaussian band-shape with 0.3 eV applied to generate the spectra.

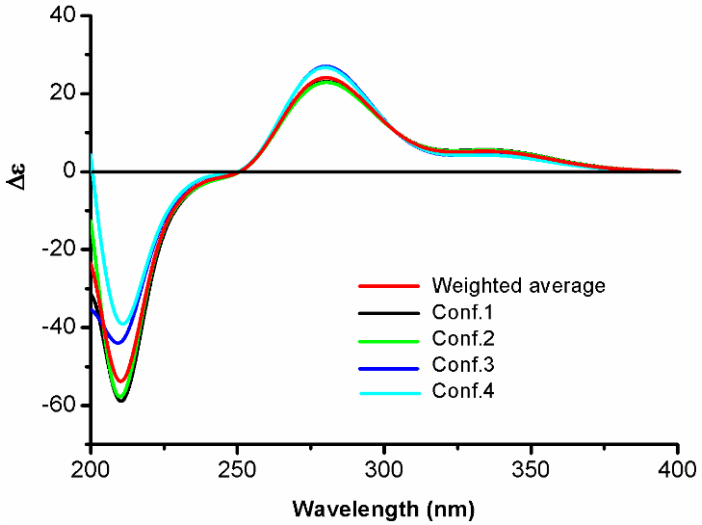

Figure S15-4. TDDFT-calculated spectra at B3LYP/6-31+G(d) level in methanol (PCM) for the low energy structures of (1'*S*, 1*R*, 4*S*, 5*R*, 6*R*, 7*S*)-**8**, and the weighted average using Boltzmann populations at 298K. Gaussian band-shape with 0.3 eV applied to generate the spectra.